DEVELOPMENT OF FUNCTIONAL POLYCARBONATE MATERIALS FROM METAL-CATALYZED COPOLYMERIZATION OF EPOXIDES AND CO_2

A Dissertation

by

YANYAN WANG

Submitted to the Office of Graduate and Professional Studies of
Texas A&M University
in partial fulfillment of the requirements for the degree of

DOCTOR OF PHILOSOPHY

Chair of Committee,	Donald J. Darensbourg
Committee Members,	Timothy R. Hughbanks
	Hong-Cai Joe Zhou
	Hung-Jue Sue
Head of Department,	Simon W. North

August 2018

Major Subject: Chemistry

ABSTRACT

Using the abundant, nontoxic and inexpensive CO_2 as a renewable C1 feedstock, the catalytic coupling of CO_2 and epoxides has provided an attractive method for preparing polycarbonates. This dissertation will highlight the development of CO_2-based functional polycarbonate materials through rational monomer/polymer design and efficient post-polymerization modifications.

First, a straightforward and simple approach to synthesize amphiphilic CO_2-derived polycarbonates with controllable block lengths, narrow molecular weight distributions and various functionalities was developed. Sequential copolymerization of propylene oxide (PO)/CO_2 and allyl glycidyl ether (AGE)/CO_2 under 'immortal polymerization' conditions yielded well-defined triblock polymer. The clickable alkene groups were then modified by radical mediated thiol-ene click chemistry to install various water-soluble moieties onto the polymer backbone. The resulting amphiphilic polycarbonates underwent self-assembly in deionized water to form well-dispersed micelle structures with distinct surface charges, providing the first examples of constructing functional nanomaterials from CO_2-based polycarbonates.

To expand the repertoire of polycarbonate biomaterials, a carboxylic acid functionalized polycarbonate was synthesized. Specifically, *tert*-butyl 3,4-epoxybutanoate was copolymerized with CO_2 using bifunctional cobalt(III) salen catalysts. Hydrolysis of the resultant polymer affords poly(3,4-dihydroxybutyric acid carbonate) (PDHBAC). Notably, PDHBAC was shown to undergo complete degradation in basic

aqueous solution into nontoxic biomasses including β-hydroxy-γ-butyrolactone and 3,4-dihydroxybutyrate. In addition, PDHBAC was employed as a degradable scaffold for platinum conjugation *via* an aspartate or glycine-aspartate linker; platinum loadings of 21.3-29.5% were achieved.

Lastly, in efforts aimed at improving the thermal mechanical properties of CO_2-based polycarbonate materials, cross-linked polycarbonate films were prepared from PO/AGE/CO_2 terpolymers containing clickable alkene groups. Detailed kinetic studies of terpolymerization of PO, AGE and CO_2 revealed similar reactivity ratios between the two epoxide monomers, indicating that the vinyl group distributed randomly along the polymer backbone. Terpolymers of PO/AGE/CO_2 were then treated with multifunctional thiols to afford well-defined cross-linked networks. Investigation of the relationships between film compositions, structures and thermal mechanical properties was carried out using dynamic mechanical analysis.

DEDICATION

To mom and dad

ACKNOWLEDGEMENTS

First and foremost, I would like to extend my sincere gratitude to my research advisor, Professor Donald J. Darensbourg, for taking me under his wing and for guiding me to become a better chemist. Don has always been very supportive and encouraging, and gave me the freedom to explore projects that I found interesting. I couldn't have asked for a better boss. One privilege of working in Don's lab is to get to know another accomplished scientist, Professor Marcetta Y. Darensbourg. Don and Marcetta, your immense knowledge, great passion for science, and kindness to others, will always be a huge inspiration for me. I would also like to thank Professors Timothy R. Hughbanks, Hong-Cai (Joe) Zhou and Hung-Jue Sue for taking time out of their busy schedule to serve in my dissertation committee.

Admittedly, I came to Don's lab with little technical skills; for one thing, I had never heard of Schlenk line before. I was very fortunate to be trained and mentored by those talented (and awesome!) DJD group chemists. I must especially mention and thank Dr. Fu-Te Tsai for his patience in teaching me those inorganic synthetic skills, including using Schlenk technique to handle air-/moisture-sensitive compounds. And without the foundation Fu had laid in the new research area, I would not have completed some of my projects in a timely manner. Special thanks to my good friend, Samuel Kyran; thank you for spending many hours on correcting my writing, for sharing tasty baking goods and interesting cooking shows, and for all the positive and meaningful conversations. Thank

you also to Joanna and Andrew, for being willing to help whenever needed, and for your friendship.

Later on, after all the 'official' DJD members left, I have shared the labs, and also made friends with several newcomers, both visiting scholars and postdocs. Dr. Debangsu Sil, thank you for always being there to get my many questions answered, and for being willing to help me (many a time!) practice my interviews. Best of luck on your new postdoc journey! Thank you also to Kaihong Chen for all the discussions that have helped solving my experiment puzzles.

Outside of the DJD group, there are a few other people that I must mention. Wei, my good friend from College, thank you for always being there to listen when I need it most. Daniel Rossi, I would not have survived 'Group Theory' without your help! I also wish to extend my gratitude to Dr. Jingwei Fan and Dr. Lu Su from Professor Karen Wooley's group for their valuable input in some of my projects.

Above all, I would like to thank my family for their love and support. To my parents, I owe you my deepest gratitude. Mom and dad, thank you for all the sacrifice you've made for my sister and me. And thank you for instilling me the important values of kindness, hard-working and self-respect. I am who I am today because of you! My younger sister, Tangyue, thank you for keeping our parents' company while I am far away. I would also like to thank my parents-in-law, brother-in-law and sister-in-law, for their love and moral support. Lastly, I would like to thank my husband, my best friend and my strongest motivation, Chris Pell, for introducing me to those great books/music/movies, for always being there for me during difficult times, and most of

all for inspiring me to be a more positive and better person. This journey is made more memorable with you walking along me.

CONTRIBUTORS AND FUNDING SOURCES

Contributors

This work was supervised by a dissertation committee consisting of Professors Donald J. Darensbourg [advisor], Timothy R. Hughbanks and Hong-Cai (Joe) Zhou of the Department of Chemistry and Professor Hung-Jue Sue of the Department of Mechanical Engineering.

All work for the dissertation was completed by the student, in collaboration with Dr. Jingwei Fan (Chapter II) and Dr. Fu-Te Tsai (Chapter III).

Funding Sources

This work was made possible in part by the financial support of the National Science Foundation under Grant Numbers CHE-1057743, DMR-1309724 and CHE-1410272, and the Robert A. Welch Foundation under Grant Numbers A-0923 and A-0001.

Its contents are solely the responsibility of the authors and do not necessarily represent the official views of the funding agencies.

TABLE OF CONTENTS

Page

Page

LIST OF FIGURES

Page

Page

Page

Page

LIST OF TABLES

Page

LIST OF SCHEMES

Page

Page

CHAPTER I

INTRODUCTION AND LITERATURE REVIEW

Brief Review of Polycarbonates

Polycarbonates (PCs) are a class of thermoplastic polymers containing carbonate units in their chemical structure. They are widely used in numerous industrial applications including automotive interiors, sunglasses, bulletproof windows, medical devices, et al.[1] The global market for polycarbonate exceeded 4.3 million tons in 2015 and is expected to grow by about 6.9% each year to 2024.[2] The most common type of polycarbonates in the market is bisphenol A (BPA) polycarbonate. It is an aromatic polycarbonate with a high glass transition temperature (T_g) of 140-155 °C. BPA polycarbonates are widely used as an engineering thermoplastic due to their outstanding physical and mechanical properties, including transparency, durability, high impact resistance, tensile strength of ~75 MPa and good electrical insulation.[3]

Compared to aromatic polycarbonates, aliphatic polycarbonates have received little commercial attention due to their low heat resistance and high susceptibility to hydrolysis. Their industrial applications are mostly limited to low molecular weight polycarbonate polyols for polyurethane production. Recently, aliphatic polycarbonates have attracted significant attention in the biomedical field due to their biocompatibility and biodegradability. One of the most investigated aliphatic polycarbonates is poly(trimethylene carbonate) (PTMC). PTMC is a highly flexible amorphous polymer with a low glass transition temperature of ~-20 °C. Unlike other degradable polymers

like polyester, PTMC degrades into non-acidic diols and carbon dioxide which are less likely to cause adverse effects such as inflammation. PTMC and its copolymers have been fabricated into nanoparticles,[4] sutures[5] and hydrogels[6] for applications in tissue engineering and drug delivery.

Synthesis of Polycarbonates and CO_2/Epoxides Copolymerization

Polycarbonates can be synthesized *via* several routes. Industrially, they are typically produced through the polycondensation reaction of a diol and phosgene in a biphasic reactor. There are several major drawbacks involved in the process including the use of highly toxic phosgene as a monomer, requirement of volatile CH_2Cl_2 as the solvent, generation of a large amount of waste water and high equipment maintenance cost.[7] In order to overcome these drawbacks, an alternative and greener route has been developed which proceeds by melt polymerization of diols and diphenyl carbonate.[7] However, this process requires high temperatures and high vacuum and thus is very energy consuming.

A third approach to synthesize polycarbonate is ring-opening polymerization (ROP) of six- or seven-membered cyclic carbonates.[8] This route is commonly practiced in research labs. Advantages of ROP include controlled molecular weight and tunable structures. However, the synthesis of substituents containing cyclic carbonates is a multiple-step process and usually involves the use of phosgene.

A new recent discovery in polycarbonate synthesis was reported by Tomshige and co-workers.[9] They demonstrated the direct copolymerization of CO_2 and diols using

CeO_2 as a catalyst and 2-cyanopyridine as a promoter to produce polycarbonates (Scheme I-1). Unfortunately, only oligomers were obtained.

Beginning with Inoue's discovery in 1969,[10] the catalytic coupling of CO_2 and epoxides has become a viable alternative for the production of polycarbonates (Scheme I-2). This synthetic routes provide many advantages. It uses the nontoxic and inexpensive CO_2 as a carbonyl source instead of the toxic phosgene. Polycarbonates made from this route can contain up to 50% (by moles) of CO_2 and therefore will rely less on fossil-based feedstocks and will have a significantly reduced carbon footprint. This process usually does not require extraneous solvent as many epoxides themselves are liquid and can dissolve the catalyst and the resulting polymer. One possible byproduct in the reaction is a five-membered cyclic carbonate. It should be noted that cyclic carbonates also find use in industrial applications as high-boiling aprotic solvents and as electrolytes in lithium-ion batteries.[11]

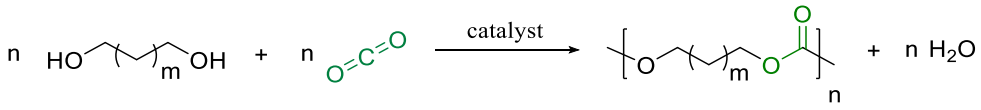

Scheme I-1. Direct polymerization of diols and CO_2 to produce polycarbonate.

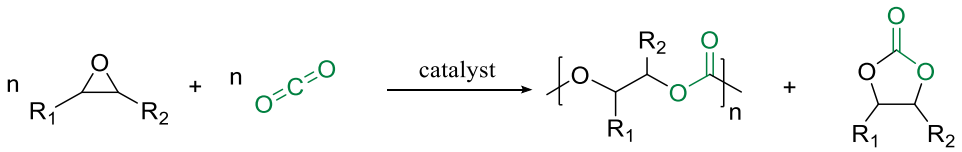

Scheme I-2. Coupling between epoxide and CO_2 to yield the desired copolymer, and cyclic carbonate side-product.

Mechanistic Aspect of Metal-Catalyzed Pathways

The coupling reaction between CO_2 and an epoxide usually requires the application of a metal catalyst. The generally accepted mechanism for production of polycarbonates is depicted in Scheme I-3. The copolymerization is initiated by the coordination of the epoxide and its subsequent ring-opening by the nucleophilic cocatalyst (X^-) to provide a metal-alkoxide species. This metal alkoxide intermediate then undergoes CO_2 insertion to form a metal-carbonate. The successive alternating incorporation of epoxides and CO_2 produces linear polycarbonates. It is generally proposed that the rate-determining step involves epoxide ring-opening by the growing anionic polymer chain rather than CO_2 insertion.[12]

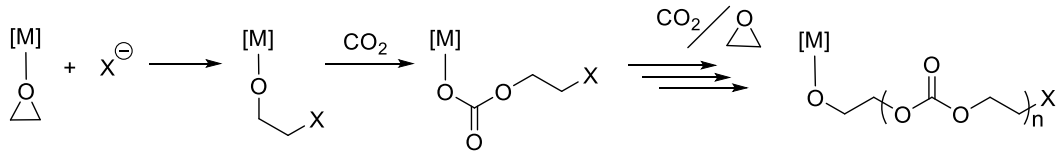

Scheme I-3. Generalized mechanism for the production of polycarbonates.

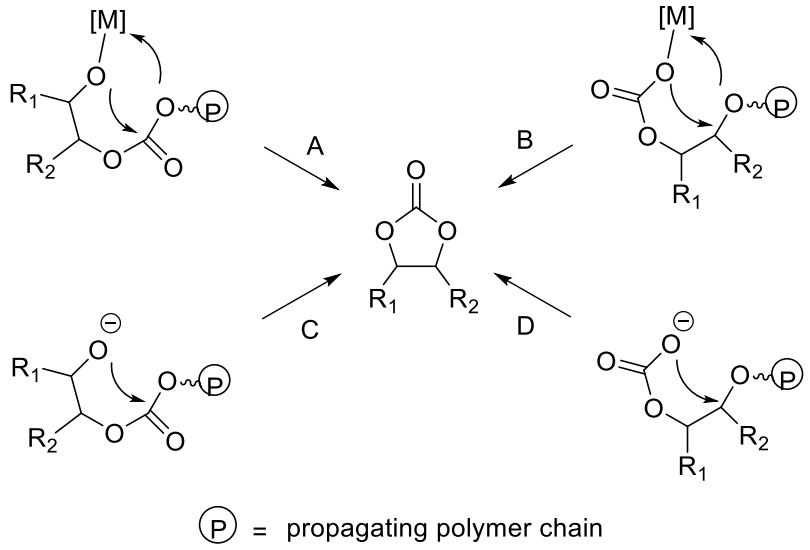

Scheme I-4. Formation of cyclic carbonates *via* backbiting reactions.

One side reaction that can occur in the process is the formation of ether linkages due to consecutive ring-opening of epoxides. Such ether linkages, though reduce the amount of CO_2 being incorporated, can be beneficial for some applications especially when low viscosity is desired. Five-membered cyclic carbonates can also form as by-products through the back-biting mechanism (Scheme I-4). This side reaction is proposed to occur *via* four pathways involving both metal-bound (path A and B) and metal-free (path C and D) polymer chains. The latter process has a much lower activation barrier and can be enhanced upon increasing reaction temperatures and/or adding excessive cocatalysts.

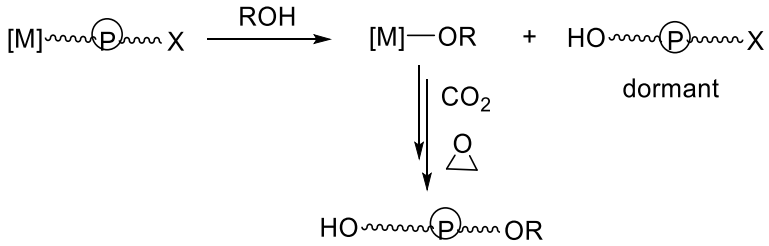

Scheme I-5. Chain transfer reactions in the presence of protic compounds.

Along with the normal chain propagation process, chain transfer reactions also need to be considered (Scheme I-5).[13] In this case, the growing polymer anion (initiated by nucleophile X^-) can undergo rapid exchange with added protic compounds, such as alcohols or water, to generate a 'free' polymer chain and an initiating metal alkoxide species. Importantly, the liberated polymer is not 'dead', but can be re-enter the chain-growing process due to the reversibility of chain transfer reactions. This phenomenon is also referred to as "immortal polymerization", first introduced by Inoue in 2000.[14] Immortal polymerization can be exploited to achieve precise control of molecular weights which are determined by the concentration of both the catalyst and chain transfer agents.

Catalysts Development for the Copolymerization of CO_2 and Epoxides

Inoue first discovered the coupling of CO_2 and propylene oxide in 1969 utilizing a heterogeneous catalyst based on diethyl zinc and water.[10a] Since then, numerous catalysts, both heterogeneous and homogeneous, have been developed for this transformation. The most widely applied heterogeneous catalysts include zinc glutarate

(or other carboxylates) and double metal cyanides.[15] These catalysts usually require more forcing reaction conditions (high catalyst loading, elevated temperature and CO_2 pressure) than homogeneous catalysts and often result in polymers with a significant amount of ether defects and broad molecular weight distribution. In addition, it is difficult to investigate the reaction mechanisms using these heterogeneous catalysts due to the lack of active-site control. Nevertheless, these catalysts are quite robust and easy to prepare from inexpensive starting materials, and thereby are currently applied in industrial processes for CO_2-based polycarbonate production. The first single-site catalyst for CO_2/epoxides copolymerization was discovered by Inoue and co-workers in 1986.[16] In this instance, the catalyst system employed was an aluminum-porphyrin complex coupled with a quaternary organic salt or triphenylphosphine. Despite the low activity of these catalysts, they provided polymers with almost perfect alternating structures and narrow molecular weight distributions. Following Inoue's discovery, various homogeneous systems have been developed to achieve improved activity and polycarbonate selectivity. The representatives are zinc phenoxides,[17] β-diiminate zinc alkoxides,[18] metalloporphyrins,[19] metal-salen or –salan complexes[20] as well as bimetallic macrocyclic derivatives.[21]

To date, the most widely studied catalysts are derived from salen cobalt complexes.[22] The first generation of this type of catalysts is a binary system comprising of a (salen)$Co^{III}X$ complex (X = Cl^{-1}, N_3^{-1} or 2,4-dinitrophenolate, *etc.*) and an exogenous onium salt co-catalyst, typically quaternary ammonium ($^nBu_4NX$) or phosphonium salt (PPNX) (Figure I-1). Recent kinetic studies revealed a fractional reaction order between

1 and 2 in catalyst concentration,[23] indicating concurrent bimetallic and monometallic pathways in the rate-limiting ring-opening step (Figure I-2). The binary catalysts yield copolymers with perfect alternating structures and can achieve good levels of regio- and stereochemistry control when chiral ligands are used. Unfortunately, a considerable amount of cyclic byproducts are produced at elevated temperatures and/or at higher degree of conversion. In addition, due to the binary nature, these systems typically exhibit a long induction period and low activity at low catalyst loadings.

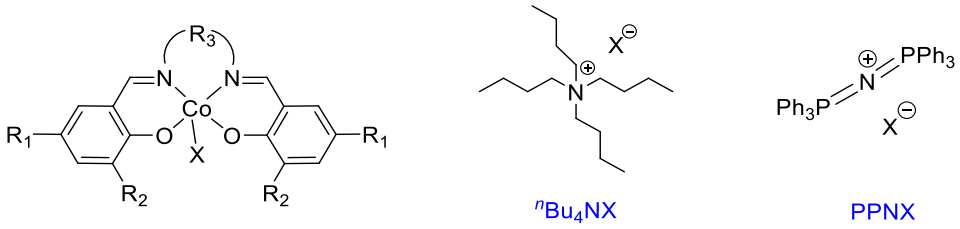

Figure I-1. (Salen)$Co^{III}X$ catalyst (left) with onium salt cocatalysts (right).

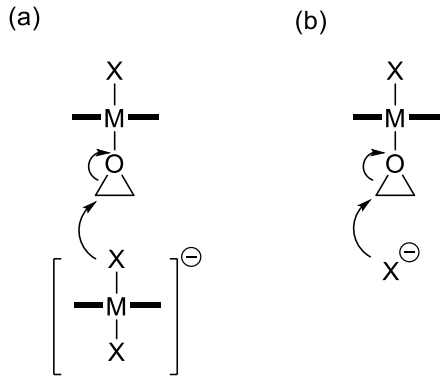

Figure I-2. Possible pathways for epoxide ring opening by binary catalysts: (a) bimetallic ring-opening and (b) monometallic ring-opening.

To overcome these limitations, the second generation of (salen)Co^{III} catalysts were developed by covalently attaching the cocatalyst to the ligand backbone and as such were named bifunctional catalysts (Figure I-3).[24] As the catalyst and cocatalyst are linked within one molecule, these compounds can maintain high activity at extremely low catalyst loadings. The appended ammonium arms can attract the dissociated anionic polymer chain through electrostatic interaction and prevent it from drifting into the bulk solution. This allows the polymeric chain to quickly return to the metal center and continue chain growth. Furthermore, the electrostatic interaction suppresses the back-biting process resulting in high polycarbonate selectivity (Figure I-3). These bifunctional catalysts are by far some of the most active catalysts for CO_2/epoxides copolymerization and unlike their simple counterparts can operate at high temperatures (70-120 °C) without losing polycarbonate selectivity.

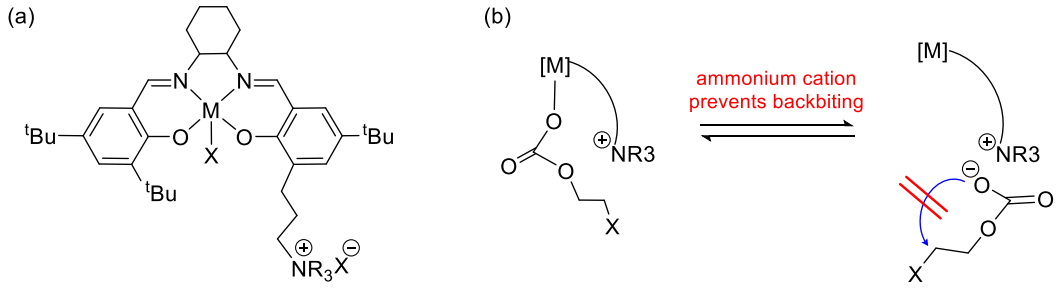

Figure I-3. (a) Bifunctional (salen)Co^{III} catalyst, (b) proposed mechanism for preventing backbiting by bifunctional catalysts.

Most Common CO_2-Based Copolymers

Two of the most investigated epoxides are cyclohexene oxide (CHO) and propylene oxide (PO). Generally, copolymerization of CHO and CO_2 can proceed readily using a variety of catalysts under mild conditions and exhibit a high polycarbonate selectivity even at high temperatures. PO can also react with CO_2 quiet easily to form polycarbonate. However, judicious choice of catalysts and reaction temperatures are usually required to eliminate formation of the cyclic by-products. Poly(cyclohexene carbonate) (PCHC) and poly(propylene carbonate) (PPC) burn cleanly and completely in air without emitting harsh residues, and thus can be used as sacrificial binders in electronics and ceramics manufacturing. Compared to PCHC, PPC exhibits more favorable mechanical properties and has found wider applications. For instance, PPC is already finding use as a degradable packaging material, and its low M_w polyols can substitute traditional petro-based polymers in polyurethane production. To date, PPC and PCHC have been commercially synthesized from CO_2 by many companies such as Saudi Aramco,[25] Empower Materials,[26] Econic Technologies[27] and Covestro[28].

Despite the advantages of PPC and PCHC, their lack of functionalities and relatively low glass transition temperatures (T_g = 37 °C for PPC, 115 °C for PCHC) have limited their use in high value-added and functional materials. In order to expand the application scope of CO_2-based polycarbonates, two topics are of current interest. One is the synthesis of more diverse polycarbonates with different functionalities. For clarification, functional polycarbonates discussed here are not characterized by their thermal properties, but rather by their inherent functionalities. Both pendant and terminal

functional groups can be incorporated into the polymer. The second topic of interest is the preparation of CO_2-PCs with high thermal resistance, characterized by a high glass transition temperature (T_g) and/or melting temperature (T_m).

Development of Functional Polycarbonates from CO_2

Introduction of pendant functional groups allows for the tailoring of material properties, such as solubility, biodegradability, stimuli-response and self-healing ability. Functional polycarbonates with pedant functionalities can be prepared *via* i) direct copolymerization of a functional monomer with CO_2, or ii) post-polymerization modification of polymer scaffolds bearing reactive groups. End functionalized polycarbonates are also of interest. The presence of terminal functional groups can lead to block copolymer formation, or for some applications such as coatings and adhesives, can improve the compatibility between different polymers. For CO_2-epoxides copolymers, end functionalities can be introduced through addition of chain transfer agents.

Direct Polymerization of Functional Monomers. With the development of highly efficient catalyst systems, a large family of functional epoxides have been successfully copolymerized with CO_2 to produce polycarbonates with pendant functionalities. The functional epoxides can be classified into four main categories based on their structures: terminal epoxides, glycidyl ethers, 4-substitutented cyclohexene oxides, and other functional alicyclic epoxides. Some of these epoxide monomers can be prepared from renewable feedstocks.[29]

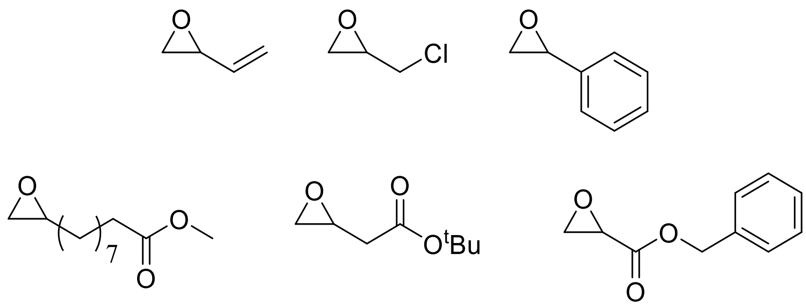

Figure I-4. Selected terminal epoxides used in CO_2 copolymerization reactions.

Terminal Epoxides

Copolymerization of CO_2 and terminal epoxides (Figure I-4) with electron-withdrawing groups (EWG), such as styrene oxide (SO),[30] epichlorohydrin (ECH)[31] and 2-vinyloxirane (VIO),[32] has been extensively studied, in comparison with propylene oxide/CO_2 coupling, to understand the influence of substituents on reaction activity, regioselectivity, and product selectivity. Generally, electron-withdrawing substituents reduce the epoxides' coordination ability to the metal center, resulting in a higher activation energy compared to propylene oxide. With regard to regioselectivity, the methine C-O bond is more prone to ring-opening due to a more electrophilic carbon center. This in turn would facilitate the formation of cyclic carbonate byproducts *via* backbiting to the methine carbon of the adjacent carbonate unit. When the binary (salen)$Co^{III}X$/PPNX (X = 2,4-dinitrophenolate (DNP)) catalyst system was employed, copolymerization of CO_2 and VIO[32] or ECH[31a] produced significant amounts of cyclic carbonates at 25˚C, the latter one showing only 10% polymer selectivity. On the other hand, the bifunctional (salen)$Co^{III}X$ complex exhibited much higher polymer selectivities (92% ~ 100%), affording high molecular weight copolymers with low

polydispersities. For SO/CO_2 coupling reactions, whereas both the binary and bifunctional systems (DNP as the initiating anion) yielded polymers with more than 99% selectivity, the latter catalyst showed much higher activity and could maintain its high performance at very low catalyst loadings.[30e]

Several terminal epoxides containing ester functionalities have been applied to produce CO_2 copolymers. In 2014, Qi *et al*. reported the catalytic coupling of epoxy methyl 10-undecenoate (EMU) and CO_2 using a double metal complex [Zn-Co^{III} DMCC] to produce an ester functionalized polycarbonate.[33] Notably, the epoxy monomer can be obtained from a bio-renewable feedstock. The EMU/CO_2 copolymers displayed low T_g values of -38 °C to -44 °C depending on the molecular weights as a result of the long alkyl side chain.

Another two ester functionalized CO_2 copolymers, poly(benzyl glycidate carbonate) (PBGC)[34] and poly(*tert*-butyl 3,4-dihyroxybutyrate carbonate) (P^{t}BuDHBC)[35], have been prepared by the Grinstaff group and the Darensbourg group respectively (Figure I-5). The monomers employed in both studies carried a bulky substitute at the methine carbon which in turn promoted ring-opening to occur predominantly at the sterically less hindered C_β-O bond during the copolymerization reactions. Hydrogenolysis of PBGC afforded poly(glyceric acid carbonate) (PGAC) which was shown to degrade in aqueous solutions. Similarly, the *tert*-Butyl group in P^{t}BuDHBC could be cleaved to produce degradable poly(3,4-dihydroxybutyric acid carbonate) (PDHBAC) which compared to PGAC contained one extra carbon between the polymer backbone and the COOH group. Of importance, a detailed degradation study

of PDHBA showed that it could degrade readily in basic solutions into 3,4-dihyroxyl butyric acid, which is a normal human metabolite. PDHBA provides a human-friendly and environmentally benign platform for biomedical applications.

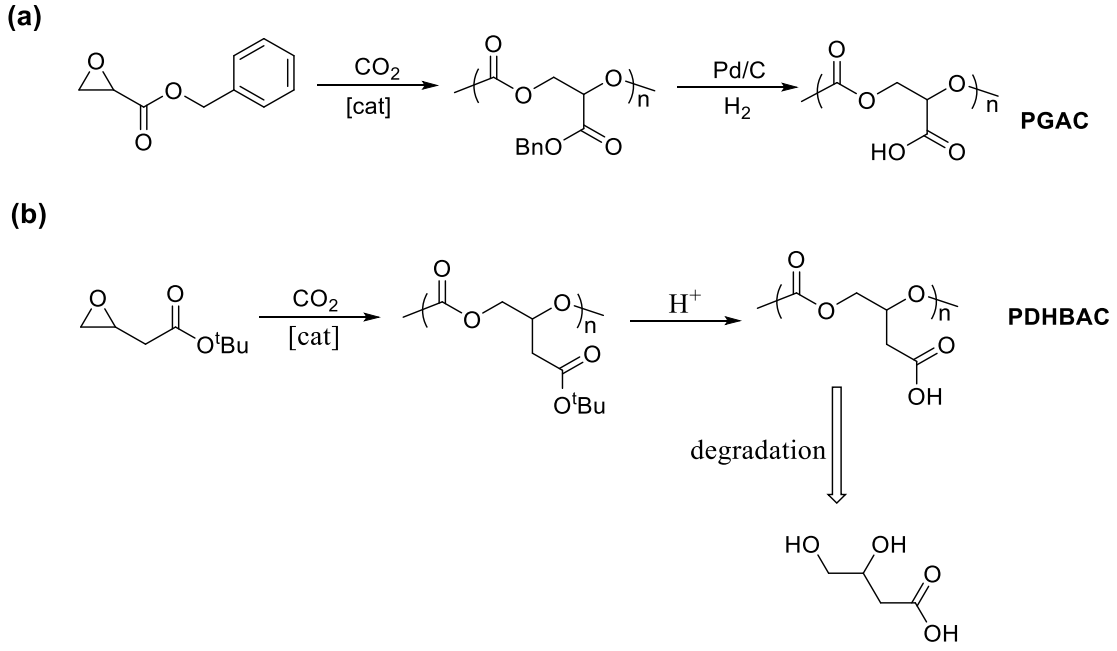

Figure I-5. (a) Synthesis of poly(glyceric acid carbonate) (PGAC) through copolymerization of benzyl glycidate and CO_2 followed by hydrogenolysis; (b) synthesis of poly(3,4-dihyoxyl butyric acid) (PDHBA) through copolymerization of *tert*-butyl 3,4-epoxybutanoate and CO_2 followed by hydrolysis.

Glycidyl Ethers

Glycidyl ethers can be readily prepared from substitution reactions between epichlorohydrin and functional alcohols. To date, a large family of glycidyl ethers (Figure I-6) have been successfully copolymerized with CO_2 using Co or Zn catalysts to produce functional polycarbonates.[36] The structure versatility of glycidyl ethers allows

access to various copolymers with desired physicochemical properties suitable for different applications. Moreover, using monomers containing reactive groups as alkyne,[37] alkene[38] and furfuryl[39] enables introduction of multiple different functionalities onto a single polymer chain through post polymerization functionalization. A few representative functional polycarbonates derived from glycidyl ethers will be highlighted below; these polycarbonates all bear hydrophilic moieties along the polymer backbone. For a full summary of glycidyl ether and CO_2 copolymers, see the excellent review by Frey and Scharfenberg.[36]

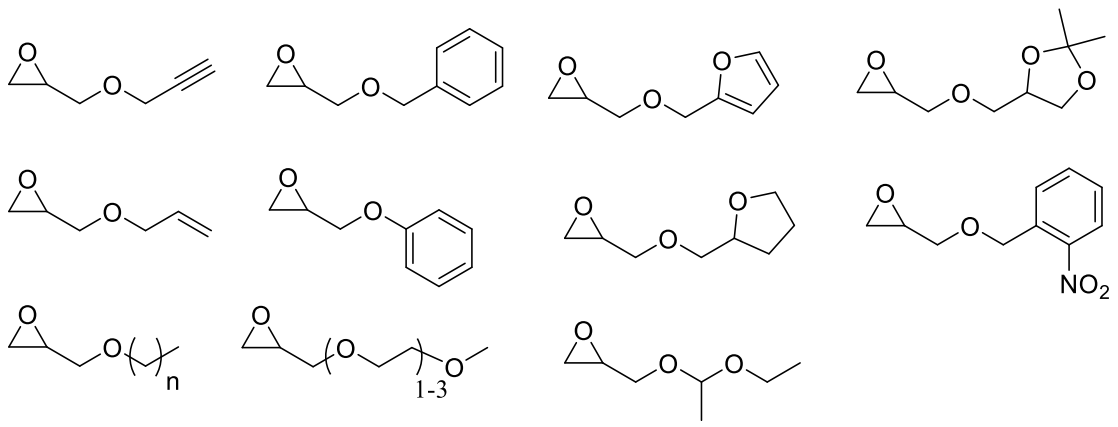

Figure I-6. Selected glycidyl ethers used in CO_2 copolymerization reactions.

The groups of Frey[40] and Grinstaff[41] independently reported the synthesis of poly(1,2-glycerol polycarbonate) through copolymerization of benzyl glycidyl ether (BGE) or ethoxyethyl glycidyl ether (EEGE) with CO_2 followed by cleavage of the protecting groups (Figure I-7). Of note, synthesis of poly(1,2-glycerol carbonate) from

direct coupling of glycidol and CO_2 is not feasible due to the interference of chain transfer reactions. Poly(1,2-glycerol carbonate) was not soluble in common organic solvents like dichloromethane, toluene, and chloroform, indicating its enhanced hydrophilicity due to the presence of hydroxyl pendant groups. In contrast to poly(1,3-glycerol carbonate) prepared from ROP, poly(1,2-glycerol carbonate) exhibited a strikingly faster degradation rate with a $t_{1/2} \approx$ 2-3 days.[41] The increase in degradation was attributed to the lower activation energy required for the pendant primary OH in poly(1,2-glycerol carbonate) to undergo intramolecular attack onto the carbonate linkage, compared to the secondary OH in the 1,3 isomer.

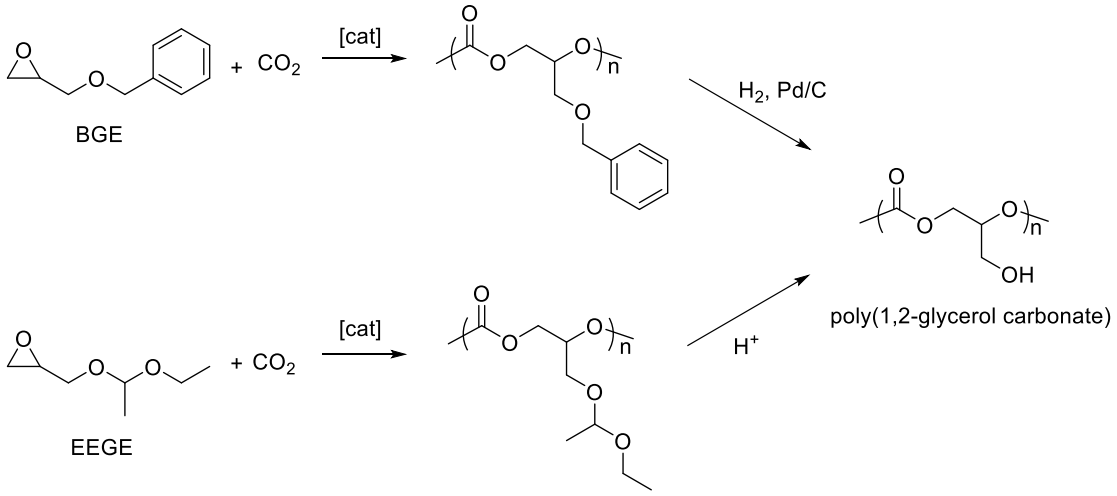

Figure I-7. Synthesis of poly(1,2-glycerol carbonate) *via* copolymerization of BGE or EEGE with CO_2 followed by deprotection.

Thermal-responsive polymers have been widely studied for their biomedical applications, such as drug delivery and tissue engineering.[42] The first examples of thermal-responsive polycarbonates derived from CO_2 were reported by Wang and co-workers.[43] Epoxides (ME_nMO, Figure I-8) containing pendant oligo(ethylene glycol) groups were copolymerized with CO_2 using the binary (salen)Co^{III} catalyst. The copolymer derived from ME_2MO/CO_2 coupling exhibited a rapid and reversible thermo-responsive phase transition in water, possessing a lower critical solution temperature (LCST) of ~ 44.7 °C.[43] Furthermore, terpolymerization of $ME_2MO/ME_1MO/CO_2$ were conducted with various feeding ratios, yielding terpolymers with a wide range of LCST values from 0 °C to 43 °C. Soon after this work, the same group reported the synthesis of $PO/ME_3MO/CO_2$ terpolymers, which also exhibited thermal-responsive solubility in water.[44] This new class of 'smart' materials could provide a powerful platform for biomedical applications.

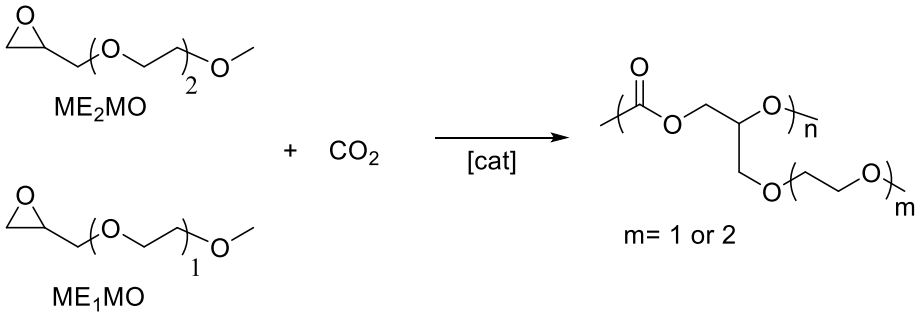

Figure I-8. Synthesis of thermo-responsive polycarbonates through coupling of ME_nMO and CO_2.

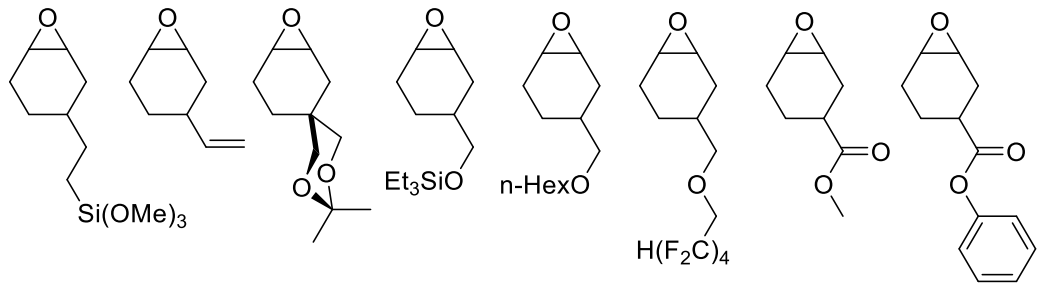

Figure I-9. Selected 4-substituted cyclohexene oxides used in CO_2 copolymerization reactions.

4-Substituted Cyclohexene Oxides

4-Substituted cyclohexene oxides (Figure I-9) have also been investigated in the copolymerization reaction with CO_2 to produce functional polycarbonates. An interesting example was reported by the Darensbourg group, describing the coupling of CO_2 and 2-(3,4-epoxycyclohexyl)ethyl-trimethoxysilane to form a CO_2 soluble polycarbonate.[45] Upon dissolution of the crude polymer in supercritical CO_2 and subsequent release of CO_2 pressure, the metal catalyst was effectively removed. Furthermore, the trimethoxysilane functionality could be utilized to prepare a cross-linked network through Si-O-Si bond formation.

Coates and co-workers employed a [(BDI)ZnOAc] complex to study the catalytic coupling of CO_2 with a variety of 4-substituted cyclohexene oxides containing vinyl, ketal, triethylsiloxy, polyethylene glycol (PEG), alkyl and fluorophilic functionalities.[46] The copolymerization reactions were demonstrated to behave in a living manner. Furthermore, various multiblock copolymers containing lipophilic, hydrophilic and fluorophilic units in a single chain were prepared by sequential addition of different monomers upon complete consumption of a former monomer.

Two ester-functionalized PCHC derivatives were synthesized by Gruter and co-workers through copolymerization reactions between CO_2 and 3,4-cyclohexene-oxide-1-carboxylic acid methyl ester or 3,4-cyclohexene-oxide-1-carboxylic acid phenyl ester using a BDI zinc catalyst.[47] A thorough MALDI-TOF-MS analysis of the isolated polycarbonates revealed the occurrence of transesterification side reactions. Consequently, branched and cyclic polymer structures were formed, which led to a broadening of the molecular weight.

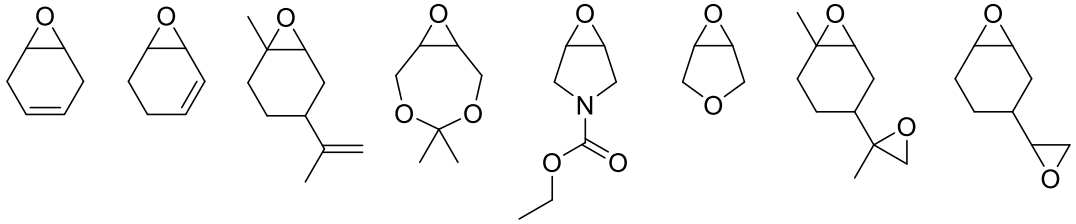

Figure I-10. Functional alicyclic epoxides used in CO_2 copolymerization reactions.

Other Functional Alicyclic Epoxides

Several other functional alicyclic epoxides (Figure I-10) in addition to 4-substituited cyclohexene oxides have been employed in the copolymerization reactions with CO_2. The Darensbourg group and others reported the synthesis of fully renewable functional polycarbonates from the catalytic coupling of CO_2 and a bio-derived epoxide, 1,4-cyclohexadiene oxide (1,4-CHDO).[48] Several catalyst systems have been employed for the copolymerization reaction, including di-zinc and di-magnesium macrocyclic catalysts,[48c] Cr- and Co-based salen complexes,[48a, 48c] and a (porphyrin)$Co^{III}Cl$/4-

dimethylaminopyridine (DMAP) system.[48b] The highest activities were observed with the binary (salen)$M^{III}X$/PPNX (M = Co or Cr, X = Cl^{-1} or 2,4-dinitrophenolate) catalysts. In the process catalyzed by (salen)Co^{III} catalyst, high copolymer selectivity (>99%) was observed, whereas employing the Cr^{III} system at its operation temperatures of 80-90 °C, the reactions gave a significant amount of cyclic carbonates in addition to the desired polymer. [37a] Both *cis*- and *trans*- cyclic carbonates were produced (Figure I-11).

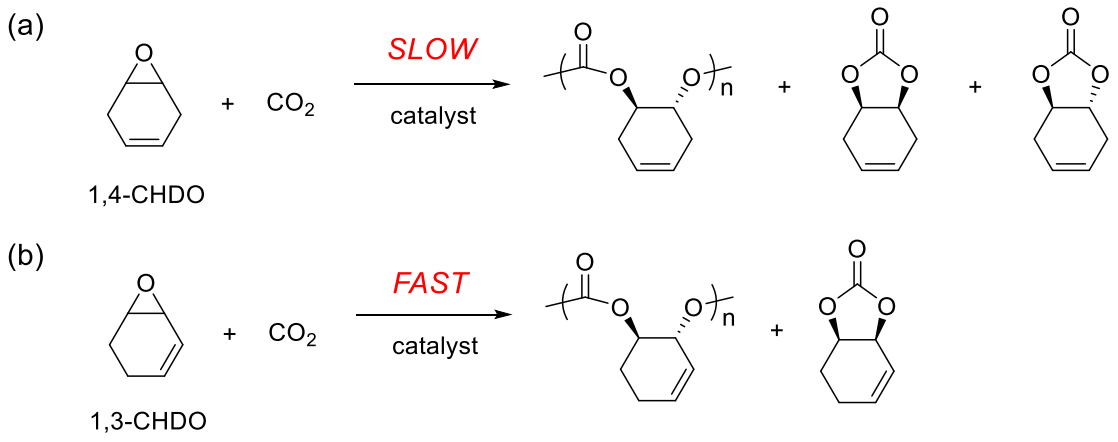

Figure I-11. (a) Copolymerization of 1,4-CHDO with CO_2 to produce polycarbonate and *cis*- and *trans*-cyclic carbonate byproducts. (b) Copolymerization of 1,3-CHDO with CO_2 to yield polycarbonate and *cis*-cyclic carbonate byproduct.

1,3-cyclohexadiene oxide (1,3-CHDO), an isomer of 1,4-CHDO, was also investigated in the copolymerization reaction with CO_2 to produce polycarbonates.[49] Notably, under the same reaction conditions, 1,3-CHDO exhibited a strikingly faster rate in the coupling reaction with CO_2 than its 1,4-analogue. In reactions catalyzed by Cr^{III} catalysts, cyclic carbonate byproducts were observed, but only exiting in the *cis*- form. This is in stark contrast to the copolymerization of 1,4-CHDO and CO_2. A detailed computation study was performed to understand the dramatic behavioral differences between the two epoxide isomers. Poly(1,3-cyclohexadiene carbonate) displayed a T_g of 104-108 °C, about 15 °C lower than its 1,4-copolymer counterpart.

A particularly attractive epoxide for polycarbonate production is *R*-limonene oxide (LO) as it can be readily obtained from a bio-derived precursor (limonene, which is a major component of citrus oils).[50] Catalytic coupling of *R*-LO and CO_2 was first achieved by Coates and co-workers in 2004 using BDI zinc catalysts, affording copolymers with moderate molecular weight (10.8 kg/mol) and high regio- and stereoregularity.[51] Very recently, significant progress has been made in poly(limonene carbonate) (PLC) production. New catalysts based on BDI zinc derivatives[52] and Al amino-triphenolate complexes[53] were developed and showed moderate to high activities towards *R*-LO/CO_2 copolymerization. Notably, Greiner was able to scale up PLC production to kilograms per batch and achieve high molecular weights of >100 kg/mol.[54] Moreover, the thermal, mechanical and gas permeability properties of PLC have been fully analyzed by Reiger and co-workers.[54-55] High M_w PLC exhibits a wide range of attractive properties, *e.g.* high thermal stability, excellent transparency, good hardness

as well as high gas permeability, rendering PLC a promising material for 'breathing glass' applications.[55]

Limonene dioxide (LDO), the diepoxide counterpart of LO, was reported to undergo chemoselective alternating copolymerization with CO_2 in the presence of a BDI Zn catalyst to yield poly(limonene-8,9-oxide carbonate) (PLOC) with epoxy pendant groups.[56] No branching or crosslinking was observed. The resultant polycarbonate PLOC displayed a high T_g of up to 135 °C. In a separate report by Kleij, PLOC was synthesized by epoxidation reaction of PLC.[57]

Lu and co-workers reported the copolymerization of CO_2 with a number of functional epoxides fused with five- or seven-membered rings.[58] For instance, they synthesized a series of meso-3,5-dioxaepoxides and investigated their coupling reactions with CO_2 using chiral catalyst systems based on biphenol-linked dinuclear $Co^{(III)}$ complexes.[58b] For the dimethyl substituted dioxaepoxide, 4,4-dimethyl-3,5,8-trioxabicyclo[5.1.0]octane (CXO), its CO_2 copolymer PCXC was highly isotactic (ee > 99%) and semicrystalline possessing a high T_m of 242 °C. Moreover, PCXC could undergo hydrolysis to generate two pendant hydroxyl groups and was subsequently applied as macroinitiators for lactide ring-opening. Very recently, the same group prepared a completely recyclable polycarbonate based on a N-hetero-epoxide, 1-benzyloxycarbonyl-3,4-epoxy pyrrolidine (BEP).[58c] At 60 °C, BEP was selectively converted to the corresponding polycarbonate using dinuclear chromium complexes coupled with a PPNX (X = NO_3^{-1}, N_3^{-1}) cocatalyst. Upon heating up to 100 °C, the copolymer degraded readily back into the epoxide monomer in quantitative yield.

Remarkably, this copolymerization/depolymerization process could be recycled several times by simply switching the temperature (Scheme I-6).

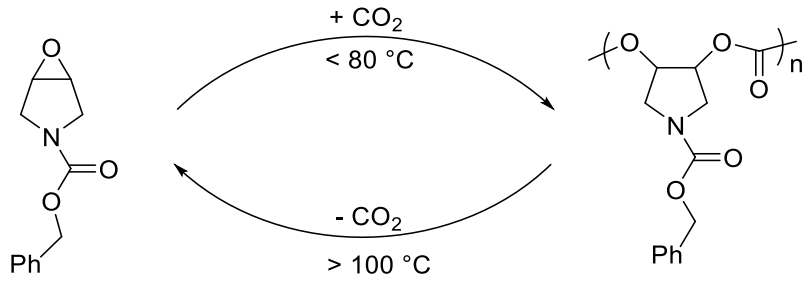

Scheme I-6. Temperature-dependent copolymerization and depolymerization of poly(BEP carbonate).

Postpolymerization Functionalization. Postpolymerization functionalization provides a powerful synthetic tool to access multiple functional polymers through a single scaffold and more importantly allows the introduction of functionalities that are incompatible with the polymerization process. As mentioned earlier, CO_2-derived polycarbonates containing reactive alkyne, alkene, furfuryl and epoxy groups have been prepared by many research groups. These copolymers can be modified *via* postpolymerization functionalization to yield polymers with a wide range of properties.

With advantageous features like high efficiency, little oxygen inhibition, quantitative conversion and absence of side products,[59] thiol-ene click chemistry has been widely employed to anchor new functionalities onto the polymer backbone. For instance, the Darensbourg group functionalized poly(1,2-vinyloxirane carbonate) *via* thiol-ene click chemistry with –OH and –COOH functionalities.[32] As a result, the

hydrophilicity of the polymer was greatly enhanced. Following this work, the same group demonstrated the modification of a block copolymer P(allyl glycidyl ether carbonate)-*b*-PPC-*b*-P(allyl glycidyl ether carbonate) with various thiols to yield amphiphilic polycarbonates with negatively- or positively- charged functionalities.[38a] These amphiphilic polymers were shown to undergo self-assembly to form micelles upon dissolution in deionized (DI) water. To our knowledge, this marked the first time that polymeric nanoparticles have been prepared from CO_2-derived block polycarbonates. Another example of this thiol-ene chemistry is the functionalization of poly(4-vinyl cyclohexene carbonate) to generate pendant hydroxyl groups.[60] Subsequent ring-opening polymerization of ε-caprolactone initiated by the –OH yielded well-defined brush copolymers.

Fully renewable poly(limonene carbonate) (PLC) was also subjected to 'thiol-ene' click chemistry (Scheme I-7), affording polymers with a wide range of properties.[61] Modification of PLC with 2-mercaptoethanol or mercaptoacetic acid greatly enhanced its hydrophilicity; the latter functionality endowed the material with pH-dependent solubility in water. Addition of butyl-3-mercaptopropionate followed by curing transformed the engineering thermoplastic into an elastic rubber, resulting in a decrease in Young's modulus by three orders of magnitude and a T_g drop by 125 °C. PLC was also treated with 2-(diethylamino)ethantiol and subsequent quaternation with benzyl bromide produced a cationic polymer possessing antibacterial properties. Besides 'thiol-ene' reactions, the double bond of PLC can undergo acid-catalyzed electrophilic addition with OH-end capped polyethylene glycol to enhance its hydrophilicity. However this

reaction was limited to short reaction times and thereby only partial (~18%) conversion of the double bond was achieved.

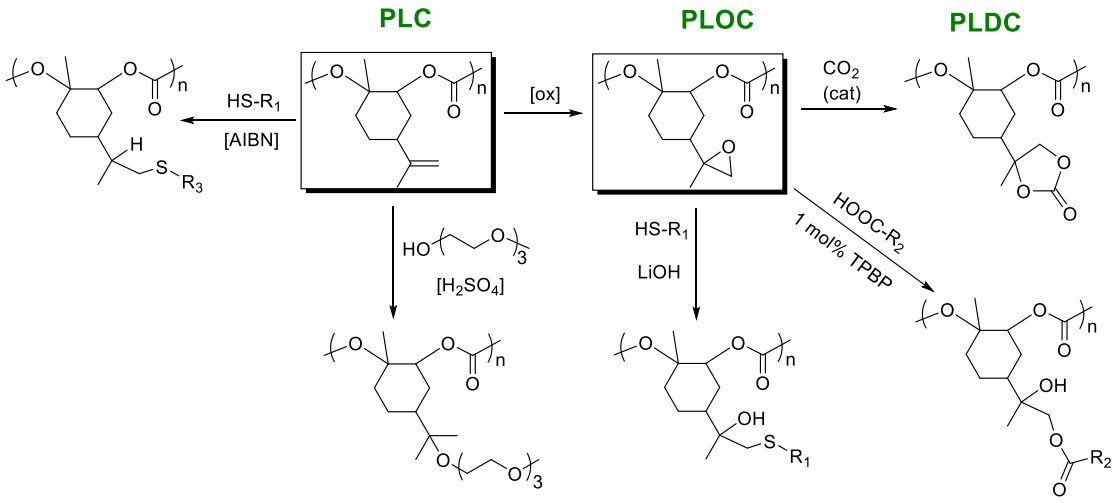

Scheme I-7. Modifications of poly(limonene carbonate) and poly(limonene-8,9-oxide carbonate).

As discussed previously, poly((limonene-8,9-oxide carbonate) (PLOC) carrying epoxide functionalities was synthesized through chemoselective copolymerization of limonene dioxide and CO_2.[56] PLOC can be modified by epoxide ring-opening reactions using various nucleophiles including thiols and carboxylic acids, without causing degradation of the polycarbonate backbone (Scheme I-7). Moreover, the pendant epoxide can undergo CO_2 insertion to produce a poly(limonene)dicarbonate (PLDC) with cyclic carbonate functionalities. T_g values of these resulting PLOC derivatives expand a wide range of 13-146 °C depending on the structure of the anchored functionalities. Remarkably, PLDC (M_n = 11.2 kg/mol) exhibited a high T_g of 146 °C,

very close to that of BPA-based polycarbonates. Alternatively, PLDC was synthesized by a 'two-step' process from PLC by Kleij.[57] The polymer had a higher molecular weight of 15.0 kg/mol and its T_g was reported to be up to an unprecedented 180 °C.

The Frey group prepared propargyl-functionalized poly(carbonate)s through terpolymerization of glycidyl propargyl ether (GPE), glycidyl methyl ether (GME) and CO_2 using a simple zinc-pyrogallol catalyst system.[37] Further functionalization of the polymer was achieved through copper-catalyzed Huisgen 1,3-dipolar cycloaddition reaction between the pendant alkyl groups and benzyl azide.

The Wang group utilized Diels-Alder (DA) reactions to post-modify a furfuryl glycidyl ether (FGE)/CO_2 copolymer (PFGEC).[62] PFGEC tends to cross-link upon exposure to air due to the presence of furfuryl functionalities. Stabilization of the copolymer was achieved by DA reaction between the furfuryl ring and N-phenylmaleimide. Frey and co-workers prepared terpolymers of FGE, GME and CO_2 and later functionalized these terpolymers *via* Diels-Alder chemistry using various maleimide derivatives.[39] Furthermore, this transformation was demonstrated to be reversible.

Terminal Functionalization *via* Addition of Chain Transfer Agents. It is desired to synthesize polycarbonates with multiple hydroxyl end functionalities (PC polyols) as they can be used as building blocks to obtain more complex polymer structures. Typically, the hydroxyl end groups are introduced by addition of chain transfer agents (CATs), such as water,[13b, 38a, 63] diols,[13a] dicarboxylic acids[13a, 64] or other

compounds containing -OH or –COOH groups. One of the potential applications of the PC polyols is in the industrial production of polyurethane.

While most CO_2-derived polycarbonate polyols reported are telechelic polymers due to ease of synthesis, it is also of interest to investigate multifunctional branched polymers. To date, several groups have been able to synthesize star-shaped[65] and hyperbranched[66] polycarbonate polyols. These structures possess unique rheological, mechanical and self-assembly properties and exhibit improved solubility due to the large number of functional groups.[67] Very recently, Frey and co-workers employed hyperbranched poly(ethylene oxide) or poly(butylene oxide) polyether polyols as macro CATs in the copolymerization reaction of CO_2 and ethylene oxide or 1,2-butylene oxide.[65b] Multiarm star polymers with high content of hydroxyl end groups were synthesized; their glass transition temperatures and intrinsic viscosities could be tuned in a broad range by varying the ratio of polyether units and polycarbonate units.

Hyperbranched polymers can be synthesized by employing an 'inimer' (initiator-monomer) in the copolymerization reaction.[66] Using this strategy, again the Frey group prepared hyperbranched polycarbonate polyols from terpolymerization of CHO, (4-hydroxymethyl)cyclohexene oxide (HCHO) and CO_2 (Figure I-12).[66b] HCHO is an inimer as it contains a polymerizable epoxy ring and an initiating (through chain transfer) hydroxyl group. Consequently, the incorporation of HCHO in the coupling reactions leads to the branching of the polymer. By varying the ratio of HCHO and CHO, the degree of branching and the number of hydroxyl end groups could be adjusted. Compared to their linear counterpart, the hyperbranched polycarbonates displayed lower

glass transition temperatures and intrinsic viscosities. These multifunctional polycarbonate polyols can be used in rigid polyurethane foam applications.

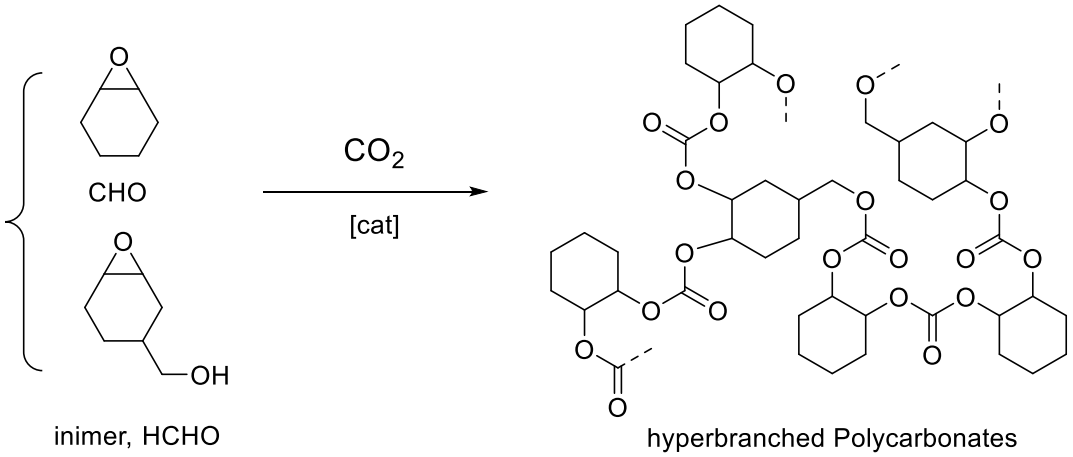

Figure I-12. Synthesis of hyperbranched polycarbonates based on (4-hydroxymethyl)cyclohexene oxide (HCHO), cyclohexene oxide (CHO), and CO_2.

Development of CO_2 Copolymers with Improved Thermal Properties

Most CO_2-based polycarbonates are amorphous, and their low glass transition temperatures have prevented their use in many applications, especially as structural materials. In order to improve the thermal deformation resistance of CO_2-PCs, several synthetic strategies have been employed, including (i) incorporation of bulky and rigid monomers, (ii) controlling the stereochemistry of epoxide enchainment, (iii) construction of terpolymers or block polymers , and (iv) formation of cross-linked networks.

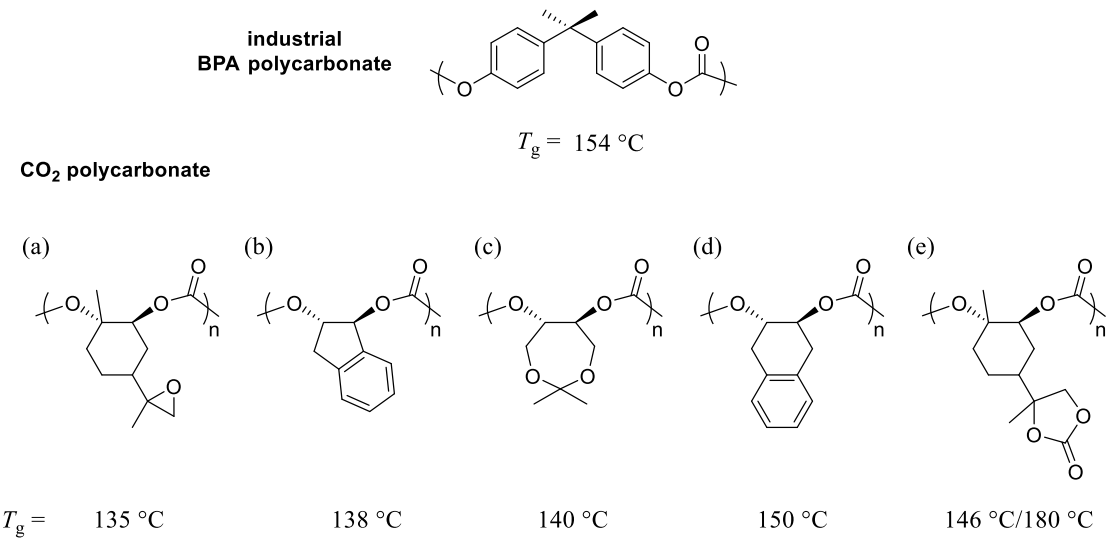

Figure I-13. (a) Poly(limonene-8,9-oxide carbonate) (PLOC), (b) Poly(indene carbonate) (PIO), (c) PCXC, (d) Poly(1,4-dihydronaphthalene carbonate) (PCDC), and (e) Poly(limonene)dicarbonate.

Incorporation of Bulky and Rigid Monomers. The rigidity of the polymer backbone exerts a significant influence on the glass transition temperature of the material. The presence of a bulky rigid moiety along the backbone can hinder segmental mobility of the polymer and therefore increase its T_g. By introducing a bulky epoxide in the copolymerization reaction, it is relatively straightforward to enhance the thermal resistance of the resulting polycarbonate. And thanks to the development of novel transition metal catalysts, several challenging epoxides with bulky structures have been successfully copolymerized with CO_2 to produce polycarbonates (structures see Figure I-13) with T_g values that are comparable to those of industrial BPA polycarbonate.

In a seminal work, Darensbourg and Wilson reported the catalytic coupling of indene oxide (IO) and CO_2 to produce the corresponding poly(indene carbonate) (PIO)

with a T_g of up to 138 °C.[68] This is the first example of incorporating an aromatic group in the backbone of CO_2-based polycarbonates. Both the binary and bifunctional (salen)Co^{III} catalysts were employed for the copolymerization; the latter catalyst exhibited a much higher polymer selectivity under the same reaction conditions. However, the catalytic activity still remained low (TOF = 12 h^{-1}) and only moderate molecular weights (no more than 9700 g/mol) were achieved. Moreover, the asymmetrical nature of IO renders difficulty to further tune the thermal properties by controlling the stereochemistry of the ring-opening process.

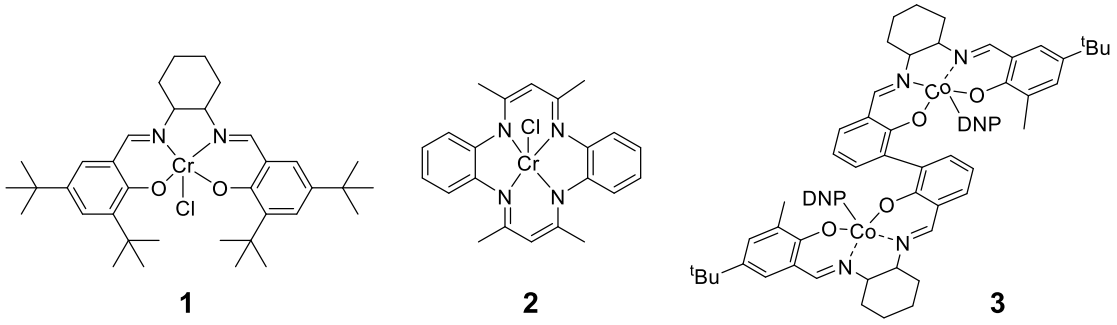

Figure I-14. Catalysts utilized for the copolymerization of 1,4-dihydronaphthalene oxide (CDO) with CO_2: the sterically crowded catalyst (salen)$Cr^{III}Cl$ **1**, tetraazaannulene-derived (tmtaa)$Cr^{III}Cl$ **2**, and biphenol-linked dinuclear (salen)$Co^{III}DNP$ **3**.

Later, the same group investigated the copolymerization reaction of 1,4-dihydronaphthalene oxide (CDO) and CO_2 using various Cr^{III} catalysts.[69] It was found that the copolymer formation was highly dependent on the steric environment around the active metal center. Traditional (salen)$Cr^{III}Cl$ (Figure I-14, **1**)/PPNCl system bearing bulky *tert*-butyl groups exhibited a low TOF of 8 h^{-1} at a 0.2% loading and yielded polycarbonate with 78% selectivity. In contrast, when a less sterically demanding tetramethyltetraazaannulene (tmtaa) catalyst, (tmtaa)$Cr^{III}Cl$ (Figure I-14, **2**) was employed for the copolymerization reaction, catalytic activity was increased by two folds and polymer selectivity was increased to ~ 89%. The highest molecular weight that was obtained in this study was 6.7 kg/mol and displayed a T_g of 136 °C. Parallel to this work, Lu and co-workers studied the catalytic coupling of CDO and CO_2 using chiral biphenol-linked dinuclear Co^{III} complexes.[70] At a 0.2% loading, the dinuclear cobalt complex **3** (Figure I-14) coupled with 2 equiv of PPNDNP cocatalyst showed a very high activity of 247 h^{-1}, yielding only the copolymer with ≥98% enantioselectivity at 25 °C. Moreover, high molecular weight of up to 40.7 kg/mol could be achieved. An intramolecular bimetallic synergistic effect was proposed to account for **3**'s excellent catalytic activity, polymer selectivity and enantioselectivity.[23c] High M_W isotactic poly(1,4-dihydronaphthalene carbonate) (PCDC) exhibited a high T_g of 150 °C, which is very close to that of BPA polycarbonate.

Employing an achiral dinuclear (salen)Co^{III} catalyst, the Lu group synthesized atactic PCXC from copolymerization of dioxaepoxide CXO and CO_2. Atactic PCXC, with fused seven membered rings in the backbone structure, displayed a high glass

transition temperature of 140 °C.[58b] When the chiral analogue of the dinuclear cobalt catalyst was used, the resultant polycarbonate is highly isotactic, possessing a semicrystalline structure with a T_m of 242 °C (*vide supra*). This influence of tacticity on the thermal properties of CO_2-based polycarbonates will be discussed later in more detail.

Despite the high thermal stability of PIO, PCDC and PCXC, these polymers are based on petroleum feedstocks, and thus it is of great interest to develop high performance CO_2-based polycarbonates from sustainable natural resources. Notably, poly(limonene-8,9-oxide carbonate) (PLOC), derived from biorenewable limonene dioxide limonene dioxide (LDO), displayed a T_g of up to 135 °C[56] and could be further modified through CO_2 insertion onto to its pendent oxirane to produce a PLDC with an even higher T_g of 146 °C[56] /180 °C[57] (*vide supra*).

Controlling the Stereochemistry of Epoxide Enchainment. The relative stereochemistry of neighboring chiral centers within polymeric chains (also referred to as tacticity) has a significant effect on the physical properties of the material. Considering that stereoselective copolymerization of epoxides and CO_2 has been reviewed in numerous articles,[22, 71] the focus here will be on highlighting recent advances in the field, including stereocomplexed polycarbonate formation, with an emphasis on the improvement of thermal properties.

As alicyclic polycarbonates usually possess relatively high T_gs, much effort has been made to tune their stereoregularity for further improvement of the thermal properties, hoping to match the performance of some commercial engineering plastics.

In this respect, stereoselective copolymerization of CHO and CO_2 has been widely investigated and several chiral catalysts of Zn(II),[72] Co(III)[73] and Al(III)[74] have been developed. Notably, both Lu[72b] and Coates[72a] were able to achieve high enantioselectivity (90-98% ee) and precise molecular weight control for CHO/CO_2 coupling under mild reaction conditions by employing chiral dinuclear (salen)Co^{III} catalysts and C_1-symmetric ZnBDI catalysts, respectively. It was worth noting that the use of chiral dinuclear Co^{III} catalysts predominantly provided polymer products with the same stereochemistry, *i.e.* (*S,S,S,S*)-configured catalysts yielded *S,S*-configured repeating units, whereas chiral ZnBDI complexes afforded polymers with opposite configurations. Unlike atactic PCHC which is an amorphous polymer, highly isotactic PCHC has a semicrystalline structure and its melting point is greatly effected by the ee% of the polymer chain. Interestingly, a systematic thermal analysis performed by Coates showed that T_m of isotactic PCHC increased almost linearly with ee% over the tested tacticity range (78% to >99%).[72a] Highly isotactic PCHC (M_n = 11 KDa, >99% ee) displayed a T_m of 267 °C.

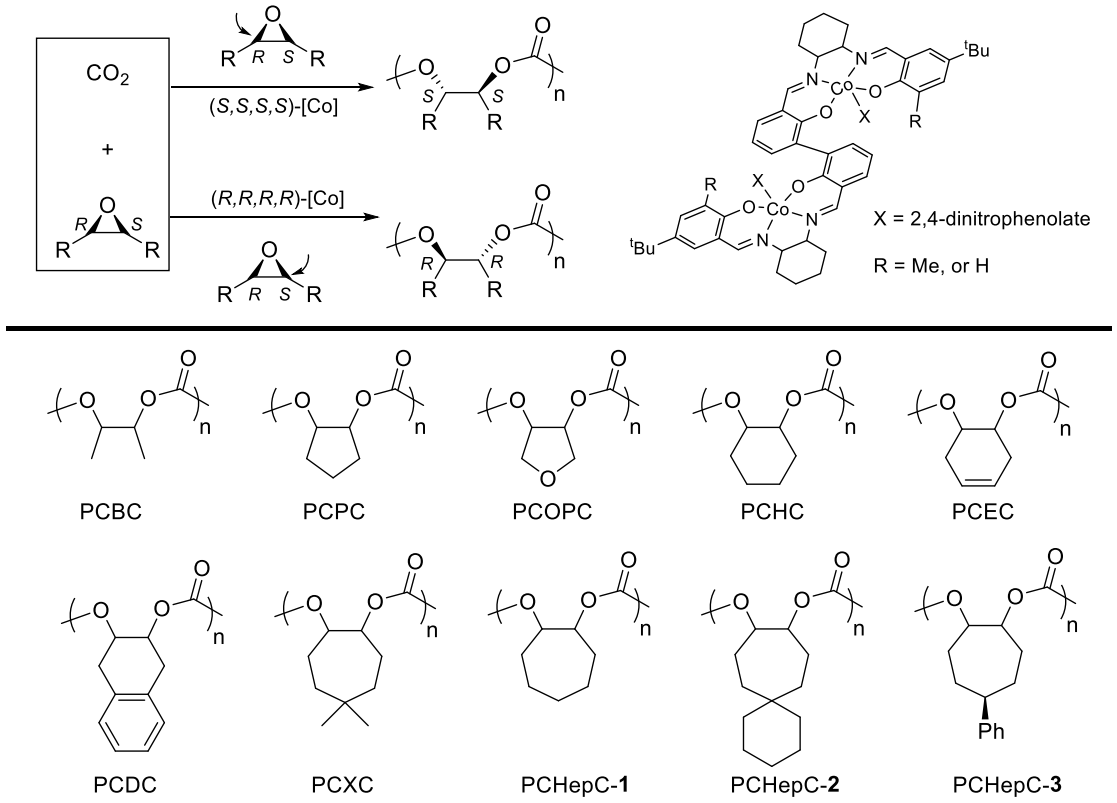

Figure I-15. Enantioselective copolymerization of CO_2 and *meso*-epoxides to enantiopure isotactic polycarbonates.

Following their success with preparing highly isotactic PCHC, Lu and co-workers have synthesized a series of highly enantiopure alicyclic polycarbonates from asymmetric copolymerization of CO_2 and various *meso*-epoxides utilizing the same chiral dinuclear $Co^{(III)}$ complexes (Figure I-15).[58a, 58b, 70, 73b, 75] Both (*R,R*)- and (*S,S*)-polycarbonates were formed from the corresponding chiral catalysts. Among these isotactic polycarbonates, some are semi-crystalline polymers possessing T_ms of 179-271 °C depending on the structure. Now with both (*R,R*)- and (*S,S*)-configured isotactic polycarbonates in hand, the same group investigated the stereocomplexation between

enantiomers of opposite configuration. Various crystalline stereocomplexes have been prepared from both crystalline and amorphous isotactic polymers, resulting in a significant improvement in thermal properties. For instance, the 3,4-epoxytetrahydrofuran (COPO)/CO_2 copolymer (PCOPC) stereocomplex exhibited a T_m of 300 °C, some 30 °C higher than its parent isotactic enantiomer.[75a] Upon mixing equal amounts of amorphous (*S,S*)- and (*R,R*)-PCDC, a crystalline stereocomplex was formed and displayed a very high T_m of 373 °C, the highest T_m yet reported in the field.[70] A summary of the thermal properties of selected isotactic polymers and their corresponding stereocomplexes can be found in Table I-1. Furthermore, the same group demonstrated that amorphous enantiomeric polymers having different chemical structures can cocrystallize to form hetero-stereocomplexes.[70] Wide-angle X-ray diffraction (WAXD) analysis revealed that hetero-stereocomplexes have different crystalline structures from that of the corresponding homo-stereocomplexes.

Coates *et al.* prepared a novel crystalline stereocomplex by mixing equal amounts of isotactic poly(*R*-limonene carbonate) (P*R*LC) and poly(*S*-limonene carbonate) (P*S*LC).[76] P*R*LC and P*S*LC were synthesized from regioselective copolymerization of CO_2 and (*R*)-and (*S*)-limonene oxide, respectively. Both enantiomers were amorphous with a T_g of ~ 120 °C and a decomposition temperature (T_d) of ~ 250 °C. On the other hand, their stereocomplex had a crystalline structure and exhibited a 15 °C increase in decomposition temperature, although its T_g remained the same as the individual enantiomer. T_m of the stereocomplex was not observed in DSC (differential scanning calorimetry) as the polymer started to degrade before reaching the transition. A detailed

structural analysis revealed that the formation of stereocomplex was promoted by the tight interdigitation between alternating P*R*LC and P*S*LC chains and by the dipolar interaction between carbonyl groups.[76-77]

Table I-1. Thermal properties of selected isotactic polycarbonates (Figure I-15) and their stereocomplexes.

	Isotactic PC			Stereocomplex	Ref.
	M_n (kg/mol)[a]	ee (%)	T_g/T_m (°C)	T_m (°C)	
PCBC	39.3	99	73/--[b]	177	75a
PCPC	29.8	99	85/--[b]	199	75a
PCOPC	10.9	99	--[c]/271	300	75a
PCHC	35.6	98	--[c]/272.4	--[f]	73b
PCEC	29.8	99	130/--[b]	314[e]	70
PCDC	24.5	99	150/--[b]	373[e]	70
PCXC	17.5	99	--[c]/242	--[d]	75a
PCHepC-**1**	7.4	92	118/--[c]	--[f]	58b
PCHepC-**2**	12.6	>99	--[c]/179	--[f]	58b
PCHepC-**3**	8.9	--[f]	123/257	--[f]	58b

[a] Reported M_n of (*S*)-polycarbonate. The corresponding (*R*)-polycarbonate has similar M_n. [b] Amorphous polymer. [c] Not detectable. [d] $T_d > T_m$. [e] Measured by fast-scan chip-calorimeter (FSC). [f] Not applicable.

Stereoselective copolymerization of mono-substituted aliphatic epoxides and CO_2 has also been investigated. In this case, formation of highly isotactic polymers requires regioselective ring-opening at the methylene C_β-O bond of the terminal epoxides (Figure I-16). By tuning the chiral and steric environment around the active metal center, high regio- and stereo-selectivity can be achieved. Many research groups

have reported the synthesis of isotactic PPC, by either the enantioselective polymerization of racemic monomers, or the simple regioselective polymerization of enantiopure substrates.[78] The thermal properties of PPC are greatly enhanced by controlling the stereochemistry of the polymer chain. Highly isotactic PPC was reported to have a glass transition temperature of 47 °C, which is 10-12 °C higher than completely atactic PPC.[78h] And a stereogradient PPC prepared by Nozaki *et al.* displayed a much higher decomposition temperature (T_d = 273 °C) than its stereoirregular counterparts (T_d ~ 240 °C).[78e]

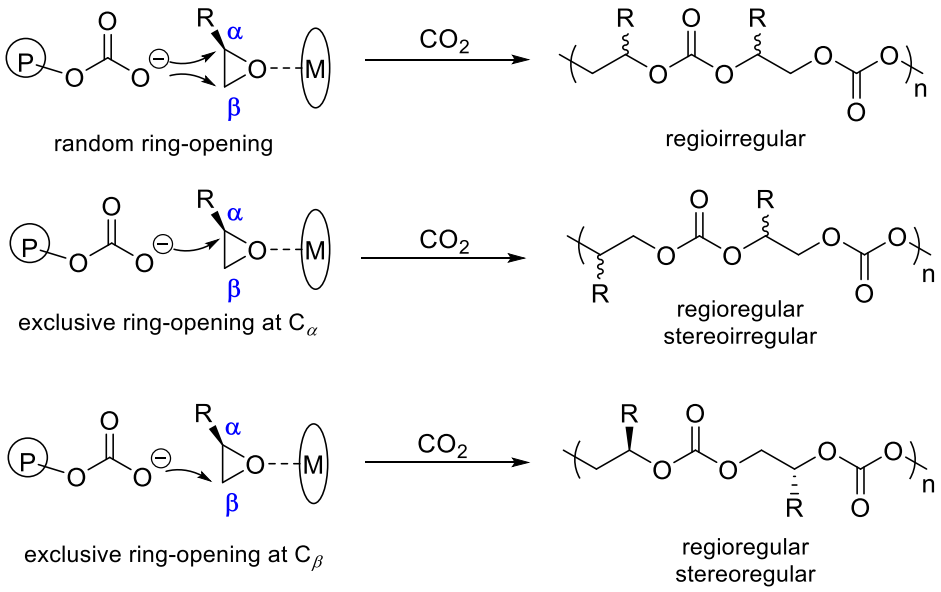

Figure I-16. Stereochemistry involved in the copolymerization of CO_2 and enantiopure mono-substituted aliphatic oxides.

Epoxides with electron withdrawing substituents have also been copolymerized stereoselectively with CO_2.[30a, 79] Wu *et al.* reported the coupling reaction of epichlorohydrin and CO_2 using bifunctional (*S,S*)-(salen)Co^{III} catalysts.[79b] It was found that bulkier substituents on the ligand promoted ring-opening at the least hindered Cβ-O bond. The highest regioselectivity was observed when complex **4** (Figure I-17) bearing an adamantane group and an appended bulky dicyclohexyl ammonium salt was used as the catalyst. When enantiopure (*R*)-epichlorohydrin is utilized in the coupling reaction, **4** predominantly ring-opens at the methylene carbon, allowing for the retention of the stereochemistry at the methine carbon. Isotatic poly(chloropropylene carbonate) (94% ee) is a typical semicrystalline polymer with an improved T_g of 42 °C (T_g = 31 °C for atatctic polymer) and a T_m of 108 °C.

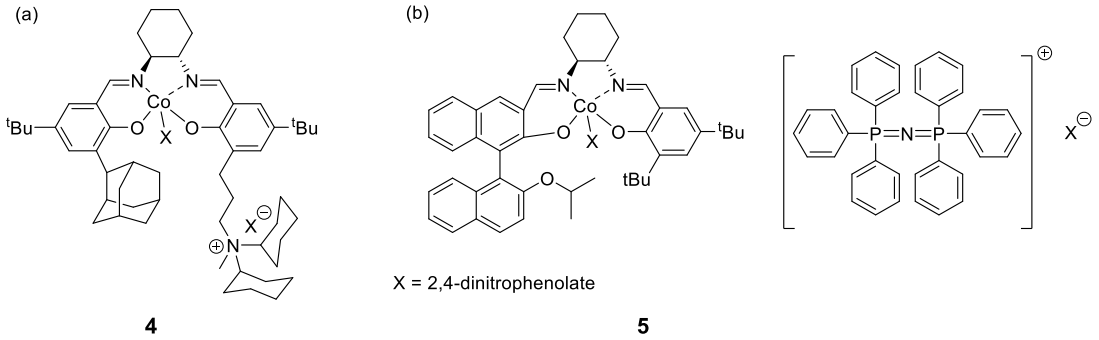

Figure I-17. Catalyst systems utilized in the stereospecific copolymerization of enantiopure terminal epoxides and CO_2.

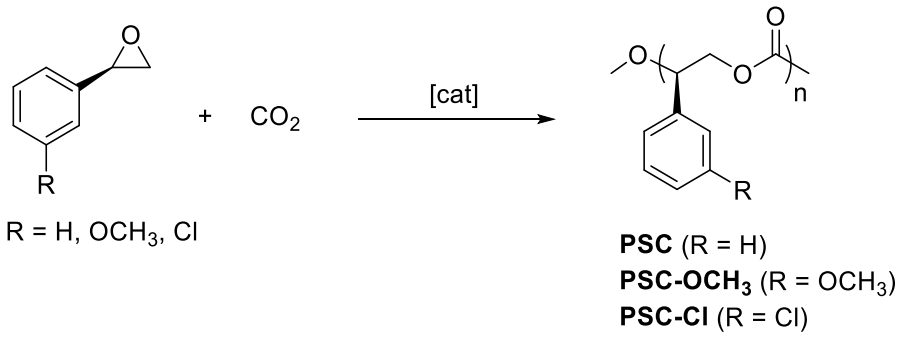

Figure I-18. Regioselective copolymerization of CO_2 and (*R*)-configuration styrene oxide and its derivatives.

Very recently, the Lu group prepared highly stereoregular poly(styrene carbonate) (PSC) and its derivatives from regioselective copolymerization of (*R*)-configured epoxides and CO_2 using a multichiral (*S,S,S*)-(salen)Co(III) complex **5** (Figure I-17) coupled with a PPNX (X = DNP) cocatalyst.[79a] Ring-opening predominantly occurred at the methine carbon to afford (*R*)-configured polycarbonates (Figure I-18). Similarly, (*S*)-configured polymer were synthesized from regioregular coupling of (*S*)-epoxides and CO_2 with the (*R,R,R*)-(salen)Co(III) catalyst system. Highly isotactic poly(styrene carbonate) and PSC-OCH_3 are typical semicrytalline polymers with T_ms of 137.3 and 90 °C, respectively. On the contrary, isotactic polymer PSC-Cl is amorphous possessing a T_g of 83.8 °C. Interestingly, 1:1 mixture of (*R*)-PSC and (*S*)-PSC can cocrystallize to form a stereocomplex with an enhanced T_m of 164.1°C, about 27 °C higher than its parent enantiomers. A crystalline stereocomplex with a T_m of 147.3 °C was also formed after mixing amorphous (*R*)-PSC-Cl and (*S*)-PSC-Cl in equal mass. Of importance, these are the first examples of stereocomplex formation that

is based on terminal epoxides/CO_2 copolymers. Attempt to cocrystallize PSC-OCH_3 of different configurations was not successful.

Construction of Terpolymers or Block Polymers. Modification of thermal properties can be achieved by combining different monomers to form either random (statistical) copolymers or block copolymers. Generally, a random copolymer displays only one glass transition temperature that falls between the T_g values of each homopolymer and is dictated by the fraction of each component. One the other hand, a block copolymer can display one T_g or two distinctive T_gs depending on the compatibility between different blocks. Various catalysts and synthetic strategies have been developed to prepare these two types of copolymers with enhanced thermal properties.

As discussed previously, PPC has good mechanical properties but its application as structural materials has been marred by a low T_g of 35-45 °C. To address this problem, there has been a lot of interest in the terpolymerization of PO, CHO and CO_2. In 2006, the Lu group reported the synthesis of random PO/CHO/CO_2 terpolymers utilizing a (salen)Co^{III} catalyst system.[73c] With about 40 mol% of PCHC, the terpolymer exhibited a single T_g of 68.8 °C. (Note that a block polymer PPC-*b*-PCHC prepared by the Darensbourg group exhibited two T_gs.[20c]) The T_g value could be adjusted between 50 and 100 °C by controlling the molar fraction of PCHC. Although PO/CO_2 copolymerization occurred much faster (~ 6 times) than CHO/CO_2 coupling under the same conditions, a matched reactivity for the two epoxides was observed during the terpolymerization reaction. This was attributed to a balanced coordination ability and ring-opening reactivity of the two epoxides, *i.e.* CHO has a stronger coordination ability but its ring-

opening rate is slow, PO the opposite. Later the same group utilized a bifunctional (salen)Co^{III} catalyst bearing a quaternary ammonium arm for the PO/CHO/CO_2 terpolymerization reaction.[24e] This catalyst exhibited a high reactivity (TOF = 3590 h^{-1}) and polymer selectivity at 90 °C and provided high molecular weight terpolymers. The Lee group also investigated the terpolymerization of PO, CHO and CO_2 using a (salen)Co catalysts tethered by four quaternary ammonium salts.[80] Reactivity ratio of PO and CHO was studied using Fineman-Ross analysis to reveal that the terpolymer had a tapered structure. Nevertheless, only one T_g was observed for the terpolymer.

Terpolymerization of PO, 1,3-cyclohexadiene oxide (1,3-CHDO) and CO_2 has been investigated by Darensbourg and Chung.[49] Fineman-Ross kinetic analysis revealed a matched reactivity between the two epoxides. The resultant polymer with about 20% 1,3-cyclohexadiene carbonate units displayed a T_g of 68.9 °C, approximately midway between the T_gs of the respective copolymers. An attempt to incorporate 1,4-CHDO into PPC failed due to the much lower copolymerization activity of 1,4-CHDO than PO.

Liu and co-workers studied the terpolymerization of PO, 4-vinyl cyclohexene oxide (VCHO) and CO_2 using a bifunctional salcy$Co^{III}NO_3$ complex.[81] It was found that the feed ratio of VCHO had a great effect on both the catalytic activity and polycarbonate selectivity. A PO/VCHO/CO_2 terpolymer with 27% vinyl cyclohexene carbonate (VCHC) units displayed a T_g of 56 °C, about 20 °C higher than that of PPC. Moreover, the thermal properties of the terpolymer can be further improved by transforming the pendant alkene groups into epoxide or cyclic carbonate functionalities.

Block copolymers have also been prepared to modify the thermal properties of PPC. Darensbourg and Wu reported the one-pot synthesis of novel poly(lactide-*b*-propylene carbonate-*b*-lactide) triblock copolymers.[63b] Copolymerization of PO and CO_2 was carried out in the presence of water utilizing a binary (salen)CoTFA/PPNTFA (TFA = trifluoroacetate) system to generate PPC polyol intermediate. PPC diols were subsequently used as macroinitiators for 1,8-diazabicyclo[5.4.0]undec-7-ene (DBU)-catalyzed ring-opening polymerization of *D*-lactide (LA). The resulting block polymers exhibited a much higher thermal resistance ($T_g \approx 45$ °C, $T_m > 110$ °C) than the parent PPC diols.

Formation of Cross-linked Network. Another effective way to increase the thermal stability of polymers is to form cross-linked networks (thermosets) by interconnecting polymer chains *via* covalent bonds or ionic bonds. Other properties such as mechanical strength and chemical resistance can also be improved through crosslinking. As discussed before, a wide range of epoxides have been coupled with CO_2 to produce polycarbonate bearing different side chain groups, such as hydroxyls, carboxylic acids, alkynes, alkenes and epoxies. These pendant functionalities have been exploited through a variety of chemical reactions to form cross-linked polycarbonate networks.

In an interesting study, Coates reported the transformation of linear polycarbonates with pendant vinyl groups into organic nanoparticles through intramolecular olefin cross-metathesis reactions.[82] At 76% cross-linking, the T_g of the particles increased to 194 °C from an initial value of 114 °C. In 2015, the Frey group

utilized well-established Diels-Alder reactions to transform polycarbonates bearing pendent furfuryl groups into a cross-linked gel.[39] The cured samples exhibited much high T_gs (~50 °C) than their linear counterparts (T_gs are below 0 °C). Furthermore, this cycloaddition transformation was shown to be fully reversible and offers promise for the development of self-healing materials.

'Thiol-ene' click chemistry has been widely employed to prepare cross-linked materials by connecting the olefin groups present in the polycarbonate chains. Pescarmona *et al*. reported the curing of poly(vinylcyclohexene carbonate) with 1,3-propanedithiol.[83] The resultant crosslinked polymer exhibited a substantial increase in T_g from 75 °C to 130 °C. The group of Darensbourg prepared crosslinked polycarbonate films using various ratios of a tetrafunctional thiol linker.[38b] The films exhibited an increase in T_g with increasing cross-linking densities.

Recent efforts have been focused on developing new cross-linked materials derived from renewable feedstocks. In this context, both Kleij[84] and Koning[85] have utilized 'thiol-ene' chemistry to prepare thermoset materials based on poly(limonene carbonate). Kleij and co-workers prepared a series of LO/CHO/CO_2 terpolymers with a variable ratio of limonene carbonate units.[84] The terpolymers were cured with a stoichiometric amount of a dithiol reagent under concentrated conditions to obtain cross-linked materials with improved thermal properties. Compared to the parent terpolymers, the decomposition temperatures of these cross-linked polycarbonates are increased by 15-77 °C and the glass transition temperatures by 19-54 °C. The Koning group synthesized low M_W poly(limonene carbonate)s and subsequently cured them with a

trifunctional thiol reagent.[85] A detailed kinetic study by ATR-IR was performed to investigate the effects of different variables, *i.e.* polymer molecular weight, ene/thiol stoichiometry and curing temperatures, on the extent of network formation. The resultant thermosets exhibited high T_gs of >100 °C and good homogeneity. The PLC/thiol system was also evaluated for coating applications, showing promising properties such as high transparency, good acetone resistance and high pencil hardness.

Besides the aforementioned methods, other types of chemical reactions have also been employed to form cross-linked polycarbonate networks, including free radical coupling,[86] thiol-epoxy addition,[56] hydrolysis and polycondensation of alkoxy silane,[45] isocyanate-hydroxy reaction[87] as well as ring opening of aziridine with carboxylic acids.[40]

Scope of the Dissertation

As described in this chapter, a lot of research efforts have been directed towards the development of more diverse CO_2-PCs with different functionalities. In this regard, we have been particularly interested in designing functional CO_2-PCs towards biomedical applications. In Chapter II, a diverse variety of amphiphilic triblock CO_2 copolymers were prepared from a sequential copolymerization and chemical transformation strategy. These triblock polymers further assembled into a family of nanostructures with various functionalities and surface charges. In Chapter III, we designed and prepared a novel polycarbonate structure carrying carboxylic acid pendant groups. This polymer was further modified to construct polymer-drug conjugates. Due

to their aliphatic nature, most commonly studied CO_2-PCs have relatively low glass transition temperatures, making them unsuitable for structural material applications. To overcome this limitation, we employed cross-linking to improve the thermal mechanical properties of CO_2-derived polycarbonates, as discussed in Chapter IV.

CHAPTER II

CONSTRUCTION OF VERSATILE AND FUNCTIONAL NANOSTRUCTURES DERIVED FROM CO_2-BASED POLYCARBONATES*

Introduction

Using the abundant, nontoxic and inexpensive CO_2 as a renewable C1 feedstock, the coupling of CO_2 and epoxides provides an attractive method for preparing polycarbonates. This environmentally more benign approach for polycarbonates synthesis has attracted a lot of attention in both academic and industrial research.[22, 71b, 71d, 71e, 88] With the recent development of catalytic systems, both heterogeneous and homogeneous, CO_2/epoxides coupling has been commercialized by many companies throughout the world.[25-28] A new trend on CO_2-based polycarbonates is the production of poly(propylene carbonate) diols which can undergo condensation reaction with diisocyanates to afford polyurethane. Nevertheless, the hydrophobic nature and lack of functionalities of the commonly studied CO_2-based polycarbonate have prevented their use in functional materials, especially for biomedical applications.

In order to expand the use of CO_2-based polycarbonates towards improved material performances, it is necessary to synthesize more diverse CO_2-based polymers with functionalities. There are a few reports on the development of functional aliphatic polycarbonates from CO_2 containing hydroxy,[40-41, 89] furfuryl,[62, 90] and oligoethylene

* Portions reprinted (adapted) with permission from "Construction of Versatile and Functional Nanostructures Derived from CO_2-based Polycarbonates." Wang, Y.; Fan, J.; Darensbourg, D. J. *Angew. Chem. Int. Ed.*, **2015**, *54*, 10206-10210. Copyright 2015 WILEY-VCH.

glycol (OEG) [43-44] groups. In these examples, preparation of monomers is usually required and only one type of functional group can be prepared at a time. More importantly, restrained by the reactivity of catalysts available, the type of functionality is usually limited by direct coupling of functional monomers and CO_2. An alternative methodology is to incorporate orthogonal, 'click' chemistry into the material design. We and others have employed 'thiol-ene' click reactions to successfully anchor various functionalities onto polycarbonates with a vinyl pendant group.[32, 49, 60-61]

In the last few decades, amphiphilic block polymers have been extensively studied due to their potential applications in material science and biomedicine. Owing to their unique biodegradability and biocompatibility, aliphatic polycarbonates have received considerable attention in the construction of amphiphilic polymers. To date, most of the amphiphilic block polymers consisting of polycarbonates are based on the ring-opening polymerization of functional six-membered cyclic carbonate monomers.[4b, 91] Generally, polyethylene glycol is used as a macroinitiator and is the hydrophilic component in the resulting block polymers. To the best of our knowledge, amphiphilic polymers with hydrophobic and hydrophilic components both derived from CO_2-based polycarbonates have not been reported. Compared to the ring-opening polymerization, this alternative route from directive CO_2/epoxides copolymerization eliminates the need for the separate preparation of cyclic carbonate. In this chapter, we demonstrate the facile preparation of CO_2-based amphiphilic block polycarbonates by a sequential copolymerization and chemical transformation strategy. The obtained amphiphilic polymers were demonstrated to undergo self-assembly in dionized (DI) water to form

well-dispersed nanoparticles, providing the first examples of constructing functional nanostructures from CO_2-based polycarbonates.

Results and Discussion

Amphiphilic block copolymers are macromolecules that have covalently connected hydrophilic and hydrophobic components. These block polymers can form a variety of supramolecular structures in aqueous solution and have shown great potential in biomedical applications, such as diagnostic imaging and drug delivery.[92] Since the polycarbonate backbone is known to be highly hydrophobic, one key challenge in synthesizing amphiphilic polycarbonates is to identifiy a monomer for the production of a hydrophilic chain segment. A strategy which can be employed to overcome the hydrophobic nature of the polycarbonate backbone is the introduction of water-soluble functional groups by postpolymerization modification. In our previous report, we demonstrated that water soluble CO_2-based polycarbonates can be produced employing thiol-ene click chemistry in the postpolymerization functionalization of CO_2/2-vinyloxirane copolymers.[32] However, polymerization of 2-vinyloxirane and CO_2 requires the use of a bifunctional catalyst (catalyst **7**, Figure II-1) in order to achieve high polymer selectivity. The synthesis of catalyst **7** is quite tedious with low overall yields. From a practical view, we choose another epoxide, allyl glycidyl ether (AGE), which can couple with CO_2 using easily accessible catalyst **6** (Figure II-1). The AGE/CO_2 copolymer can be modified to install hydrophilic moieties to the polymer backbone. Related chemistry has been utilized in AGE based polyethers.[93]

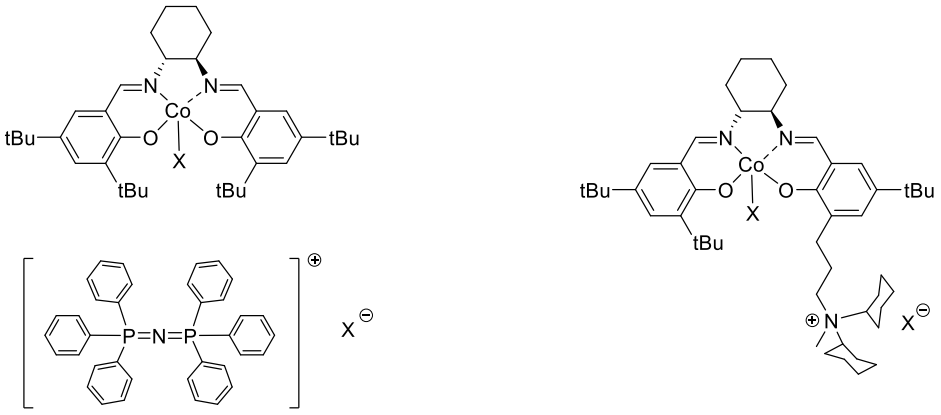

Figure II-1. Catalyst systems utilized in the copolymerization of epoxides and CO_2. X = Cl^{-1}, N_3^{-1}, trifluoroacetate (TFA), 2,4-dinitrophenolate (DNP), etc.

Due to the living nature[20c, 24a, 46] of the coupling reaction of epoxides/CO_2 catalyzed by (salen)Co system, we hypothesized that block polymers can be synthesized by a 'two step, one-pot' strategy by adding different monomers sequentially. For polymerization of epoxides and CO_2 catalyzed by the (salen)CoX/PPNX (X^- = Cl^-, AcO^-, Br^-, 2,4-dinitrophenolate, etc) binary catalyst system, it is inevitable for chain-transfer reaction to occur due to trace water impurity.[94] Thus, the coupling of epoxides and CO_2 gives polymers with differing end groups, OH-PC-OH and OH-PC-X. Upon addition of the second epoxide, an undesired mixture of both ABA and AB block polymers will be produced. To circumvent this problem, a certain amount of water is intentionally added into the system. The resulting hydroxy end-capped polymers can serve as macroinitiators in the subsequent copolymerization reaction.[13a, 95] A (salen)CoTFA[63b]/PPNTFA (TFA = trifluoroacetate) catalyst system will be employed due to the fact that trifluoroacetate can undergo hydrolysis more easily and rapidly than other end-groups.[13b, 63]

The overall synthetic route for amphiphilic CO_2-based polycarbonate is shown in Figure II-2. Two epoxides are employed in the sequential polymerization reaction, one is propylene oxide (PO) that leads to the hydrophobic segment, the other is allyl glycidyl ether that carries an alkene functionality for copolymerization followed by modification to the hydrophilic blocks.

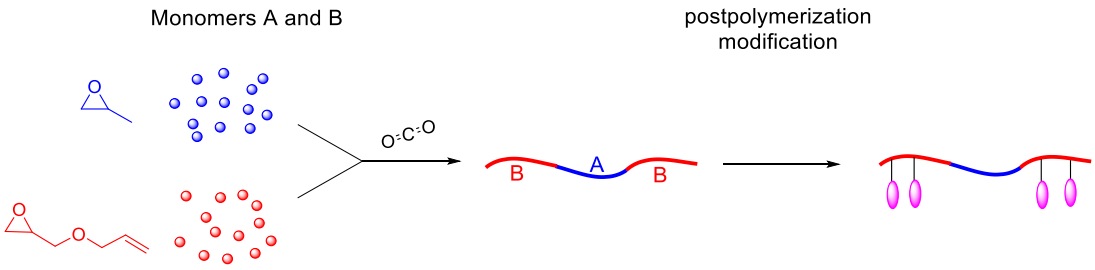

Figure II-2. Schematic presentation of synthesis of CO_2-based amphiphilic polycarbonates.

One-Pot Sequential Ring-Opening Copolymerization. To prepare the triblock polycarbonate, we first examined the copolymerization of PO and CO_2 using catalyst **6** (X = trifluoroacetate; 0.1 mol% loading) in the presence of 20 equiv. of water (to the catalyst). The polymerization reaction was carried out at ambient temperature for 48 hours to ensure the complete conversion of PO in order to minimize tapering when the second monomer (AGE) is added. Consistent with the result we reported before where a lager catalyst loading was used,[63b] the resulting polymer shows an extremely narrow polydispersity index (PDI; 1.01) in gel permeation chromatography (GPC) and the MALDI-TOF mass spectrometry showed only one series of signals assigned to two hydroxy end groups (Figure II-3). The result indicates that water not only acts as a chain-

transfer agent to protonate the anion of the growing polymer chain but also completely hydrolyzes the initiating trifluoroacetate groups at the chain end.[13b, 63]

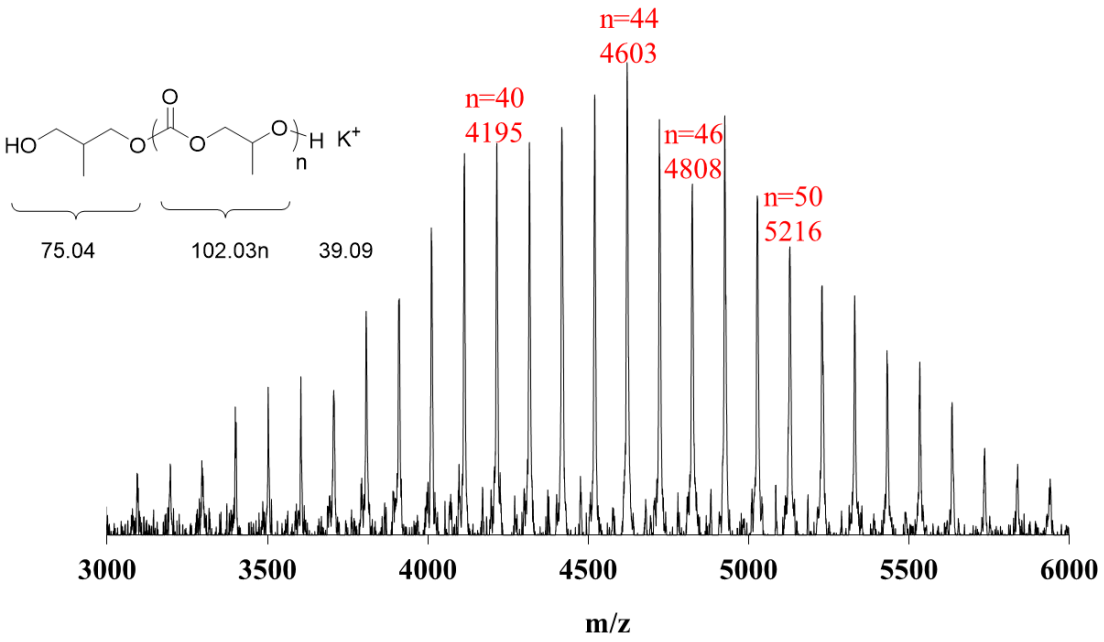

Figure II-3. MALDI-TOF mass spectrum of poly(propylene carbonate) end-capped with –OH groups. The polymer was obtained from propylene oxide/CO_2 copolymerization with 20 equiv. water under catalyst 1/PPNX (X = trifluoroacetate), 48h, 2.5 MPa CO_2.

Subsequently, after careful release of CO_2, various amounts of AGE were added into the reactor followed by recharging with CO_2. Triblock polycarbonates with different molecular weight and composition were produced (Table II-1). The GPC traces of the resultant copolymers were shown in Figure II-4, which shows an increase in the copolymer's molecular weight with an increase in AGE loading. The fact that the measured M_W is close to the theoretical values together with the really narrow PDI of these triblock copolymers confirm that the reaction system maintained its living character during the course of chain extension. Differential scanning calorimetry (DSC) measurements revealed decreasing T_g (glass transition temperature) values with a larger poly(allyl glycidyl ether carbonate) (PAGEC) ratio. This is attributed to the long flexible pendant group of the PAGEC blocks.

Table II-1. Results from "two-step, one-pot" strategy to prepare ABA triblock polycarbonate. m/n is the molar ratio of allylglycidylether carbonate units to propylene carbonate units.

	$MW_{in\ theory}$ (g/mol)	**MW_{GPC}[(b)] (g/mol)**	**PDI[(b)]**	**T_g[(c)] (°C)**
PPC diol	–	4600	1.01	23
m/n=1/2	8100	7000	1.01	7
m/n=2/3	9300	8100	1.01	4
m/n=1/1	11700	10300	1.01	-1

(*a*) See the Experimental section for the exact procefure. (*b*) Determined by GPC. PDI = M_w/M_n. (*c*) Determined by DSC.

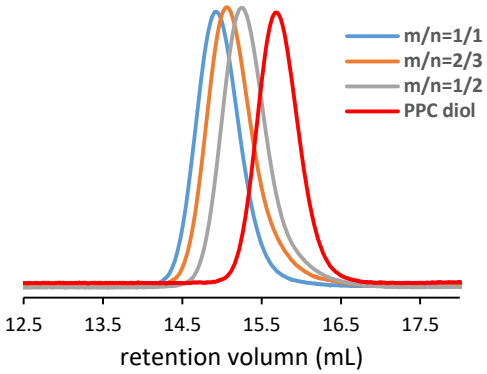

Figure II-4. GPC traces of triblock polycarbonates with different composition (table II-1).

Functionalization by Thiol-Ene Reactions. The functionalization of PAGEC-*b*-PPC-*b*-PAGEC (m/n=1) triblock polycarbonates was achieved by radical mediated thiol-ene click reaction with various thiols including mercaptoacetic acid, 2-(Boc-amino)ethanethiol and boc-*L*-cysteine, to give polymers **P1**, **P2**, and **P3**, respectively (Scheme II-1). In order to avoid possible chain-chain coupling reactions, 20 equivalents of thiols to alkene groups were used in the thiol-ene reaction under UV irradiation with dimethoxy-2-phenylacetophenone (DMPA) as a photoinitiator. The resulting polymers were readily purified and their structures were confirmed. The disappearance of the terminal alkene protons in the ^{1}H NMR spectra of the three resulting polymers confirmed the complete conversion of the alkene groups. GPC analysis of each of these polymers shows a really narrow single peak without any tailing at the high molecular weight portion, confirming the successful suppression of crosslinking side reactions.

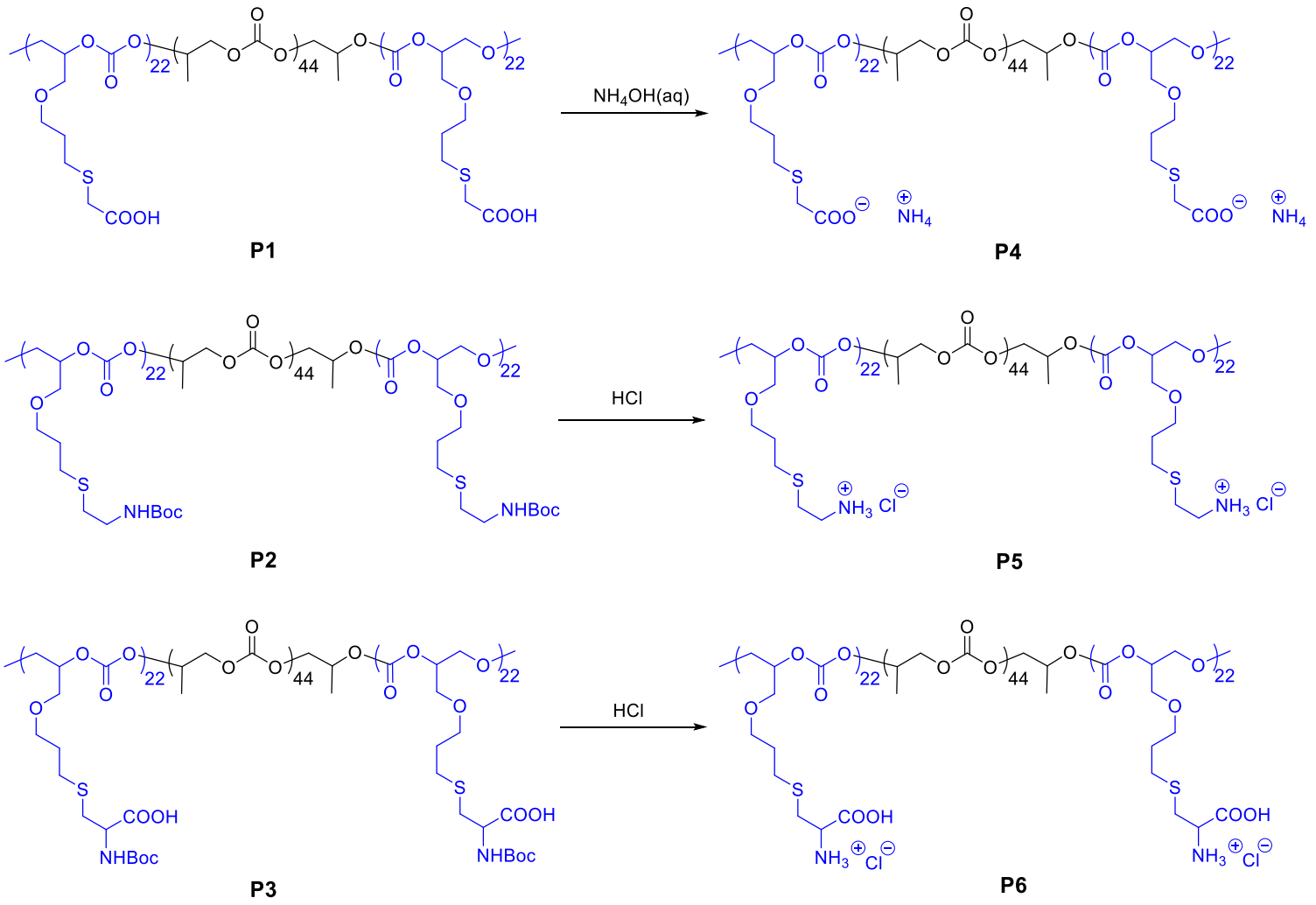

Scheme II-1. Synthesis of amphiphilic block polycarbonates with different charges. Boc = *tert*-butoxycarbonyl.

In order to provide high hydrophilicity of the end blocks, the deprotonation of the pendant carboxylic acid of polymer **P1** and the Boc deprotection of polymer **P2**/**P3** were conducted in THF, giving the corresponding negatively-charged **P4** and positively-charged **P5**/**P6** triblock amphiphilic polycarbonates.

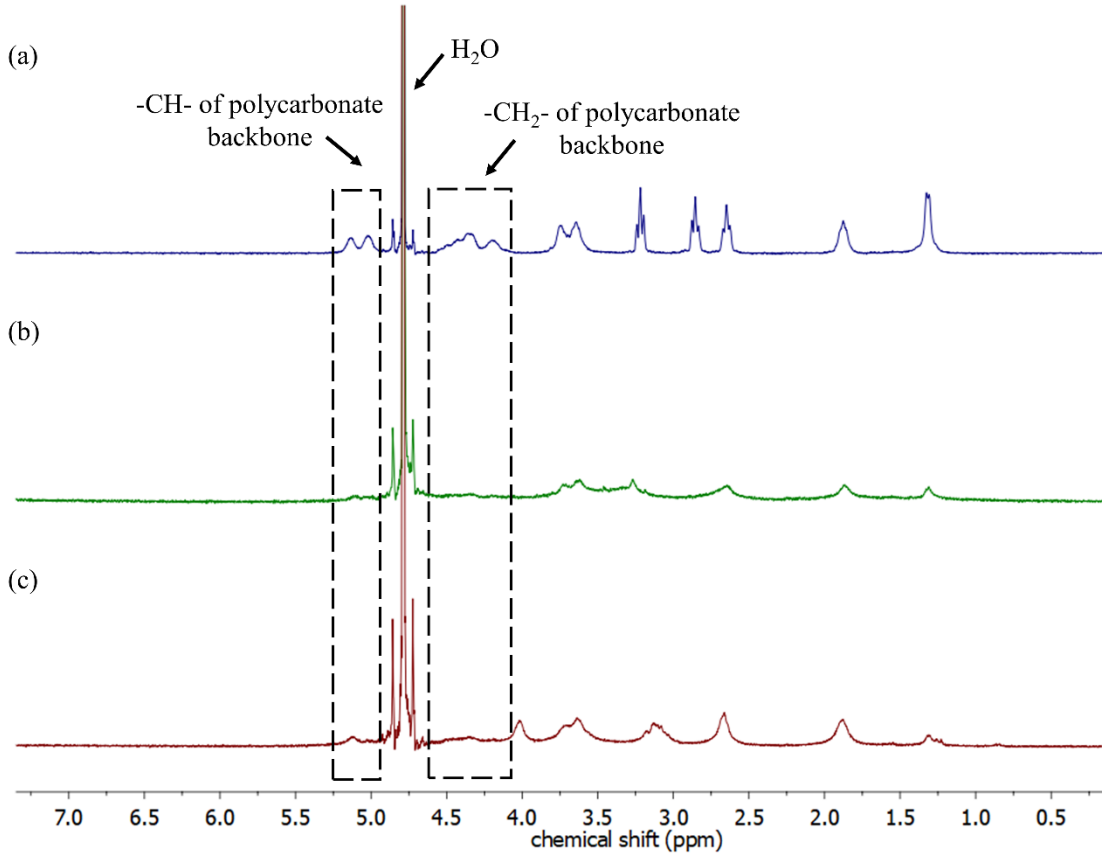

Figure II-5. ^{1}H NMR spectra of amphiphilic triblock polycarbonates (a) cationic polymer **P4**, (b) anionic polymer **P5** and (c) cationic polymer **P6** in D_2O.

Self-Assembly of Amphiphilic Polycarbonates. All three amphiphilic polycarbonates were dissolved in DI water by sonication for 10 min at room temperature.

The morphology of the resulting nanostructures were characterized by dynamic light scattering (DLS) and transmission electron microscopy (TEM). DLS analysis shows no hydrodynamic diameter distribution for the aqueous solution of polymer **P5**, consistent with its ^{1}H NMR spectrum in D_2O in which the proton signal from the hydrophobic PPC was only slightly shielded (Figure II-5, a). This result indicates that no shell-core structure was formed. In contrast, the DLS studies of anionic block polymer **P4** and cationic polymer **P6** showed that they underwent assembly to form nanoparticles with high uniformity, giving a similar intensity-averaged hydrodynamic diameters of 26±15 nm (Figure II-6, a and b). The formation of micelles can also be confirmed by ^{1}H NMR spectra of polymers **P4** and **P6** in D_2O (Figure II-5, b and c). TEM images revealed that the morphologies of both nanoparticles formed by **P4** and **P6** are spherical (Figure II-6, c and d). The surface charge densities of the resulting nanoparticles in DI water were characterized by zeta potential analysis. Zeta potential values of -59 mV for polymer **P4** and +28 mV for polymer **P6** indicated the anionic and cationic surface characteristics of these nanoparticles. It is noted that an attempt to make zwitterionic triblock polycarbonate by removal of HCl from polymer **P6** resulted in a non-soluble polymer, even in highly polar solvents as DMSO (dimethyl sulfoxide) and DMF (dimethylformamide). This is due to the strong interchain charge interaction between $-COO^-$ and $-NH_3^+$ which is unbreakable through solvation. Both polymers **P4** and **P6** displayed a similar critical micelle concentration (CMC) of 66 μg/mL in DI water, determined by pyrene fluorescence measurements at room temperature.

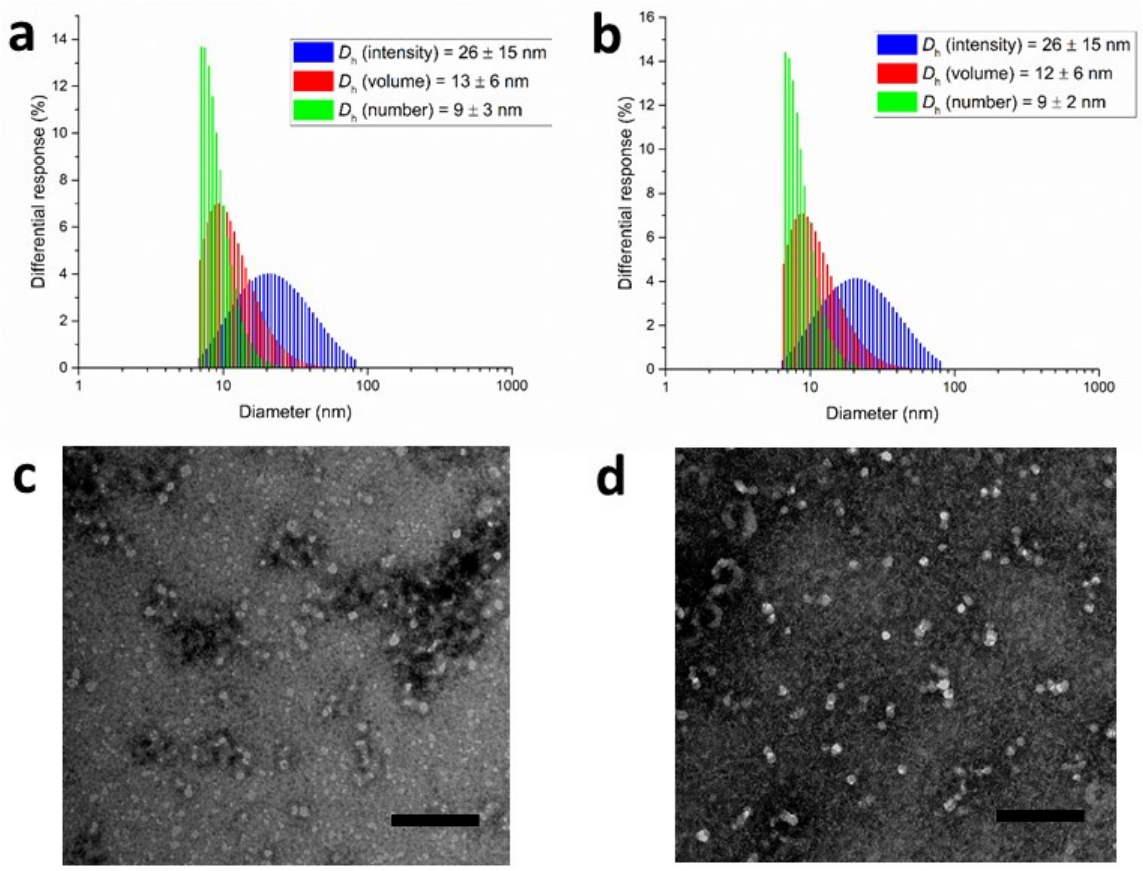

Figure II-6. (a) DLS results of anionic nanoparticles **P4**: D_h (intensity) = 26 ± 15 nm, D_h (volumn) = 13 ± 6 nm, D_h (number) = 9 ± 3 nm. (b) DLS results of cationic nanoparticles **P6**: D_h (intensity) = 26 ± 15 nm, D_h (volumn) = 12 ± 6 nm, D_h (number) = 9 ± 2 nm. TEM images for anionic (c) and cationic (d) nanoparticles. The scale bars in both TEM images are 100 nm.

Conclusions

Herein, we have demonstrated the facile construction of CO_2-based versatile and functional amphiphilic polymer with negatively and positively charged functionalities from a sequential copolymerization and chemical transformation strategy. By the judicious use of water as a chain-transfer reagent, well-defined ABA triblock polycarbonates were prepared by a "two-step, one-pot" strategy. The living nature of the

(salen)CoX catalyst systems for epoxides/CO_2 coupling enabled the preparation of multiblock polymers with precise control of block chain lengths. Furthermore, the clickable alkene groups were then modified to install different functionalities and charges onto the polymer backbones, yielding amphiphilic CO_2-based polycarbonates. This emerging class of polycarbonates derived from CO_2 could provide a powerful platform for biomedical applications.

Experimental

Materials and Methods. All manipulations involving air- or/and moisture-sensitive compounds were carried out in a glovebox or with standard Schlenk technique under an Argon (Ar) atmosphere. Allyl glycidyl ether (97%, Alfa) and propylene oxide (98%, Alfa) were distilled over CaH_2 prior to use. 2-aminoethanethiol and dimethoxy-2-phenylacetophenone (DMPA) were purchased from TCI. *L*-cysteine hydrochloride anhydrous and mercaptoacetic acid were acquired from Amresco and Alfa Aesar, respectively. Di-*tert*-butyl dicarbonate was purchased from Chem Impex Int'l Inc. Tetrahydrofuran (THF), dichloromethane (DCM), and toluene were purified using an MBraun manual solvent purification system packed with Alcoa F200 activated alumina desiccant. Bone-dry carbon dioxide supplied in a high-pressure cylinder and equipped with a liquid dip tube was purchased from Scott Specialty Gases.

Characterization Techniques. ^{1}H NMR spectra were recorded on a Mercury 300 MHz spectrometer. The peak frequencies were referenced versus an internal standard (TMS) shifts at 0 ppm.

Molecular weight determinations were performed with a Malvern modular GPC apparatus equipped with ViscoGEL I-series columns (H&L) using THF as eluent. Polystyrene standards were used to calibrate the system. The absolute molecular weight and distribution of polycarbonates was determined by size-exclusion chromatography coupled with Refractive Index (RI), Right Angel Light Scattering (RALS) and Low Angel Light Scattering (LALS) detectors.

DSC measurements were performed with a polymer DSC instrument by Mettler Toledo. The glass transition temperature (T_g) of polymers was determined from the second heating at a heating rate of 5 °C/min.

MALDI-TOF mass spectroscopy measurements were performed on a Waters MALDI Micro MX mass spectrometer, equipped with a nitrogen laser delivering 3 ns laser pulses at 337 nm. α-Cyano-4-hydroxycinnamic acid (J&K, 97%), was used as a matrix. CH_3COOK (Aldrich, 98%) was added for ion formation.

DLS measurements were conducted using a Delsa Nano C (Beckman Coulter, Inc., Fullerton, CA) equipped with a laser diode operating at 658 nm. All measurements were made in DI water at 25 °C. The concentration of the amphiphilic block polycarbonates was 2 mg/mL. Scattered light was detected at 165° angel and analyzed using a log correlator over 70 accumulations. The photomultiplier aperture and the attenuator were automatically adjusted to obtain a photon counting rate of ca. 10 kcps. The calculation of the particle size distribution and distribution averages was performed using CONTIN particle size distribution analysis routes using Delsa Nano 2.31 software. The peak

averages of histograms from intensity, volume and number distributions out of 70 accumulations were reported as the average diameter of the particles.

The ζ-potential of the nanoparticles was determined by Delsa Nano C particle analyzer (Beckman Coulter, Inc., Fullerton, CA) equipped with a 30 mW laser diode (658 nm). The ζ-potential of the particles in suspension was obtained by measuring the electrophoretic movement of charged particles under an applied electric field. Scattered light was detected at a 30° angle at 25 °C. The ζ-potential was measured at five regions in the flow cell and a weighted mean was calculated. These five measurements were used to correct for electroosmotic flow that was induced in the cell due to the surface charge of the cell wall. All determinations were repeated three times.

Transmission electron microscopy (TEM) images were collected on a JEOL 1200 EX (Tokyo, Japan) operating at 100 kV and micrographs were recorded at calibrated magnifications using a SLA-15C CCD camera. Samples for TEM measurements were prepared as follows: 10 μL of the dilute polymer solution was deposited onto a carbon-coated copper grid, and after 1 min, the excess of the solution was quickly wicked away by a piece of filter paper. The samples were then negatively stained with 1 wt % uranyl acetate aqueous solution. After 30 s, the excess staining solution was quickly wicked away by a piece of filter paper and the samples were left to dry in vacuum overnight.

The CMC values of polymers in DI water were estimated by fluorescence spectroscopy using pyrene as a probe. The measurements was conducted on a RF-5301PC spectrofluorophotometer system (Shimadzu Corp., Kyoto, Japan) and analyzed using Panorama Fluorescence v. 2.1 software. The sample solutions were prepared by mixing 1

mL polymer aqueous solution with 1 mL pyrene aqueous stock solution ($6.0*10^{-7}$ mol/L). Samples with polymer concentrations ranging from 2 mg/mL to 4 μg/mL were prepared and left to equilibrate at room temperature for 24 hours. The fluorescence spectra were recorded from 360 to 450 nm at an emission wavelength of 334 nm. The intensity (peak height) ratios of I_{373}/I_{384} were plotted against the concentrations of polymer in the sample solutions. The CMC was taken as the intersection of the tangent to the curve at the inflection with tangent through the points at high polymer concentration.

Synthesis of Boc-*L*-cysteine. Boc-*L*-cysteine was synthesized following the procedure in literature.[96] A mixture of *L*-cysteine hydrochloride (50 mmol), di-*tert*-butyl dicarbonate (50 mmol) and $NaHCO_3$ (150 mmol) in THF (18 mL) and water (45 mL) was stirred under Ar at room temperature for 30 hours. 6M HCl solution was added dropwise into the reaction mixture in an ice bath to adjust the pH to 3. The solution was extracted with ethyl acetate three times. The organic phase was combined and dried over Na_2SO_4 and evacuated in vacuo to give a slightly yellow oil (yield: 70%). ^{1}H NMR ($CDCl_3$, 300 MHz): δ 5.40-5.60 (m, 1H, N*H*), 4.74-4.48 (m, 1H, CH_2CH(COOH)NH), 3.10-2.81 (m, 2H, $CHCH_2SH$), 1.46 (s, 9H, $C(CH_3)_3$) ppm.

Synthesis of 2-(Boc-amino)ethanethiol. 2-(Boc-amino)ethanethiol was synthesized following the procedure in literature.[97] To a solution of 2-aminoethanethiol (25 mmol) in water (15 mL), a THF solution of di-*tert*-butyl dicarbonate (25 mmol) was added. The mixture was stirred under Ar at room temperature for 4 hours. The solution was extracted with CH_2Cl_2. The combined organic layers were dried over Na_2SO_4 and evacuated in vacuo to give a colorless oil (yield: 98%). ^{1}H NMR ($CDCl_3$, 300 MHz): δ

4.99 (br, 1H, N*H*), 3.47-3.14 (m, 2H, CH_2NHBoc), 2.75-2.48 (m, 2H, CH_2SH), 1.40 (s, 9H, C(CH_3)$_3$), 1.33 (t, 1H, S*H*, J = 8.5 Hz) ppm.

Representative Procedures for the Synthesis of PAGEC-*b*-PPC-*b*-PAGEC Triblock Polycarbonates. (Salen)cobalt(III)X/PPNX (X = trifluoroacetate) (0.0125 mmol), propylene oxide (0.87mL, 12.5 mmol) and 0.7 mL toluene/CH_2Cl_2 (1/1 volume ratio) with 20 equiv. water were added into a 15 mL autoclave, and pressurized to 2.5 MPa. After 48 h, the CO_2 pressure was slowly released and allyl glycidyl ether was added. The reactor was recharged with CO_2 to 2.5 MPa. The pressure was released after 48 h. The crude polymer was dissolved in CH_2Cl_2 and precipitated from methanol. This process was repeated three times to completely remove the catalyst. For the first precipitation cycle, ca. 0.5 g of *p*-methoxyphenol was added to the CH_2Cl_2 solution to forestall self-crosslinking. The obtained polymer was dried under high vacuum at room temperature. NMR for samples with 50% PPC Unit. ^{1}H NMR ($CDCl_3$, 500 MHz): δ 5.86 (tdd, 1H, OCH$_2$C*H*=CH$_2$, J = 16.0, 10.5, 5.6 Hz), 5.34-5.12 (m, 2H, CH=CH_2), 5.08-4.95 (m, 2H, C*H*OCOO, C*H*OCOO), 4.51-4.07 (m, 4H, CH_2OCOO, CH_2OCOO), 4.08-3.94 (m, 2H, CH$_2$OCH_2CH=CH$_2$), 3.71-3.56 (m, 2H, CH$_2$OCH_2CH), 1.32 (d, 3H, CH_3, J = 6.5 Hz) ppm. GPC: M_n = 10300 g/mol, PDI = 1.01. DSC: T_g = -1 °C.

General Procedure of Thiol-ene Reactions of PAGEC-*b*-PPC-*b*-PAGEC Triblock Polycarbonate with Functional Thiols. A solution of ABA triblock polymer (0.30g, M_n = 10300 g/mol, 50% PPC unit, 1.15 mmol alkenes), functional thiol (23 mmol) in 25.0 mL of THF was degassed for 15 min and then refilled with Ar. DMPA (0.1 mmol) was added into the solution followed by UV irradiation (365 nm) for 2h. The reaction

mixtures were precipitated from THF into diethyl ether or hexane to remove excess functional thiols and photoinitiator by-products to give the product polymers.

The mercaptoacetic acid functionalized product was obtained in the form of a slightly yellow soft solid in a yield of 80%. ^{1}H NMR (d_6-DMSO, 300 MHz): δ 5.04-4.82 (m, 2H, C*H*OCOO, C*H*OCOO), 4.47-3.98 (m, 4H, CH_2OCOO, CH_2OCOO), 3.60 (m, 2H, overlapping residual tetrahydrofuran), 3.20 (s, 2H, CH_2SCH_2COOH), 2.58 (t, 2H, $CH_2CH_2SCH_2$, J = 7.1 Hz), 1.85-1.65 (m, 2H, overlapping residual tetrahydrofuran), 1.22 (d, 3H, CH_3, J = 6.5 Hz) ppm. GPC: M_n = 16000 g/mol, PDI = 1.01. DSC: T_g = -5 °C.

The 2-(Boc-amino)ethanethiol functionalized product was obtained in the form of a slightly yellow soft solid in a yield of 75%. ^{1}H NMR ($CDCl_3$, 300 MHz): δ 5.18-4.82 (m, 3H, C*H*OCOO, C*H*OCOO, N*H*), 4.55-3.97 (m, 4H, CH_2OCOO, CH_2OCOO), 3.70-3.39 (m, 4H, CHCH_2OCH$_2$, CH$_2$OCH_2CH$_2$), 3.29 (t, 2H, CH_2NHBoc, J = 6.5 Hz), 2.76-2.34 (m, 4H, CH_2SCH_2), 1.98-1.63 (m, 2H, overlapping residual tetrahydrofuran), 1.43 (s, 9H, C(CH_3)$_3$), 1.33 (d, 3H, CHCH_3, J = 6.5 Hz) ppm. GPC: M_n = 17600 g/mol, PDI = 1.01. DSC: T_g = 9 °C.

The Boc-*L*-cysteine functionalized product was obtained as a slightly yellow solid in a yield of 60%. ^{1}H NMR (d_6-DMSO, 300 MHz): δ 6.65 (s, 1H, N*H*), 5.06-4.80 (m, 2H, C*H*OCOO, C*H*OCOO), 4.45-3.85 (m, 6H, CH_2OCOO, CH_2OCOO, C*H*(COOH)NHBoc), 2.95-2.59 (m, 2H, SCH_2CH), 2.50 (m, 2H, overlapping DMSO), 1.86-1.64 (2H, OCH$_2$CH_2CH$_2$S, overlapping residual tetrahydrofuran), 1.37 (s, 9H, C(CH_3)$_3$), 1.22 (d, 3H, CHCH_3, J = 6.5 Hz) ppm. NMR peaks of the alkoxyalkane protons are obscured by

those of H_2O and residual tetrahydrofuran. GPC: M_n = 22300 g/mol, PDI = 1.01. DSC: T_g = 46 °C.

Deprotonation of Mercaptoacetic Acid Functionalized Triblock Polycarbonate. Mercaptoacetic acid functionalized triblock polymer was dissolved in anhydrous THF and the solution was cooled to 0 °C. 1.0 equiv (based on the mole of the pendant COOH group) of aqueous ammonium hydroxide (28 wt% $NH_4OH_{(aq)}$) was added dropwise into the solution under positive Ar atmosphere. A white suspension was formed during the course of addition. The reaction mixture was stirred for 5 min before diethyl ether was added into the reaction to precipitate the product. The white solid was isolated and dissolved in deionized water. The micelle solution was lyophilized to give the product polymer. ^{1}H NMR (d_6-DMSO, 300 MHz): δ 5.02-4.82 (m, 2H, C*H*OCOO, C*H*OCOO), 4.50-3.98 (m, 4H, CH_2OCOO, CH_2OCOO), 3.66-3.36 (m, 4H, CHCH_2OCH_2, CH_2OCH_2CH_2), 3.17 (s, 2H, CH_2SCH_2COONH_4), 2.57 (t, 2H, CH_2CH_2SCH_2, J = 7.2 Hz), 1.87-1.62 (m, 2H, OCH_2CH_2CH_2S), 1.22 (d, 3H, CH_3, J = 6.5 Hz) ppm.

BOC Deprotection of 2-(Boc-amino)ethanethiol and Boc-*L*-cysteine Functionalized Triblock Polycarbonates. 20 mL HCl saturated THF was added into 0.5 mL THF solution of 0.3g 2-(Boc-amino)ethanethiol or Boc-*L*-cysteine functionalized triblock polycarbonates. The solution was stirred at room temperature for 4 hours and a white precipitate was formed. The solid was isolated and dissolved in deionized water and lyophilized to give the product polymer.

Cationic triblock polymer **5** was obtained as a colorless solid in a yield of 70%. . ^{1}H NMR (d_6-DMSO, 300 MHz): δ 8.25 (br, NH_3), 5.05-4.82 (m, 2H, C*H*OCOO,

C*H*OCOO), 4.46-3.88 (m, 4H, C*H*$_2$OCOO, C*H*$_2$OCOO), 3.84-3.26 (m, 4H, CHC*H*$_2$OCH$_2$, CH$_2$OC*H*$_2$CH$_2$), 2.96 (m, 2H, OCH$_2$C*H*$_2$CH$_2$S), 2.75 (m, 2H), 2.56 (t, 2H, J = 6.9 Hz), 1.87-1.62 (m, 2H, C*H*$_2$NH$_3$), 1.22 (d, 3H, C*H*$_3$, J = 6.5 Hz) ppm.

Cationic triblock polymer **6** was obtained as a colorless solid in a yield of 50%. . ^{1}H NMR (d_6-DMSO, 300 MHz): δ 8.61 (br, N*H*$_3$), 5.05-4.82 (m, 2H, C*H*OCOO, C*H*OCOO), 4.48-3.92 (m, 4H, C*H*$_2$OCOO, C*H*$_2$OCOO), 3.76-3.25 (m, 5H, CHC*H*$_2$OCH$_2$, CH$_2$OC*H*$_2$CH$_2$, C*H*(COOH)NH$_3$), 3.04 (m, 2H, CH$_2$C*H*$_2$SCH$_2$), 2.60 (m, 2H, SC*H*$_2$CH(COOH)NH$_3$), 1.76 (m, 2H, OCH$_2$C*H*$_2$CH$_2$S), 1.22 (d, 3H, C*H*$_3$, J = 6.2 Hz) ppm.

Self-assembly of Amphiphilic Triblock Polycarbonates. The functional triblock copolymers (3mg/mL) were suspended into DI water (1.0mL) and sonicated for 10 min.

CHAPTER III

CARBOXYLIC ACID FUNCTIONALIZED POLYCARBONATES FROM CO_2: A VERSATILE PLATFORM FOR THE SYNTHESIS OF FUNCTIONAL POLYCARBONATES*

Introduction

Petroleum derived chemicals currently are by far the most important sources of polymeric materials. Considering their vast utilization as fuels which lead to their rapid depletion, finding alternative carbon sources for producing polymers based on renewable monomers has been the subject of numerous research programs worldwide.[98] A significant contribution to this area is the production of biodegradable polycarbonates *via* the alternating copolymerization of bio-derived epoxides and the renewable C1 feedstock, carbon dioxide.[41, 48a, 48c, 51] The recent development of single-site metal catalysts with well-defined structures have provided active catalytic systems which operate under mild reaction conditions, and in some instances afford regio-and/or stereo-selective copolymers. [22, 71]

Because of their biocompatibility, biodegradability, and approval for use in biomedical devices by the US Food and Drug Administration (FDA), aliphatic polycarbonates are very important synthetic biomaterials.[99] In our continued efforts

* Portions reprinted (adapted) from "Environmentally Benign CO_2-Based Copolymers: Degradable Polycarbonates Derived from Dihydroxybutyric Acid and Their Platinum-Polymer Conjugates." Tsai, F.; Wang, Y.; Darensbourg, D. J. *J. Am. Chem. Soc*. **2016**, *138*, 4626-4633. Copyright 2016 American Chemical Society.

towards the development of polycarbonate biomaterials, we have designed and prepared a novel CO_2-derived polycarbonate structure that can undergo degradation to yield nontoxic metabolites in biological environment. As is shown in scheme III-1, poly(3,4-dihydroxybutyrate carbonate) (PDHBAC) can be synthesized from copolymerization reaction of *tert*-butyl 3,4-epoxybutanoate (^{t}Bu 3,4-EB) and CO_2 followed by cleavage of the *tert*-butyl protection group. The isotactic structure of PHBAC (*S*- form) is particularly attractive, as it can degrade into (*S*)-3,4-dihdroxybutyric acid ((*S*)3,4-DHBA), a normal human urinary metabolite. Biologically, (*S*)-3,4-DHBA originates from the degradation of carbohydrates or from the metabolism of γ-hydroxybutyrate, a naturally occurring substance found in the human central nervous system. Normal adults excrete (0.37±0.15) mmol of 3,4-dihydroxybutyrate per 24 hr. The compound is also detectable in blood (18.0 (0.0-54.0) mM) and in cerebrospinal fluid (CSF) (15.0±15.0 mM).[100] Moreover, (*S*)-3,4-DHBA is a highly useful chiral intermediate in synthesizing statin-class drugs such as CRESTOR®, LIPITOR® and carnitine.

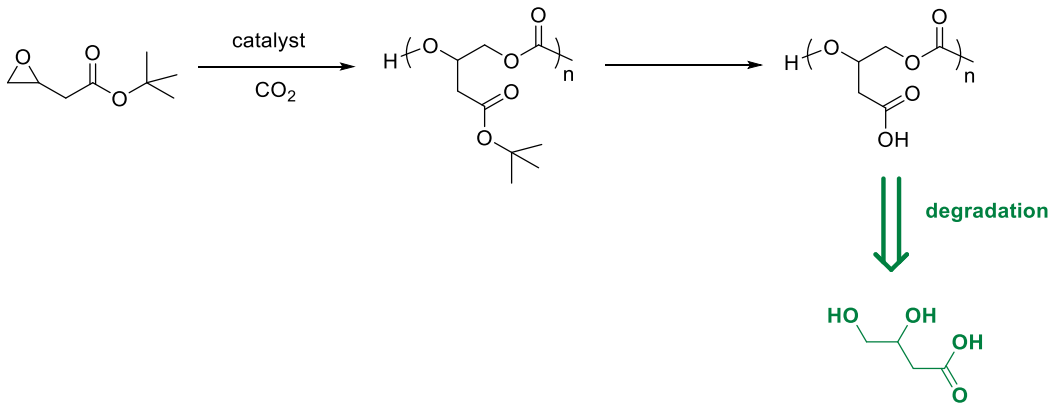

Scheme III-1. Synthesis of poly(3,4-dihydroxybutyrate carbonate) and its degradation.

In chemotherapy-based small-molecule platinum-containing drugs, cisplatin, carboplatin, and oxaliplatin have been extensively used in the treatment of solid cancers, such as ovarian, bladder, testicular and non-small-cell lung cancers. However, clinical use of platinum-containing drugs has been limited due to several major side effects, including nephrotoxicity and neurotoxicity. Because of the drug's non-selectivity, normal and transformed cells are equally affected. Further, poor water solubility leads to suboptimal distribution in the circulation. The electrophilic nature of platinum in its aquated form, which is partly present when dissolved in the circulation system, results in its high affinity for amino acids. Because of these limitations, research efforts in creating carrier-bound platinum complexes are aimed at the development of platinum-polymer conjugates. Hence, it has been proposed to employ poly(3,4-dihydroxybutyrate carbonate) as a carrier for the delivery of platinum to protect the drugs from nonspecific binding, to increase circulation time and to use the enhanced permeation and retention effect (EPR) of cancer cells.[101] In order to construct the platinum-polymer conjugates, postpolymerization functionalization was conducted by anchoring aspartate/glycine-aspartate and (DACH)$PtCl_2$ (DACH = (*1R, 2R*)-diaminocyclohexane) onto the bio-related polycarbonate scaffold.

Results and Discussion

Epoxide Synthesis. Synthesis of *tert*-butyl 3,4-epoxybutanoate (^{t}Bu 3,4-EB) was achieved by the two-step process depicted in Scheme III-2. The coupling reaction of 3-butenoic acid with *tert*-butyl acetate was triggered by a catalytic quantity of $BF_3 \cdot OEt_2$ to

afford *tert*-butyl 3-butenoate. Epoxidation of *tert*-butyl 3-butenoate was carried out with *m*CPBA (*meta*-chloroperoxybenzoic acid) to provide the epoxide in good yield.

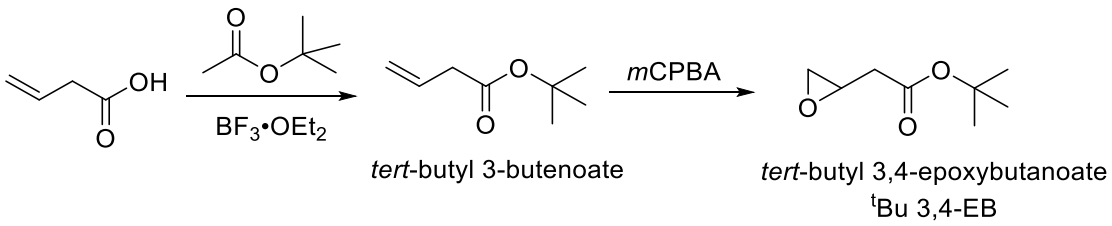

Scheme III-2. Synthesis of *tert*-butyl 3,4-epoxybutanoate.

Copolymerization Reactions. Initially, the copolymerization reactions of twice-distilled over CaH_2 (~0.043% water content) *rac*-^{t}Bu 3,4-EB with CO_2 were carried out employing bifunctional catalysts **7-X** (X = Cl^-, N_3^-, DNP^-, structure see Figure II-1). As noted in Table III-1, in the absence of *added* water only catalyst **7-Cl** afforded any coupling product which was exclusively the corresponding cyclic carbonate. However, upon adding 10 equiv of water to catalyst **7-DNP**, copolymerization of CO_2/*rac*-^{t}Bu 3,4-EB readily occurred at 40 °C. A similar reactivity pattern was observed under identical reaction conditions for the copolymerization process involving the sterically less hindered *rac*-methyl 3,4-epoxybutanoate (*rac*-Me 3,4-EB) monomer and CO_2 (Table III-2). These results suggest that small, good nucleophiles with poor leaving group properties, that is, resulting from chain-transfer with water or the diol resulting from epoxide hydrolysis, initiates the alternating copolymerization process.

Table III-1. Coupling reaction of CO_2 and twice-distilled *tert*-butyl 3,4-epoxybutanoate (^{t}Bu 3,4-EB)[a]

catalysts	conversion[e] (%)	TOF (h^{-1})	delectivity[e] (polymer %)	M_n (GPC) (kg/mol)	PDI
1-DNP[b]	0	0	-	-	-
1-DNP[c]	91.3	25.4	98.5	5.6	1.19
1-DNP[d]	81.8	9.3	91.8	12.6	1.57
1-Cl[b]	50	13.9	0	-	-
1-N_3[b]	0	0	-	-	-

[a]All the coupling reactions were conducted in neat *rac*-^{t}Bu 3,4-EB in a 25 mL autoclave for 18 hours. Temperature and pressure were held at 40 °C and 3.0 MPa, respectively. [b]Catalyst/epoxide = 1/500. [c]Catalyst/H_2O/epoxide = 1/10/500. [d]Catalyst/H_2O/epoxide = 1/10/1000. [e]Characterized by ^{1}H NMR spectrum of crude product.

Table III-2. Coupling reaction of CO_2 and twice-distilled methyl 3,4-epoxybutanoate (Me 3,4-EB)[a]

catalysts	conversion[e] (%)	TOF (h^{-1})	selectivity[e] (polymer %)	M_n (GPC) (kg/mol)	PDI
1-DNP[b]	0	0	-	-	-
1-DNP[c]	88.7	24.6	97.7	5.4	1.53
1-Cl[b]	69.7	19.4	0	-	-
1-N_3[b]	0	0	-	-	-

[a]All the coupling reactions were conducted in neat *rac*-Me 3,4-EB in a 25 mL autoclave for 18 hours. Temperature and pressure were held at 40 °C and 3.0 MPa, respectively. [b]Catalyst/epoxide = 1/500. [c]Catalyst/H_2O/epoxide = 1/10/500. [d]Characterized by ^{1}H NMR spectrum of crude product.

Table III-3. Coupling reaction of CO_2 and once-distilled (> 0.5% water content) *tert*-butyl 3,4-epoxybutanoate (^{t}Bu 3,4-EB)[a]

catalysts	t (h)	T (°C)	conversion[e] (%)	TOF (h^{-1})	selectivity[e] (polymer %)	M_n(GPC) (kg/mol)	PDI
1-DNP[b]	22	25	98.5	22.4	100	15.8	1.07
1-DNP[c]	22	25	96.1	21.8	100	14.7	1.08
1-DNP[b]	8	40	100	62.5	100	16.9	1.04
1-DNP[d]	16	40	100	62.5	100	20.8	1.08

[a]The coupling reaction was conducted in neat ^{t}Bu 3,4-EB in a 25 mL autoclave at 3.0 MPa CO_2 pressure. [b]Catalyst/*rac*-^{t}Bu 3,4-EB = 1/500. [c]Catalyst/(*S*)-^{t}Bu 3,4-EB = 1/500. [d]Catalyst/*rac*-^{t}Bu 3,4-EB = 1/1000. [e]Characterized by ^{1}H NMR spectrum of crude product.

To further examine this hypothesis, the use of once-distilled *rac*-^{t}Bu 3,4-EB monomer which contains traces of adventitious water was subjected to the copolymerization process with CO_2. As shown in Table III-3, the catalyst **7-DNP** was found to selectively copolymerize CO_2 and *rac*-^{t}Bu 3,4-EB to afford the corresponding polycarbonate with greater than 99% carbonate linkages. The isolated copolymers exhibited narrow molecular weight distributions with PDI values less than 1.10 and displayed bimodal distributions. The main-chain sequence of the resulting poly(*tert*-butyl 3,4-dihydroxybutyrate carbonate) (P^{t}BuDHBC) was characterized by ^{1}H and ^{13}C NMR spectroscopy. In the ^{1}H NMR spectrum, the resonance of the methine CH was observed at 5.24 ppm, and signals at δ = 3.3-3.6 ppm assignable to ether linkages were not evident. By way of contrast with poly(methyl 3,4-dihydroxybutyrate carbonate) (PMeDHBC) which exhibited 91.8% head-to-tail region-selectivity, the ^{13}C NMR spectrum of the atactic P^{t}BuDHBC copolymer shows it to consist of 100% head-to-tail regio-chemistry

(Figure III-1). This observation implies that the sterically congested *tert*-butyl group promotes ring-opening of *rac*-^{t}Bu 3,4-EB to occur exclusively at the C_{β}-O bond during its copolymerization with CO_2.

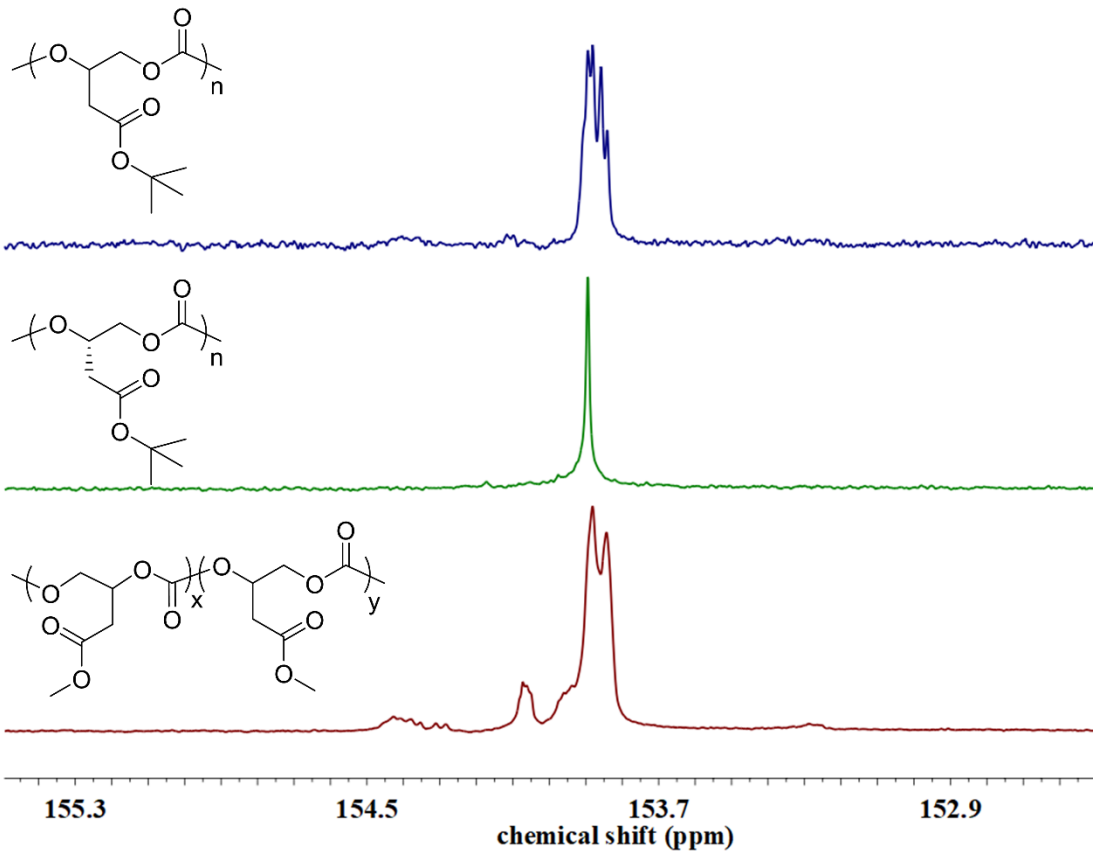

Figure III-1. ^{13}C NMR spectra ($CDCl_3$) of carbonate region for copolymers poly(*tert*-butyl 3,4-dihydroxybutanoate carbonate) (blue), poly((*S*)-*tert*-butyl 3,4-dihydroxybutanoate carbonate) (green), and poly(methyl 3,4-dihydroxybutanoate carbonate) (red).

Provided with this encouraging regioregular result, it was of interest to synthesize a chiral, isotactic version of this copolymer. To this end, a hydrolytic kinetic resolution of *rac*-^{t}Bu 3,4-EB was carried out with Jacobson's catalyst in a 44% yield (based on the racemic epoxide) to afford the *S*-enantiomer following the published procedure. Subsequent copolymerization of (*S*)-^{t}Bu 3,4-EB and CO_2 in the presence of catalyst **7-DNP** afforded an isotactic poly((S)-*tert*-butyl 3,4-dihydroxybutyrate carbonate) (*S*-P^{t}BuDHBC) with a molecular weight of 14.7 kg/mol and a PDI of 1.08 (entry 3 in Table III-3). In the ^{13}C NMR spectrum, the isotactic polymer shows 100% head-to-tail selectivity and exhibits a single sharp signal at 153.9 ppm (Figure III-1).

Synthesis of Poly(3,4-dihydroxybutyric acid carbonate) (PDHBAC). With the polycarbonates, P^{t}BuDHBC and *S*-P^{t}BuDHBC, in hand, the *tert*-butyl protecting groups of the pendent carboxylate groups were removed using trifluoroacetic acid (TFA) in dry CH_2Cl_2 at ambient temperature over 12h. Upon isolation, the resulting copolymer's ^{1}H NMR spectrum revealed the absence of the *tert*-butyl resonance at 1.43 ppm, confirming its removal from the polymer. The poly(3,4-dihyroxybutyric acid carbonate) (PDHBAC) is not soluble in water or common organic solvents, but was soluble in methanol and DMSO. However, subsequent deprotonation of PDHBAC by 0.45 equivalents of K_2CO_3 in wet MeOH afforded the water-soluble poly(potassium 3,4-dihydroxybutyrate carbonate) (PKDHBC). The thermal properties of the various isolated polycarbonates were examined by conducting DSC analyses. As shown in Table III-4, the glass transition temperatures (T_g), which are a function of changes in the polymer properties such as modulus, increase as the flexible methyl group is replaced by the sterically more congested

t-butyl group. Because of the polar carboxylic acid pendent groups and the intrinsic ionic character of the potassium salts, PDHBAC/*S*-PDHBAC and PKDHBC**,** stronger interchain interactions lead to these polycarbonates exhibiting higher T_g values than the others.

Table III-4. Glass transition temperature (T_g) for polycarbonate

Polycarbonates	**M_n (kg/mol)**	**T_g (°C) (DSC)**
PMeDHBC	5.4	18
P^{t}BuDHBC	5.6/15.8	37
S-P^{t}BuDHBC	14.7	40
PDHBAC	-	65
S-PDHBAC	-	74

Depolymerization and Degradation Reactions. It is of interest to investigate depolymerization and degradation reaction pathways of these polycarbonates under anaerobic conditions. In our previous studies, base-initiated depolymerization of polycarbonates derived from CO_2 and epoxides generally occurred *via* a backbiting process of the deprotonated copolymer chain end, resulting in an unzipping of the polymer chain to provide the corresponding cyclic carbonate.[102] As illustrated in Scheme III-3, the depolymerization of poly(*tert*-butyl 3,4-dihydroxybutyrate carbonate) is found to proceed by way of a similar end-scission pathway following deprotonation of the hydroxyl chain end by the strong non-nucleophilic base NaHMDS (sodium *bis*(trimethylsilyl)amide).

Upon addition of base, immediate depolymerization was noted as evidenced by the appearance of ^{1}H NMR resonances at δ = 3.63 and 3.25 ppm in d_8-toluene (Figure III-2). These chemical shifts are assigned to the methylene hydrogens of the generated cyclic carbonate. At 40 °C P^{t}BuDHBC slowly depolymerized cleanly to its cyclic carbonate counterpart, reaching a molar ratio of cyclic carbonate to copolymer of 1.79 after 12 days (Figure III-3).

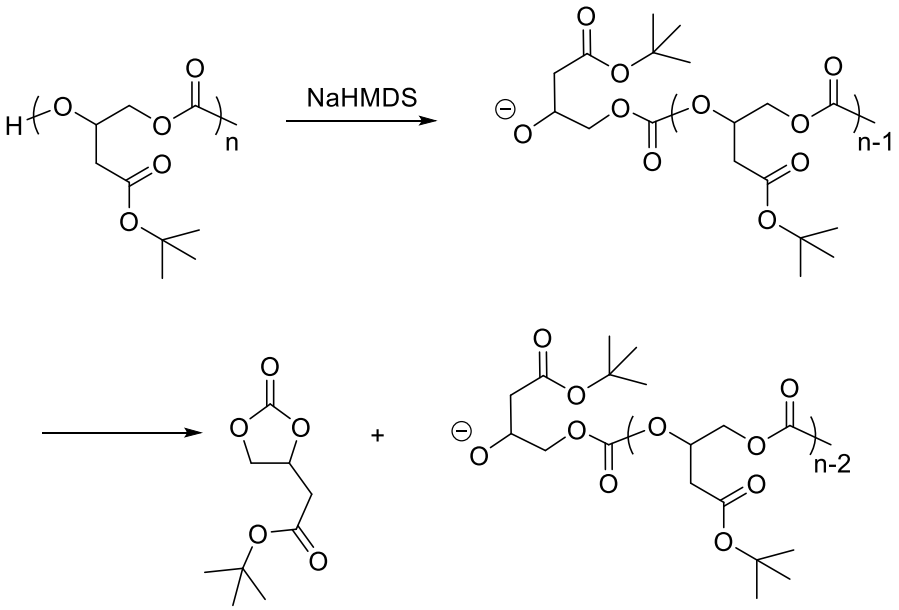

Scheme III-3. Depolymerization of poly(*tert*-butyl 3,4-dihydroxybutyrate carbonate) in the presence of sodium *bis*(trimethylsilyl)amide (NaHMDS).

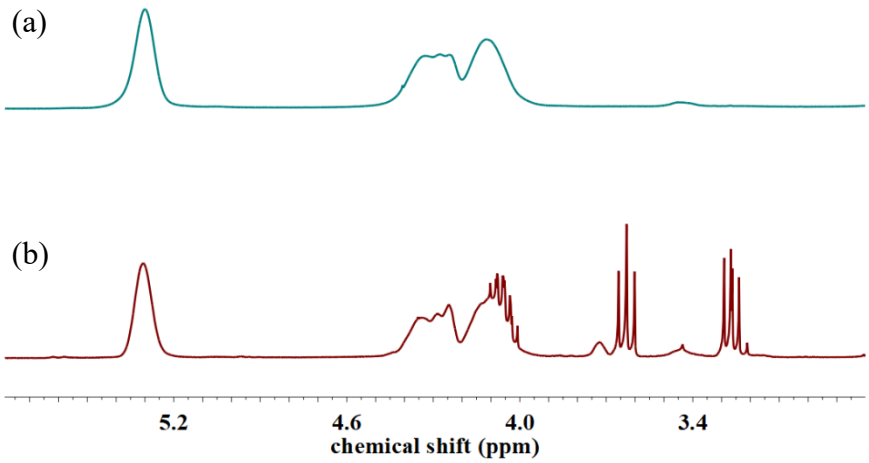

Figure III-2. ^{1}H NMR spectra of poly(*tert*-butyl 3,4-dihydroxybutanoate carbonate) in d_8-toluene: (a) before and (b) after adding NaHMDS (3h, 40 °C).

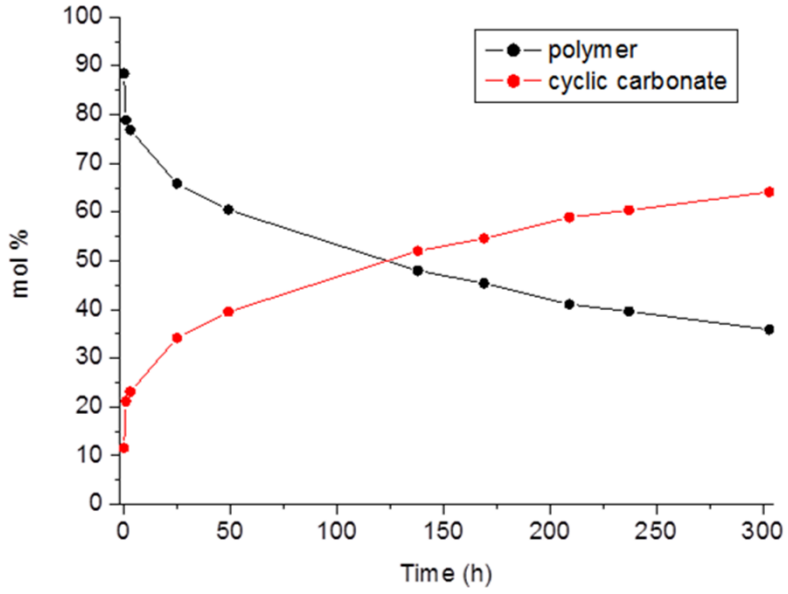

Figure III-3. Depolymerization of poly(*tert*-butyl 3,4-dihydroxybutanoate carbonate) in d_8-toluene at 40 °C subsequent to deprotonation with NaHMDS.

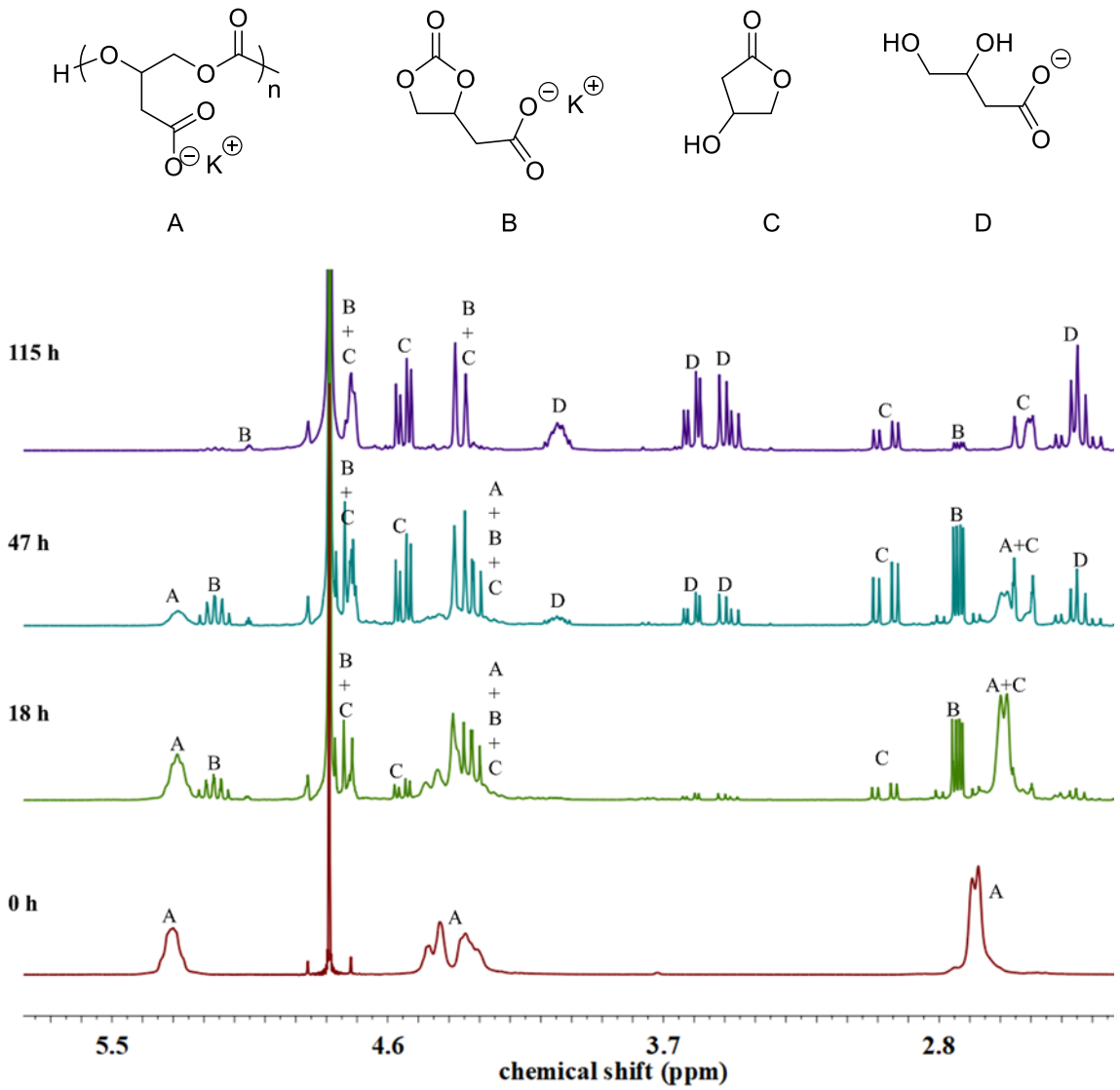

Figure III-4. ^{1}H NMR spectra monitoring the degradation process of acetyl-capped poly(3,4-dihydroxybutyrate carbonate) in aqueous solution at pH = 8 at 37 °C.

On the other hand, for poly(3,4-dihydroxybutyric acid carbonate), neither depolymerization nor degradation was observed by ^{1}H NMR spectroscopy upon heating the d_7-DMF dissolved polymer in the absence of NaHMDS at 37 °C for 12 days. This indicates that intramolecular cyclization of the carboxylic acid group onto the carbonate backbone to afford *O*-carboxyanhydride does not occur. Such an observation is likely a consequence of the lower nucleophilicity of the carboxylic acid group in PDHBAC as compared to the primary hydroxyl group in poly(1,2-glycerol carbonate).[41] In contrast, when acetyl end-capped poly(potassium 3,4-dihydroxybutyrate carbonate) was dissolved in water (D_2O, pH = 8) and heated at 37 °C, degradation occurred with formation of cyclic carbonate, *β*-hydroxy-*γ*-butyrolacetone and 3,4-dihyroxybutyrate as determined by ^{1}H NMR spectroscopy (Figure III-4). Over a 5d period, polycarbonate and cyclic carbonate fully degraded into *β*-hydroxy-*γ*-butyrolacetone and 3,4-dihyroxybutyrate. To further corroborate cyclic carbonate degradation and *β*-hydroxy-*γ*-butyrolacetone hydrolysis, samples composed of cyclic carbonate or *β*-hydroxy-*γ*-butyrolacetone were dissolved in D_2O (pH = 8) and heated at 37 °C while monitoring by ^{1}H NMR spectroscopy. The complete degradation of cyclic carbonate occurred within 3 days with the formation of *β*-hydroxy-*γ*-butyrolacetone and 3,4-dihydroxybutyrate. Similarly, the hydrolysis of *β*-hydroxy-*γ*-butyrolacetone to afford 3,4-dihydroxybutyrate was observed. Based on these results, the degradation of acetyl end-capped poly(potassium 3,4-dihyroxybutyrate carbonate) can be attributed to the more nucleophilic nature of the carboxylate in D_2O, and it is proposed that the degradation occurs randomly along the carbonate backbone. As illustrated in Scheme III-4, it is presumed that intramolecular cyclization of the

carboxylate onto the carbonate backbone forms intermediate **A** containing an *O*-carboxyanhydride.[34] Subsequent hydrolysis of *O*-carboxyanhydride furnishes the polycarbonate containing a hydroxyl chain end. Deprotonation of a hydroxyl polymer chain end in weak basic condition triggers end-scission depolymerization, leading to the formation of cyclic carbonate. Presumably, hydrolysis of cyclic carbonate and concomitant nucleophilic attack of the carboxylate at C_α-O bond in intermediate **B** yields *β*-hydroxy-*γ*-lactone, with hydrolysis generating 3,4-dihydroxybutyrate. The complete degradation of acetyl-capped poly(potassium 3,4-dihydroxybutyrate carbonate) into biomass, *β*-hydroxy-*γ*-butyrolacetone and 3,4-dihydroxybutyrate, in water (pH = 8) at 37 °C indicates that this polycarbonate is biodegradable, human-friendly and environmentally benign.

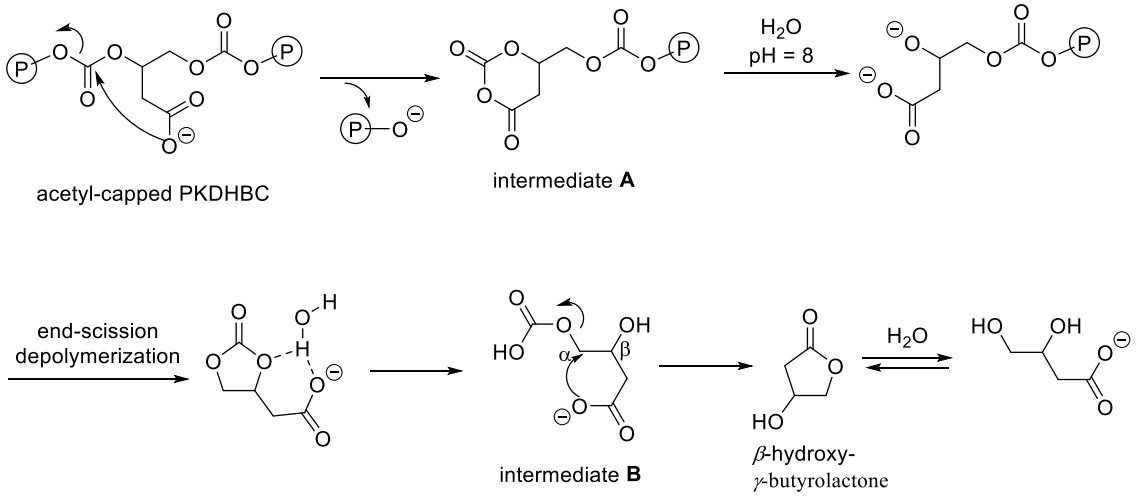

Scheme III-4. Proposed degradation mechanism of acetyl end-capped poly(3,4-dihydroxybutyric acid carbonate) in water (pH =8) into *β*-hydroxy-*γ*-butyrolacetone and 3,4-dihydroxybutyrate.

Synthesis of Platinum-polymer Conjugate. Efficient delivery of therapeutics into tumor cells to increase the intracellular drug concentration is a major challenge for cancer therapy due to drug resistance and inefficient cellular uptake. The strategy of using delivery vehicles to selectively transport more of anticancer agents to tumors is clinically attractive. This can be achieved by linking a platinum-based drug to a water-soluble, biocompatible, biodegradable polymer in order to exploit the enhanced permeability and retention (EPR) effect of macromolecules in tumors.[101] The aim of the current study is to construct water-soluble polycarbonates which can serve as anticancer drug carriers. In this regard, poly(3,4-dihydroxybutyric acid carbonate) was treated with oxalyl chloride in the presence of catalytic amounts of dimethylformamide (DMF) followed by reaction with an amine, di-*tert*-butyl-*L*-aspartate or glycine-di-*tert*-butyl-*L*-aspartate. The subsequent deprotection by TFA and dialysis against water afforded water-soluble polycarbonates PDHBAC-Asp-OH and PDHBAC-Gly-Asp-OH (Scheme III-5). The structures of PDHBAC-Asp-OH and PDHBAC-Gly-Asp-OH are confirmed by ^{1}H NMR spectroscopy. The chemical shifts at 8.20 ppm and 4.52 ppm (in DMSO) are assigned to the amide proton (−C(O)N*H*CH−) and the methine proton (−C(O)NHC*H*−) of aspartic acid, respectively. For PDHBAC-Gly-Asp-OH, the resonance of methylene protons (−C(O)NHCH_2C(O)−) of glycine was found at 3.74 ppm (in DMSO). Because of the large number of pendant carboxylic acid groups in the resulting polymers, both PDHBAC-Asp-OH and PDHBAC-Gly-Asp-OH are not soluble in CH_2Cl_2, but are completely soluble in water and DMSO.

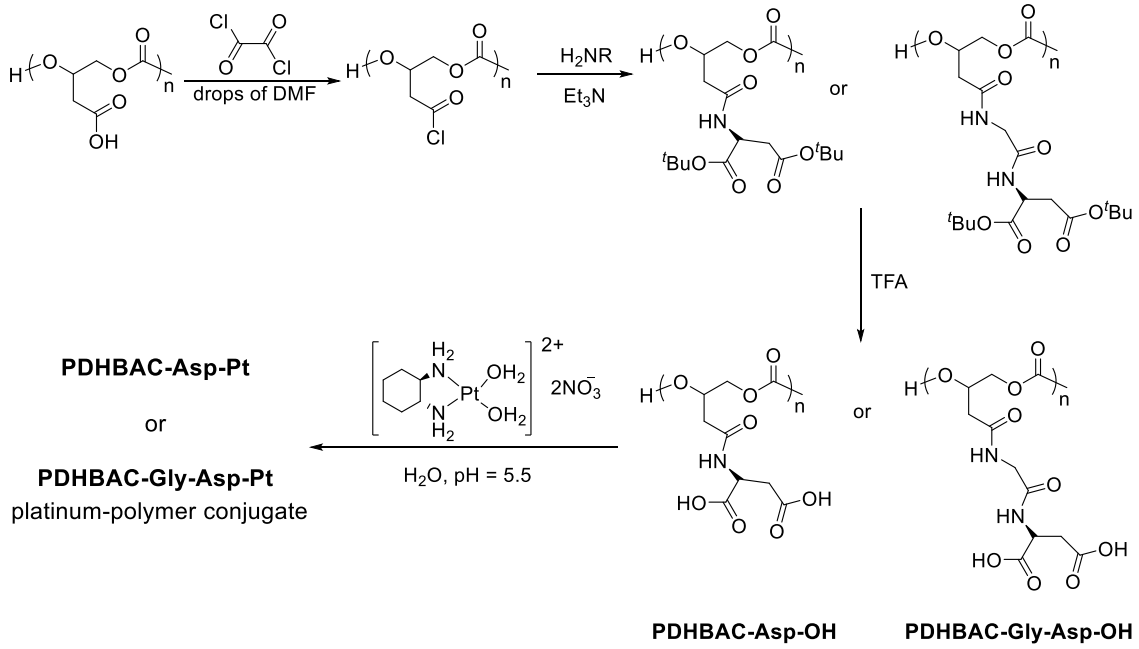

Scheme III-5. Synthesis of platinum-polymer conjugates.

In an effort to construct platinum-polymer conjugates, PDHBAC-Asp-Pt and PDHBAC-Gly-Asp-Pt, the reaction of PDHBAC-Asp-OH or PDHBAC-Gly-Asp-OH with aqueous $[(DACH)Pt(OH_2)_2][NO_3]_2$ (DACH = (*1R*, *2R*)-diaminocyclohexane) was conducted. The carboxylic acid residues from PDHBAC-Asp-OH and PDHBAC-Gly-Asp-OH were deprotonated at pH 10 using K_2CO_3, and subsequently neutralized by cautious addition of aqueous 1N HNO_3. Since the coordination bonds between water ligands and platinum are usually labile and subject to ligand substitution reactions,[101] it is presumed that carboxylate and amide (−C(O)NH−) groups would coordinate to the Pt center, generating a variety of derivatives in the aqueous environment. After removal of excess $[(DACH)Pt(OH_2)_2][NO_3]_2$ by dialysis, the light yellow solid was characterized by ^{1}H NMR spectra, and the loaded amounts of platinum were determined by neutron

activation analysis (NAA) spectrometry (Table III-5). In the ^{1}H NMR spectra (D_2O), chemical shifts ranging from 5.00 to 6.00 ppm are assigned to methine C*H* protons in the polycarbonate backbone. The broadening of methine resonance is due to the combination of various polymer conformations as Pt is coordinated by carboxylate and amide side chains. Moreover, the resonances of DACH are found within the range of 1.00−2.50 ppm. For PDHBAC-Asp-Pt, the loading was as high as 29.5% (wt/wt, relative to the polymer), while a lower loading (21.3%) was found with PDHBAC-Gly-Asp-Pt. As compared with the theoretical Pt loading (full Pt loading), the loaded percentage of Pt (86.0%) onto PDHBAC-Asp-OH is higher than that (68.3%) onto PDHBAC-Gly-Asp-OH. The water solubilities of PDHBAC-Asp-Pt and PDHBAC-Gly-Asp-Pt were determined to be 11 mg/mL and 13 mg/mL, respectively. Dynamic light scattering (DLS) analysis shows no hydrodynamic diameter distribution observed in PDHBAC-Asp-Pt and PDHBAC-Gly-Asp-Pt aqueous solutions, demonstrating platinum-polymer conjugates dissolve completely in water. In combination with NAA and DLS data, it is presumed that carboxylate, amide-chelating (*N*,*O*-coordinate mode) and amide, amide-chelating (*N*,*N*-coordinate mode) are dominant in the platinum-polymer conjugates. These results suggest that poly(3,4-dihydroxybutyric acid carbonate) and their related derivatives have the potential to serve as platinum drug delivery carrier for future anticancer pharmaceutical applications.

Table III-5. Neutron activation analyses for platinum determination.

Platinum-polymer conjugates	Pt (wt %)	Pt (wt %) (full loading)	% of Pt loading
PDHBAC-Asp-Pt	29.5	34.3	86.0
PDHBAC-Gly-Asp-Pt	21.3	31.2	68.3

Conclusions

In summary, we have synthesized new copolymers from *tert*-butyl 3,4-epoxybutanoate and carbon dioxide utilizing bifunctional cobalt(III) salen catalysts in the presence of sterically unhindered nucleophiles as initiators. The isolated polycarbonates contained more than 99% carbonate linkages and exhibited narrow molecular weight distributions. Poly(*tert*-butyl 3,4-dihydroxybutyrate carbonate) was shown to possess 100% head-to-tail regioselectivity and a glass transition temperature of 37 °C. A chiral, isotactic poly((*S*)-*tert*-butyl 3,4-dihydroxybutyrate carbonate) was synthesized which displayed a slightly higher T_g of 40 °C, and was characterized by a single ^{13}C NMR resonance in the carbonate region at 153.9 ppm. Deprotection of the pendant *tert*-butyl ester groups of poly(*tert*-butyl 3,4-dihydroxybutyrate carbonate) afforded hydrophilic poly(3,4-dihydroxybutyrate carbonate). Full degradation of acetyl-capped poly(3,4-dihydroxybutyrate carbonate) into the biomass, β-hydroxy-γ-butyrolacetone and 3,4-dihydroxybutyrate, in basic (pH = 8) aqueous solutions at 37 °C indicates that this polycarbonate is biodegradable, human-friendly, and environmentally-benign. Relevant to protecting anticancer drugs from nonspecific binding, increased circulation time, and taking advantage of the enhanced permeation and retention effect (EPR) of

macromolecules in cancer cells, platinum-polymer conjugates, PDHBAC-Asp-Pt and PDHBAC-Gly-Asp-Pt, were synthesized with platinum loading of 29.5% and 21.3%, respectively. As a result of their high Pt content (>65%) and the absence of a hydrodynamic diameter distribution being observed in PDHBAC-Asp-Pt and PDHBAC-Gly-Asp-Pt aqueous solutions, it may be concluded that carboxylate, amide-chelating (*N,O*-coordinate mode) and amide, amide-chelating (*N,N*-coordinate mode) are predominant in the platinum-polymer conjugates. Potentially, these polycarbonates and their platinum-polymer conjugates could expand the repertoire of biocompatible, biodegradable polymers available for future anticancer pharmaceutics.

Experimental Section

Materials and Methods. All manipulations involving air- or/and moisture-sensitive compounds were carried out in a glove box or with standard Schlenk technique under argon atmosphere. *Tert*-butyl 3,4-epoxybutanoate and methyl 3,4-epoxybutanoate were distilled over CaH_2 under reduced pressure prior to use. Methyl 3-butenoate was purchased from Sigma-Aldrich. Tetrahydrofuran (THF) was purified by an MBraun Manual Solvent Purification system packed with Alcoa F200 activated alumina desiccant. Bone-dry carbon dioxide supplied in a high-pressure cylinder and equipped with a liquid dip tube was purchased from Scott Specialty Gases. The bifunctional [(*1R,2R*-salen)Co(III)$(DNP)_2$] (DNP = 2,4-dinitrophenolate) catalysts were synthesized as described previously.[32]

Characterization Techniques. ^{1}H and ^{13}C NMR spectra were recorded on Mercury 300 MHz and Inova 500 MHz spectrometers. The peak frequencies were referenced versus the internal standard (TMS) shift at 0 ppm for ^{1}H NMR and against the solvent, chloroform-*d* at 77.0 ppm for ^{13}C NMR, respectively.

MALDI-TOF mass spectrometric measurement was performed on a Waters MALDI Micro MX mass spectrometer, equipped with a nitrogen laser delivering 3 ns laser pulses at 337 nm. α-Cyano-4-hydroxycinnamic acid (J&K, 97%) was used as a matrix. CH_3COOK (Aldrich, 98%) was added for ion formation.

Molecular weight determinations (M_n and M_w) were carried out with a Malvern Modular GPC apparatus equipped with ViscoGEL I-series columns (H+L) and Model 270 dual detector comprised of Refractive Index (RI) and Light Scattering detectors. The curve was calibrated using monodisperse polystyrene standards covering the molecular weight range from 580 to 460000 Da. In addition, THF was used as eluent for all GPC measurements.

Dynamic light scattering (DLS) measurements were conducted using Delsa Nano C (Beckman Coulter, Inc., Fullerton, CA) equipped with a laser diode operating at 658 nm. All measurements were made in water (n = 1.3328, η = 0.8878 cP) at 25 ± 1 °C. The concentration of PDHBAC-Asp-Pt and PDHBAC-Gly-Asp-Pt aqueous solution was 1 mg/mL. Scattered light was detected at a 15° angle and analyzed using a log correlator over 70 accumulations for a 0.5 mL of sample in a glass size cell (0.9 mL capacity). Prior to measurement, solutions were filtered through a 0.2 μm PTFE membrane filter to remove

dust particles. The photomultiplier aperture and the attenuator were automatically adjusted to obtain a photon counting rate of ca. 10 kcps.

Synthesis of *Tert*-butyl 3,4-Epoxybutanoate. To a 250 mL round-bottom flask charged with 3-butenoic acid (10.0 g, 0.116 mol) and *tert*-butyl acetate (60 mL, 0.458) was added catalytic amount of $BF_3 \cdot OEt_2$ (1 mL). The reaction mixture was stirred at ambient temperature for 48 h. The solution was quenched with water (25 mL), basified to pH = 12 with aqueous sodium hydroxide (4N) and extracted with diethyl ether (3 × 50 mL). Removal of solvent yielded *tert*-butyl 3-butenoate as a light yellow oil (yield 80%). ^{1}H NMR ($CDCl_3$, 300 MHz): δ 5.90 (m, 1H, CH_2=C*H*), 5.10-5.16 (m, 2H, C*H*$_2$=CH), 3.05-2.93 (m, 2H, C*H*$_2$COO^{tert}Butyl), 1.45 (s, 9H, C(C*H*$_3$)$_3$) ppm. To a solution of *tert*-butyl 3-butenoate (10 g, 70.4 mmol) in CH_2Cl_2 (100 mL) was added *m*-CPBA (24.0 g, 97.4 mmol, 1.4 equiv) in one portion at 0 °C. The reaction mixture was allowed to warm up to room temperature and stirred for 24 h. The white precipitate was filtered off. The filtrate was washed with saturated aqueous $NaHCO_3$ and dried over Na_2SO_4. The solution was concentrated and then distilled under a vacuum to afford the racemic epoxide as a colorless oil (yield 88%). ^{1}H NMR ($CDCl_3$, 300 MHz): δ 3.25 (m, 1H, OC*H*(CH_2)CH_2), 2.82 (t, 1H, OC*H*$_2$CH), 2.54 (m, 1H, OC*H*$_2$CH), 2.47 (t, 2H, C*H*$_2$COO^{t}Bu), 1.46 (s, 9H, C(C*H*$_3$)$_3$) ppm.

Hydrolytic Kinetic Resolution of *Tert*-butyl 3,4-Epoxybutanoate. Neat racemic *tert*-butyl 3,4-epoxybutanoate (3.0 g, 18.99 mmmol) was added to a 25 mL of round-bottom flask containing (*1S, 2S*)-salenCo(OAc) (0.06 g, 0.09 mmol). Water (0.19 mL, 10.56 mmol) was added dropwise, while the temperature was controlled, which must stay

below 15 °C. After the end of the addition, the reaction mixture was allowed to warm to room temperature (water bath was used to ensure temperature remained around 20 °C). The solution was stirred in air for 18 h and was then directly distilled under a vacuum to afford enantiomerically enriched (*S*)-*tert*-butyl 3,4-epoxybutanoate (1.32 g, 44%) as a colorless oil. ^{1}H NMR ($CDCl_3$, 300 MHz): δ 3.25 (m, 1H, OC*H*(CH_2)CH_2), 2.82 (t, 1H, OC*H*$_2$CH), 2.54 (m, 1H, OC*H*$_2$CH), 2.47 (t, 2H, C*H*$_2$COO^{t}Bu), 1.46 (s, 9H, C(C*H*$_3$)$_3$) ppm.

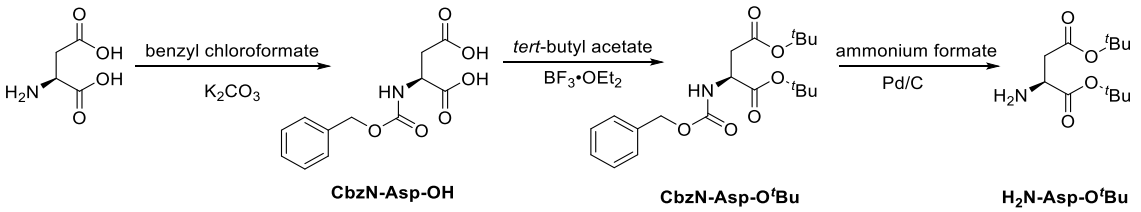

Scheme III-6. Synthesis of di-*tert*-butyl-*L*-aspartate (H_2N-Asp-O^{t}Bu).

Synthesis of Di-*tert*-butyl-*L*-aspartate (H_2N-Asp-O^{t}Bu) (Scheme III-6). Benzyl chloroformate (15 mL, 106 mmol) was added into a THF-H_2O solution (v/v = 1/2) of *L*-aspartic acid (13.31 g, 100 mmol) and K_2CO_3 (27.6 g, 200 mmol). The mixture was stirred for 12 h at room temperature, acidified with aqueous 3N HCl solution to pH = 2, and extracted with ethyl acetate. The organic layer was washed with water, and brine, and dried with Na_2SO_4. Removal of the solvent yielded CbzN-Asp-OH as a light yellow oil (yield 96%). ^{1}H NMR ($CDCl_3$, 300 MHz): δ 9.17 (brs, 2H, CH_2COO*H*, CHCOO*H*), 7.30 (m, 5H, Ar-*H*), 6.07 (s, 1H, N*H*), 5.07 (s, 2H, Ar-C*H*$_2$), 4.66 (m, 1H, CH_2C*H*NH), 2.73-3.08 (dd, 2H, CHC*H*$_2$COOH) ppm. To a solution of CbzN-Asp-OH (13.3 g, 50 mmol) in

100 mL of *tert*-butyl acetate was added catalytic amount of $BF_3 \cdot OEt_2$ (1 mL). The reaction mixture was stirred at ambient temperature for 48 h. The solution was quenched with water (25 mL), basified to pH = 12 with aqueous sodium hydroxide (4N) and extracted with ethyl acetate. The ethyl acetate layer was dried with Na_2SO_4 and the solvent was removed under reduced pressure to give CbzN-Asp-O^{t}Bu as a light yellow oil (yield 87%). ^{1}H NMR ($CDCl_3$, 300 MHz): δ 7.35 (s, 5H, Ar-*H*), 5.76 (s, 1H, N*H*), 5.12 (s, 2H, Ar-CH_2), 4.47 (m, 1H, CH_2CH(NH)COOH), 2.67-2.92 (dd, 2H, CHCH_2COOH), 1.45 (s, 9H, C(CH_3)$_3$), 1.43 (s, 9H, C(CH_3)$_3$) ppm. Pd/C (10%, 2g, 10% w/w) was added to a solution of CbzN-Asp-O^{t}Bu (19 g, 50 mmol) and ammonium formate (32 g, 500 mmol) in methanol (100 mL) and the suspension was stirred overnight at room temperature. The mixture was filtered through celite, and the solvent was removed under reduced pressure. The resultant residue was uptaken in ethyl acetate and cooled to 0 °C for overnight. The suspension was filtered and the filtrate was collected. Removed of ethyl acetate afforded H_2N-Asp-O^{t}Bu as a light yellow oil (yield 70%). ^{1}H NMR ($CDCl_3$, 300 MHz): δ 7.16 (brs, 2H, NH_2), 3.82 (s, 1H, C*H*NH_2), 2.80 (s, 2H, CHCH_2COO^{t}Bu), 1.46 (s, 9H, C(CH_3)$_3$), 1.45 (s, 9H, C(CH_3)$_3$) ppm.

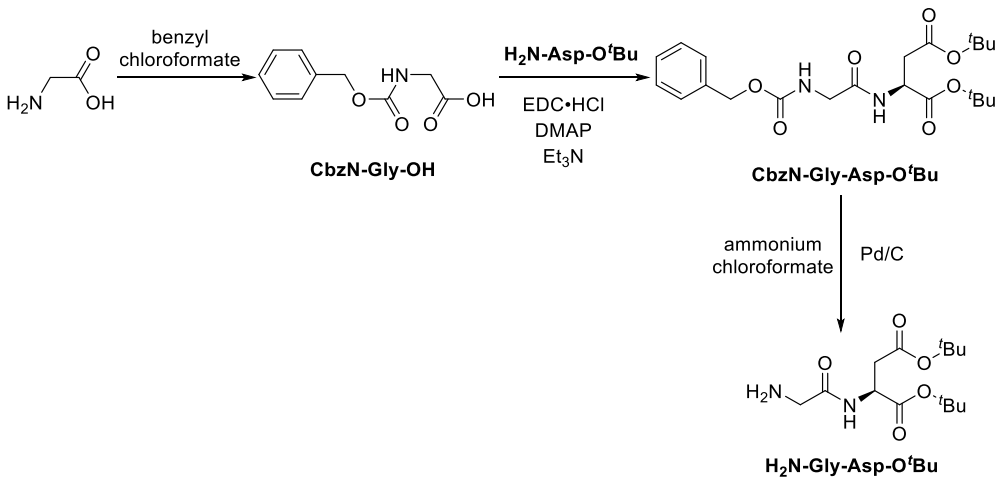

Scheme III-7. Synthesis of glycine-di-*tert*-butyl-*L*-Aspartate (H_2N-Gly-Asp-O^{t}Bu).

Synthesis of Glycine-di-*tert*-butyl-*L*-aspartate (H_2N-Gly-Asp-O^{t}Bu) (Scheme III-7). Benzyl chloroformate (15 mL, 106 mmol) was added into a THF-H_2O solution (v/v = 1/2) of glycine (7.5 g, 100 mmol) and K_2CO_3 (20.7 g, 150 mmol). The mixture was stirred for 12 h at room temperature, acidified with aqueous 3N HCl solution to pH = 2, and extracted with ethyl acetate. The organic layer was washed with water, and brine, and dried with Na_2SO_4. Addition of a large amount of diethyl ether into the concentrated solution led to the precipitation of CbzN-Gly-OH as a white solid (yield 96%). ^{1}H NMR ($CDCl_3$, 300 MHz): δ 7.35 (m, 5H, Ar-*H*), 5.25 (s, 1H, N*H*), 5.14 (s, 2H, Ar-CH_2), 4.04 (d, 2H, CH_2(NH)COOH) ppm. To a well-stirred mixture of CbzN-Gly-OH (2.09 g, 10 mmol), H_2N-Asp-O^{t}Bu (2.45 g, 10 mmol), *N*-(3-dimethylaminopropyl)-*N*′-ethylcarbodiimide hydrochloride (EDC·HCl, 2.88 g, 15 mmol) and 4-dimethylaminopyridine (DMAP, 1.22 g, 10 mmol) in dry CH_2Cl_2 (100 mL) was added trimethylamine (2.8 mL, 20 mmol) dropwise. The resulting mixture was stirred for 12 h

at ambient temperature and then quenched with 5% of aqueous citric acid (100 mL). The resulting solution was washed with brine and extracted with ethyl acetate. The ethyl acetate layer was dried with Na_2SO_4, and the solvent was removed under reduced pressure to give CbzN-Gly-Asp-O^{t}Bu as light yellow oil (yield 92%). ^{1}H NMR ($CDCl_3$, 300 MHz): δ 7.35 (s, 5H, Ar-*H*), 6.90 (s, 1H), 5.44 (s, 1H, N*H*), 5.12 (s, 2H, N*H*), 4.70 (m, 1H, C*H*(NH)COO^{t}Bu), 3.92 (s, 2H, COONHCH_2CONH), 2.67-2.92 (dd, 2H, CHCH_2COO^{t}Bu), 1.45 (s, 9H, C(CH_3)$_3$), 1.43 (s, 9H, C(CH_3)$_3$) ppm. Pd/C (10%, 2g, 10% w/w) was added to a solution of CbzN-Gly-Asp-O^{t}Bu (4.36 g, 10 mmol) and ammonium formate (6.3 g, 100 mmol) in methanol (100 mL) and the suspension was stirred overnight at room temperature. The mixture was filtered through celite, and the solvent was removed under reduced pressure. The resultant residue was uptaken in ethyl acetate and filtered. The filtrate was collected, washed with saturated $NaHCO_{3(aq)}$ and then ethyl acetate was removed to afford H_2N-Gly-Asp-O^{t}Bu as a light yellow oil (yield 70%). ^{1}H NMR ($CDCl_3$, 300 MHz): δ 8.00 (brs, 2H, N*H*), 4.70 (m, 1H, C*H*(NH)COO^{t}Bu), 3.37 (s, 2H, CH_2NH$_2$), 2.66-2.92 (dd, 2H, CHCH_2COO^{t}Bu), 1.43 (s, 9H, C(CH_3)$_3$), 1.42 (s, 9H, C(CH_3)$_3$) ppm.

Representative Procedures for the Polymerization of CO_2 with *Tert*-butyl 3,4-Epoxybutanoate. A 25 mL Parr autoclave was heated to 120 °C under vacuum for 8h, cooled under vacuum to room temperature and moved to a dry box. Catalyst **7-DNP** (11.5 mg, 0.01 mmol) and once-dried *tert*-butyl 3,4-epoxybutanoate (0.74 mL, 5 mmol, 500 equiv) were placed in the autoclave equipped with a magnetic stirrer. The autoclave was pressurized with 3.0 MPa of CO_2 and was placed in an oil bath at the desired temperature (25 or 40 °C). The CO_2 pressure was released after an allotted reaction time. A small

amount of the resultant polymerization mixture was removed from the autoclave for ^{1}H NMR analysis to quantitatively give the conversion of *tert*-butyl 3,4-epoxybutanoate. The crude polymer was dissolved in a 10 mL CH_2Cl_2/MeOH (5/1, v/v) mixture with 0.5% HCl solution and precipitated from methanol. This process was repeated 3-5 times to completely remove the catalyst, and white polymer was obtained by vacuum-drying. ^{1}H NMR ($CDCl_3$, 300 MHz): δ 5.32-5.15 (m, 1H, $CH_2CHOCOO$), 4.54-4.06 (m, 2H, $CHCH_2OCOO$), 2.79-2.51 (m, 2H, $CHCH_2COO^tBu$), 1.54-1.35 (m, 9H, $C(CH_3)_3$) ppm.

Preparation of Poly(3,4-dihydroxybutyrate carbonate). To a CH_2Cl_2 solution of poly(*tert*-butyl 3,4-dihydroxybutyrate carbonate) (0.202 g, 1 mmol) was added trifluoroacetic acid (0.23 mL, 3 mmol). The reaction mixture was stirred at ambient temperature for 12h. Addition of a large amount of diethyl ether led to the precipitation of poly(3,4-dihydroxybutyric acid carbonate) as a white solid. ^{1}H NMR (d_6-DMSO, 300 MHz): δ 12.62 (brs, 1H, COO*H*), 5.20-5.08 (m, 1H, $CH_2CHOCOO$), 4.45-4.10 (m, 2H, $CHCH_2OCOO$), 2.6 (m, 2H, CH_2COOH) ppm.

Preparation of Poly(potassium 3,4-dihydroxybutyrate carbonate). Aqueous solution (0.5 mL) of K_2CO_3 (0.062 g, 0.45 mmol) was added into methanol solution (4.5 mL) of poly(3,4-dihydroxybutyric acid carbonate) (0.146 g, 1 mmol). The resulting mixture was stirred for 1h at ambient temperature along with CO_2-releasing. A large amount of diethyl ether was added to precipitate the white solid, poly(potassium 3,4-dihydroxybutyrate carbonate). The pH value of the aqueous solution of poly(potassium 3,4-dihydroxybutyrate carbonate) was determined to be 6 using pH paper. For the study on the degradation of poly(potassium 3,4-dihydroxybutyrate carbonate) in D_2O at 37 °C,

the pH was adjusted to 8 by cautious addition of K_2CO_3 (in D_2O): ^{1}H NMR (D_2O, 300 MHz). δ 5.28 (m, 1H, $CH_2CHOCOO$), 4.55-4.18 (m, 2H, $CHCH_2OCOO$), 2.70-2.44 (m, 2H, CH_2COOK) ppm.

Synthetic Procedure for the Modification of Poly(3,4-dihydroxybutyric acid carbonate) with H_2N-Asp-O^{t}Bu or H_2N-Asp-O^{t}Bu. To a CH_2Cl_2 suspension of poly(3,4-dihydroxybutyric acid carbonate) (0.146 g, 1 mmol) and drops of anhydrous DMF was added oxalyl chloride (0.18 mL, 2 mmol) at 0 °C. The reaction mixture was stirred for 2 h at ambient temperature. Addition of a large amount of anhydrous diethyl ether into the solution led to the precipitation of poly(3,4-dihydroxybutyric acid chloride carbonate) (PDHBAC-Cl). A CH_2Cl_2 solution of amine (H_2N-Asp-O^{t}Bu: 0.49 g, 2 mmol or H_2N-Asp-O^{t}Bu: 0.604 g, 2 mmol) and trimethylamine (0.28 mL, 2 mmol) was added slowly into the CH_2Cl_2 solution of PDHBAC-Cl. The resulting mixture was stirred at room temperature for overnight. The reaction was quenched with 25 mL water and extracted with CH_2Cl_2. The organic layer was dried with Na_2SO_4 and the solvent was removed under reduced pressure. The obtained PDHBAC-Asp-O^{t}Bu or PDHBAC-Gly-Asp-O^{t}Bu crude product was dissolved in CH_2Cl_2 before adding 40 equiv of trifluoroacetic acid (3.1 mL, 40 mmol). The reaction mixture was stirred at ambient temperature for 12 h. A large amount of diethyl ether was added to precipitate PDHBAC-Asp-OH or PDHBAC-Gly-Asp-OH as white solids. For PDHBAC-Asp-OH, ^{1}H NMR (d_6-DMSO, 300 MHz): δ 12.52 (brs, 2H, CH_2COOH, $CHCOOH$), 8.40 (s, 1H, NH), 5.14 (m, 1H, $CH_2CHOCOO$), 4.70-3.95 (m, 3H, $CHCH_2OCOO$, $CH_2CH(NH)COOH$), 2.59 (m, 4H, overlapping DMSO) ppm. For PDHBAC-Gly-Asp-OH, ^{1}H NMR (d_6-DMSO, 300 MHz). δ 12.80 (brs, 2H,

CH_2COOH, $CHCOOH$), 8.53-8.03 (s, 1H, N*H*, N*H*), 5.16 (m, 1H, $CH_2CHOCOO$), 4.69-4.08 (m, 3H, $CHCH_2OCOO$, $CH_2CH(NH)COOH$), 3.74 (m, 2H, $NHCH_2CONH$), 2.59 (m, 4H, overlapping DMSO) ppm.

Synthesis of Platinum-polymer Conjugates. To the aqueous solution of polymer (PDHBAC-Asp-OH: 0.26 g, 1 mmol; or PDHBAC-Gly-Asp-OH: 0.32 g, 1 mmol) was added 4 equiv of K_2CO_3. The solution was stirred for 5 min and was filtered through a syringe filter (pore size = 0.2 μm). The pH of the filtrate was adjusted to 7.0 by cautious addition of 1N HNO_3(aq). To a 15 mL round-bottom flask containing [(DACH)$PtCl_2$] (1.14 g, 3 mmol) was added aqueous $AgNO_3$ (1.02 g, 6 mmol) with a trace amount of nitric acid, and the reaction was stirred for 12h at ambient temperature in the dark. The white precipitate, AgCl, was removed by centrifuge, and the aqueous solution was filtered through syringe filter to remove the residue AgCl particles. The platinating solution of [(DACH)Pt$(OH_2)_2$][NO_3]$_2$ was transferred into the aqueous polymer solution slowly with vigorous stirring, and the pH value of the resultant mixture was adjusted to 5.5 by careful addition of K_2CO_3. The reaction mixture was stirred for 12h at 37 °C and then filtered through a cotton ball to remove the gray solid. The collected light yellow solution was purified by dialysis against water for two days. After removal of water by lyophilization, the light yellow solid, PDHBAC-Asp-Pt and PDHBAC-Gly-Asp-Pt, was characterized by ^{1}H NMR spectroscopy (D_2O) and the loaded amount of platinum was analyzed by neutron activation analysis (NAA) spectrometry.

CHAPTER IV

TERPOLYMERIZATION OF PROPYLENE OXIDE AND VINYL OXIDES WITH CARBON DIOXIDE: COPOLYMER CROSS-LINKING AND SURFACE MODIFICATION VIA THIOL-ENE CLICK CHEMISTRY*

Introduction

In endeavors aimed at decreasing the use of petrochemical resources, the development of an alternative/additional carbon feedstock is mandatory for a sustainable chemical industry. Relevant to this long term goal, the transformation of carbon dioxide and epoxides into selective formation of biodegradable polymers or the corresponding cyclic carbonates represents a promising technology for large scale use of carbon dioxide.[22, 71b, 71d, 88a-g, 88j] Polycarbonates derived from this methodology are in general rather inert materials which lack functionality for subsequent modification to achieve desired properties. In this regard, there has been a lot of interest in preparing CO_2 copolymers bearing active side chain groups such as carboxylic acids,[34-35] alcohols,[40-41] furfuryls,[39] alkynes[37] and alkenes.[38] These functionalities allow for postpolymerization modification to yield polymers with a wide range of properties. For example, a triblock polymer, poly(allyl glycidyl ether carbonate)-*b*-poly(propylene carbonate)-*b*-poly(allyl glycidyl ether carbonate), was synthesized and subsequent functionalization with various

* Portions reprinted (adapted) from "Terpolymerization of Propylene Oxide and Vinyl Oxides with CO_2: Copolymer Cross-linking and Surface Modification *via* Thiol-ene Click Chemistry." Darensbourg, D. J.; Wang, Y. *Polym. Chem.*, **2015**, *6*, 1768-1776. Reproduced by permission of The Royal Society of Chemistry.

thiols by thiol-ene click chemistry allows for installation of different water-soluble moieties onto the polymer backbone, as demonstrated in Chapter II.

Thiol-ene click chemistry and other postpolymerization functionalization reactions can be exploited to prepare cross-linked networks by interconnecting different polymer chains using multifunctional cross-linkers. Such cross-linking may yield polymers with improved thermal and mechanical properties. For instance, Kleij and co-workers cured terpolymers of limonene oxide/cyclohexene oxide/CO_2 with a stoichiometric amount of a dithiol reagent.[84] The resultant cross-linked materials exhibited improved thermal properties with their decomposition temperature in the range of 250-280 °C and with glass transition temperature of up to 150 °C.

In this chapter, we report the preparation of cross-linked materials based on poly(propylene carbonate) (PPC). PPC is one of the mostly investigated CO_2-derived polymers and its production has been commercialized by several companies around the world. PPC exhibits many favorable properties such as biodegradability, transparency, excellent adhesion and low permeability for oxygen and water.[103] However, the low glass transition (~ 37 °C) of PPC has prevented its use in many applications, especially as structural materials. To overcome this limitation, we incorporated vinyl epoxides (VIO and AGE, Figure IV-1) into the copolymerization reaction of propylene oxide (PO) and carbon dioxide to introduce cross-linkable alkene pendant groups. The resultant terpolymer was cured with thiol reagents *via* thiol-ene click chemistry to improve their mechanical and thermal properties. A comparison of the mechanical and thermal properties of such polymeric materials will be examined based on their cross-linking

densities. Further, the preparation of surface functionalized polymer films will be described utilizing photoinitiated thiol-ene chemistry. These modified films should serve to immobilize biomolecules or metal nanoparticles on their surfaces.[104]

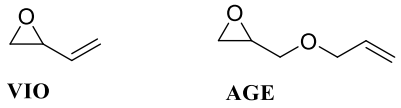

Figure IV-1. Vinyl epoxides employed in the terpolymerization reactions. VIO: 2-vinyl oxirane; AGE: allyl glycidyl ether.

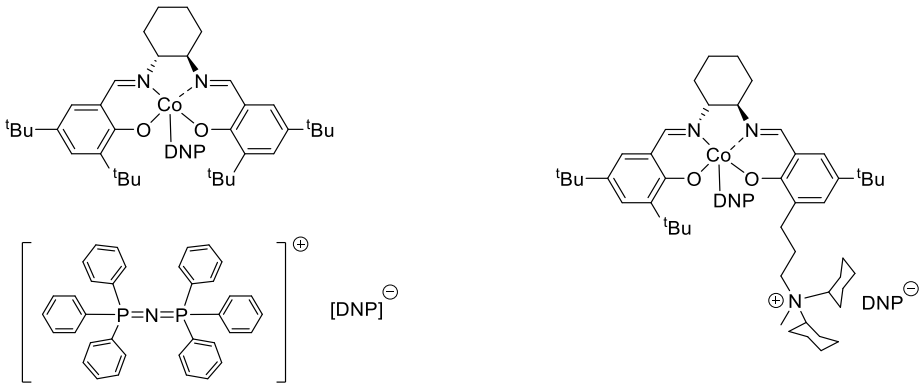

Figure IV-2. Catalyst systems utilized in terpolymerization reactions: binary catalyst (left) and bifunctional catalyst (right).

Results and Discussion

Terpolymerization Reactions of Propylene Oxide, Vinyl Oxides, and Carbon Dioxide. A useful means of expanding the range of both physical and mechanical properties of copolymers derived from CO_2 and epoxides is to synthesize polymeric materials incorporating two chemically different epoxide monomers. This methodology

as well provides an opportunity for introducing functionality into these otherwise inert polymers. Herein, we have prepared terpolymers of propylene oxide, vinyl epoxides, and carbon dioxide; whereby, the vinyl groups afford sites for postpolymerization functionalization *via* thiol-ene click chemistry. These reactions were performed using catalysts (Figure IV-2) and conditions such that the process was 100% selective for production of completely alternating copolymers, i.e., there was no spectroscopic evidence for formation of cyclic carbonates. Terpolymers with ~ 25 % vinyl groups (PO/AGE feed ratio is 3:1) are targeted. To aid in interpreting the formation of these terpolymers, kinetic studies have been carried out. Table IV-1 contains the experimental data for the terpolymerization of propylene oxide/2-vinyloxirane and carbon dioxide at different feed ratios. The Fineman-Ross plot is illustrated in Figure IV-3, where there is low conversion of reactants to product.[105] A bifunctional catalyst (Figure IV-2, right) was utilized in this study to avoid the formation of cyclic carbonate byproducts.

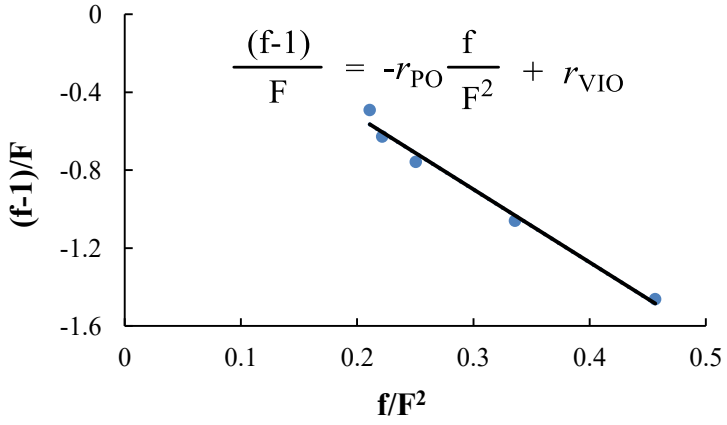

Figure IV-3. Fineman-Ross plot for the terpolymerization of PO/VIO/CO_2 at 25 °C, where the slope equals $-r_{PO}$ and the intercept equals r_{VIO}.

Table IV-1. Terpolymerization of PO/VIO/CO_2.[a]

entry	Monomer/catalyst		Reaction time (h)	Conversion (%)		F (VIO/PO) in feed	f (VIO/PO) in polymer	f/F^2	(f-1)/F
	PO	VIO		PO	VIO				
1	1127	1468	3.5	10	2.7	1.303	0.358	0.211	-0.493
2	1221	1387	3.5	9.8	2.5	1.136	0.286	0.222	-0.628
3	1315	1305	3.5	8.4	2.0	0.993	0.247	0.251	-0.758
4	1502	1142	2.5	5.8	1.5	0.760	0.194	0.336	-1.060
5	1690	979	2.75	4.6	1.2	0.579	0.153	0.456	-1.463

[a]Reaction conditions: 25 °C, 2.5 MPa CO_2 pressure.

Using a Fineman-Ross analysis, the monomer reactivity ratios of the two epoxides were determined by varying the monomer feed ratio and observing the monomer composition in the resulting copolymers by ^{1}H NMR spectroscopy during the early stages of the reactions. These kinetic measurements provide an assessment of the relative conversion rates of the two epoxide monomers. These relative conversion rates are determined by both the binding constant of the epoxide to the metal center as well as the rate constant for the ring-opening process (Scheme IV-1). A comparable set of reactions can be described where the carbonate species contains the vinyl group (**C** and **D**, Scheme IV-1) with a corresponding k_{21} and k_{22} rate constants. If we assume the carbonate binding energies are approximately the same for the two different epoxides, the equilibrium constants in pathways **A** and **C**, i.e., K_1 and K_1', and pathways **B** and **D**, i.e., K_2 and K_2' will be the same, respectively, mainly being dependent on the metal-epoxide binding energies. From the graph in Figure 1, r_{PO} and r_{VIO} were found to be 3.74 and 0.224, respectively. If these values are modified to account for their difference in the metal binding abilities of these two epoxides, where their respective pK_bs are 15.7 and 16.3, k_{11}/k_{12} and k_{22}/k_{21} are determined to be 0.941 and 0.892. That is, there is little rate difference for self-propagation *vs* cross-propagation. Nevertheless, because of the difference in metal epoxide binding constants, a 3:1 feed mixture of monomers, PO and VIO will result in a tapered terpolymer.

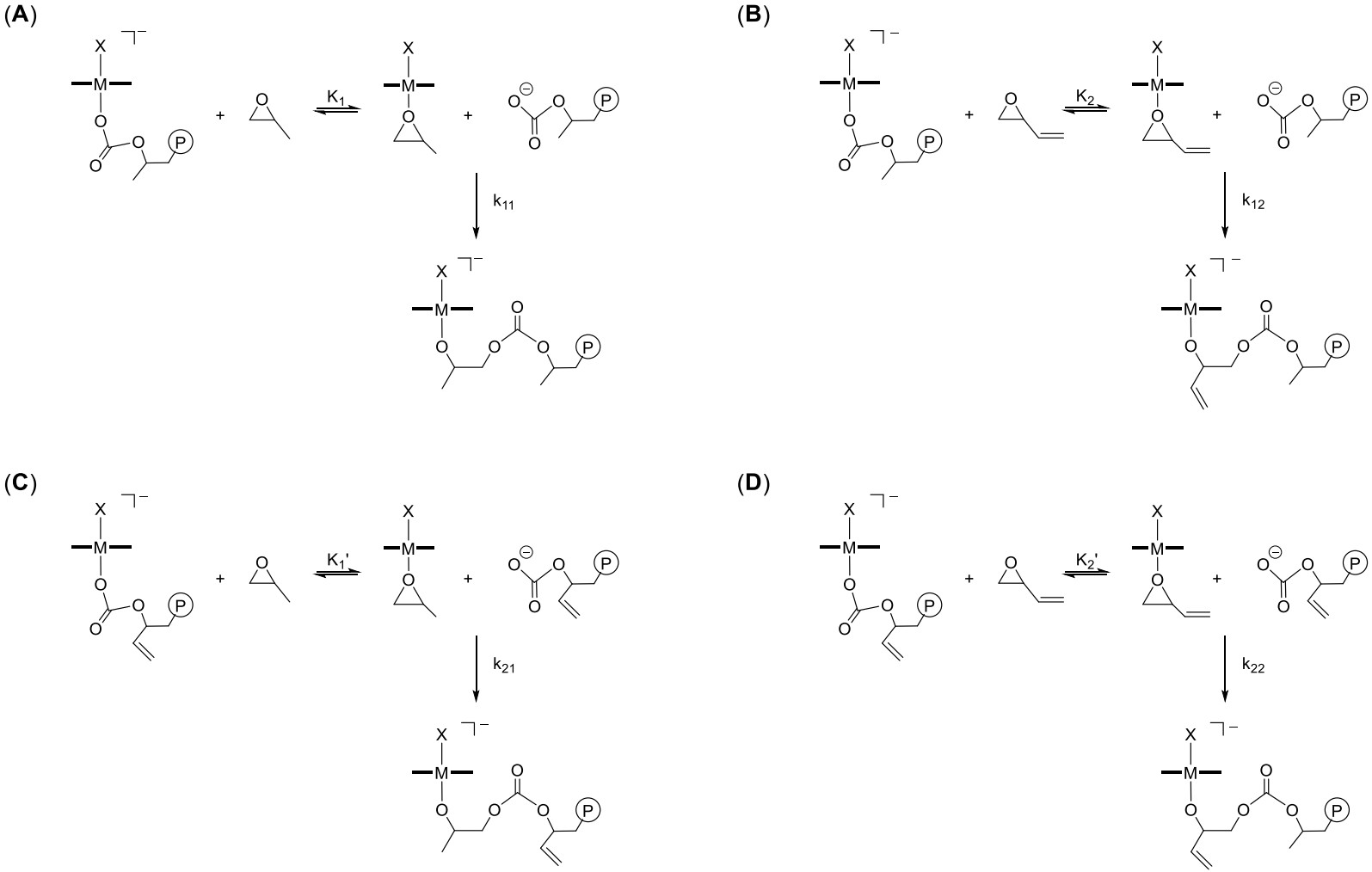

Scheme IV-1. (**A**) Self-propagation pathway for propylene oxide; (**B**) cross-propagation pathway for propylene oxide; (**C**) cross-propagation pathway for 2-vinyloxirane; (**D**) self-propagation pathway for 2-vinyloxirane.

A similar kinetic treatment of the terpolymerization reactions of propylene oxide, allyl glycidyl ether, and CO_2 was performed with the experimental findings summarized in Table IV-2. From the Fineman-Ross plot illuminated in Figure IV-4, the r_{PO} and r_{AGE} parameters were determined to be 0.755 and 0.876, respectively. Since the pK_bs of the epoxide binding sites are expected to be quite similar, these reactivity ratios likely are representative of k_{11}/k_{12} and k_{22}/k_{21}. Hence, a 3:1 feed mixture of the two monomers, PO and AGE, are anticipated to afford a rather homogeneous random terpolymer during extended reaction times.

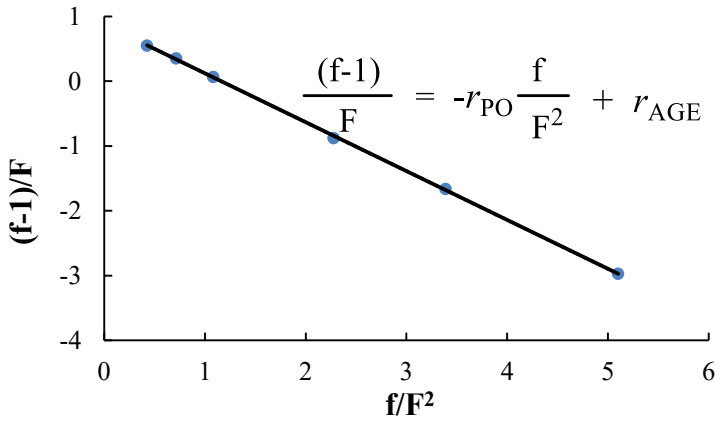

Figure IV-4. Fineman-Ross plot for the terpolymerization of PO/AGE/CO_2 at 25 °C, where the slope equals $-r_{PO}$ and the intercept equals r_{AGE}.

Table IV-2. Terpolymerization of PO/AGE/CO_2.[a]

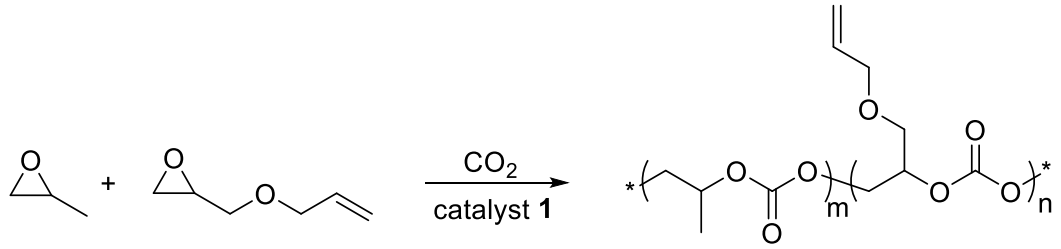

entry	Monomer/catalyst		Reaction time(min)	Conversion(%)		F (AGE/PO) in feed	f (AGE/PO) in polymer	f/F^2	(f-1)/F
	PO	AGE		PO	AGE				
1	675	1555	50	1.9	6.4	2.310	2.273	0.426	0.551
2	956	1393	50	4.8	8.5	1.457	1.515	0.714	0.354
3	1237	1227	50	7.0	8.7	0.992	1.065	1.082	0.066
4	1799	895	50	6.8	7.6	0.497	0.563	2.279	-0.879
5	2080	730	50	8.0	9.6	0.351	0.417	3.388	-1.663
6	2361	564	50	8.0	9.8	0.239	0.291	5.102	-2.972

[a]Reaction conditions: 25 °C, 2.5 MPa CO_2 pressure.

(**a**) (**b**)

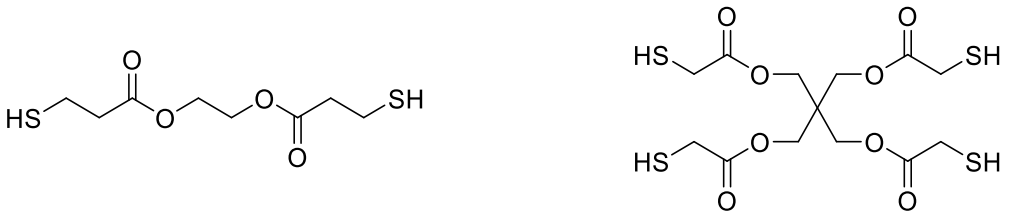

Figure IV-5. Cross-linker utilized: (**a**) ethylene glycol *bis*(3-mercaptopropionate); (**b**) pentaerythritol *tetrakis*(mercaptoacetate).

Cross-linking of Terpolymers. Because the terpolymers derived from a 3:1 mixture of PO and AGE along with CO_2 is more randomized than its vinyl epoxide analog VIO, we choose to examine the photo-induced cross-linking of this polymeric material *via* thiol-ene chemistry. For these experiments, two cross-linkers were employed, one flexible (**a**) and one more rigid (**b**) (Figure IV-5). The resulting cross-linked materials were characterized by Raman spectroscopy, where the polycarbonate exhibits a peak at 1647 cm^{-1} arising from the alkene C=C stretching vibration and a peak at 1750 cm^{-1} corresponding to the C=O vibration of the carbonate group. It is noteworthy here that the carbonate groups from the cross-linkers only account for a small portion of the overall carbonate peak intensity in the polymer. Hence, the carbonate peak at 1750 cm^{-1} can be used as a reference peak. Upon plotting the ratio of the peak areas of 1647 cm^{-1}/1750 cm^{-1} against the theoretical double bond conversion (based on added thiol), a near linear relationship was observed as shown in Figure IV-6. Full conversion of the double bond could be achieved, indicating that both SH groups of cross-linker (**a**) and all four SH groups of cross-linker (**b**) reacted quantitatively with the alkene moieties.

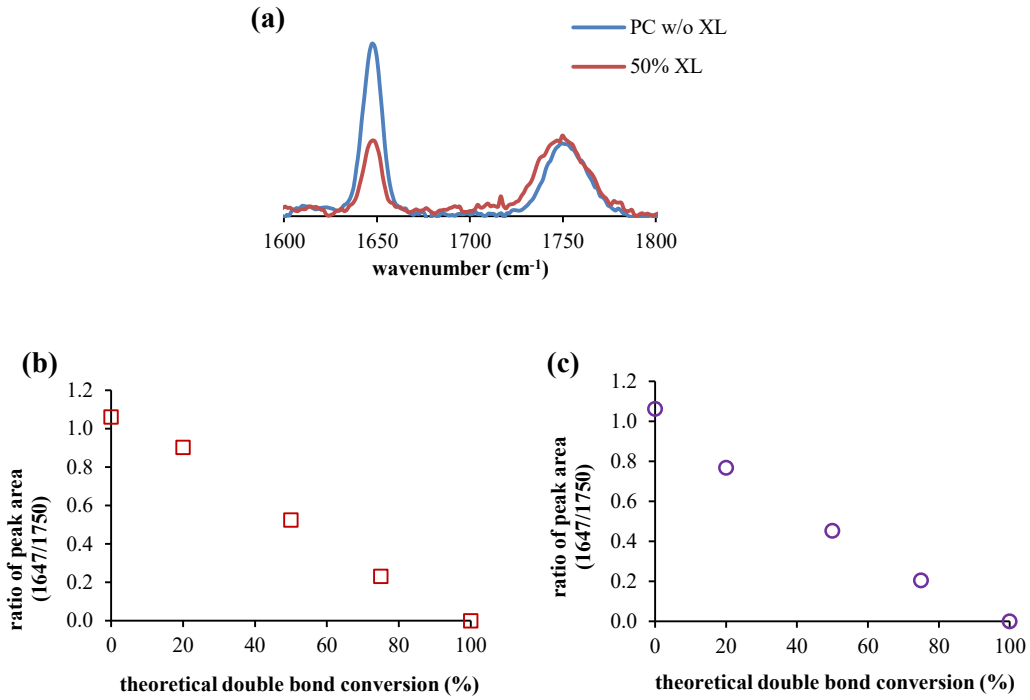

Figure IV-6. (a) Normalized FT-Raman spectrum of a polycarbonate film w/o cross-linking and an example of **a** based cross-linked film with 50% double bond conversion. (b) Plot of peak area ratio (C=C/C=O) against theoretical double bond conversion based on normalized FT-Raman spectra of **a** based cross-linked polymer films. (c) Plot of peak area ratio (C=C/C=O) against theoretical double bond conversion based on normalized FT-Raman spectra of **b** based cross-linked polymer films.

In order to examine the mechanical and thermal properties of these irradiation cured cross-linked polycarbonate films as a function of the cross-linker and cross-linking density, dynamic mechanical analysis (DMA) measurements were performed. At low conversion of C=C bonds of 20%, both (**a** and **b**) cross-linked films behave as lightly-cross-linked thermosets, featuring a decreasing rubbery modulus with increasing temperature and an unsymmetrical tanδ curve (Figures IV-7 and Figure IV-8). For polymer films with 50% or higher conversion of the double bonds, these behave as typical cross-linked networks with a rubbery modulus plateau that is constant with increasing

temperature. Tanδ peaks for these films are more symmetrical. For films with higher cross-link densities (50–100%), the cross-linker **a** based films have similar rubbery moduli as indicated in Table IV-3, whereas, for cross-linker **b** based films, there is a 50% increase in the rubbery modulus between 50% and (75–100%) C=C bond conversion. It was observed that the cross-linker **b** based films with high cross-link densities (75–100%) were noticeably harder and more brittle than those with lower cross-link densities. This is expected due to the increasing stiffness of the films.

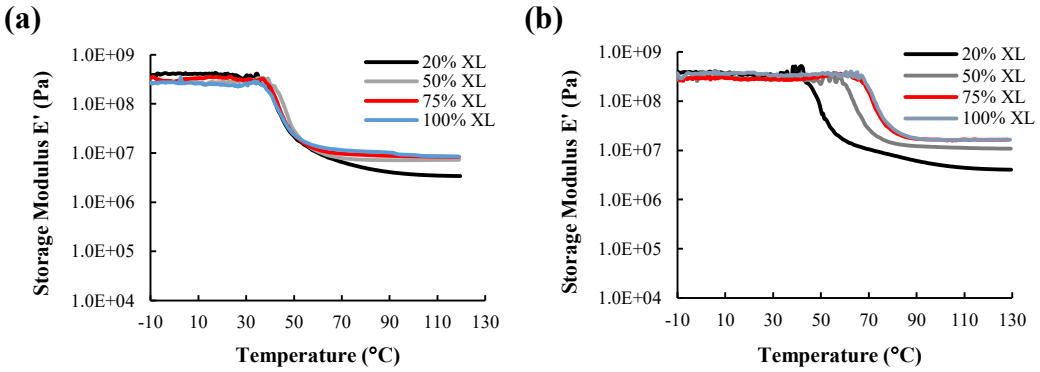

Figure IV-7. Storage modulus E' of (a) cross-linker **a** based films and (b) cross-linker **b** based cross-linked films.

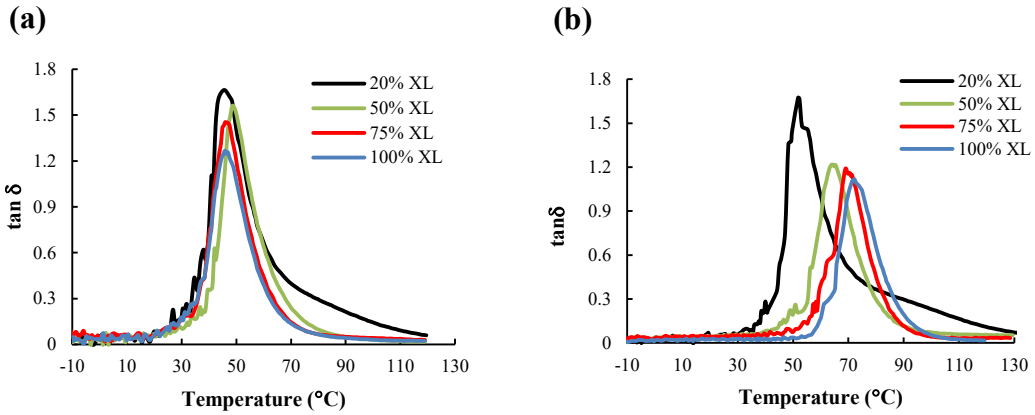

Figure IV-8. Tanδ *vs* temperature of (a) cross-linker **a** based films and (b) cross-linker **b** based cross-linked films.

Table IV-3. Rubbery moduli as a function of cross-linker and cross-link densities.

Conversion (C=C)	E′ @110°C, **a** based film (MPa)	E′ @110°C, **b** based film (MPa)
20%	3.47	4.40
50%	7.22	11.21
75%	8.41	16.64
100%	8.61	16.24

Table IV-4. Glass transition temperatures (T_gs) of cross-linked polycarbonates.

Conversion (C=C)	T_g **a** based film (°C)	T_g **b** based film (°C)
20%	45.5	51.8
50%	48.6	64.0
75%	45.9	69.1
100%	45.8	72.2

Table IV-4 summarizes the glass transition (T_g) values for the various cross-linked polycarbonate films as defined by the peak of tanδ curves (Figure IV-8). For cross-linker **a** based films, the changes in T_g with cross-linking densities are negligible. On the other hand, the films based on cross-linker **b** exhibit an increase in T_g with increasing cross-linking densities, from 52 ºC for low C=C bond conversion to 72 ºC for complete C=C bond conversion. This difference in thermal properties between the **a** and **b** based cross-linked films can be anticipated given the structures of the cross-linkers. That is, ethylene glycol *bis*(3-mercaptopropionate) is a longer flexible difunctional cross-linker, whereas, pentacrythritol *tetrakis*(mercaptoacetate) has increased functionality and has shorter bridges hinged at a central point. As a result, upon connecting two pendant groups of polycarbonate backbones, the dithiol cross-linker provides long flexible bridges. The increasing network cross-linking is counterbalanced by the flexibility of the bridges which accounts for the similar T_gs. For the tetrathiol cross-linker, the bridges between the polycarbonate backbones are much less flexible, thereby, as more cross-linking occurs higher T_gs are achieved for the films. This is depicted in the skeletal drawings in Figure IV-9.

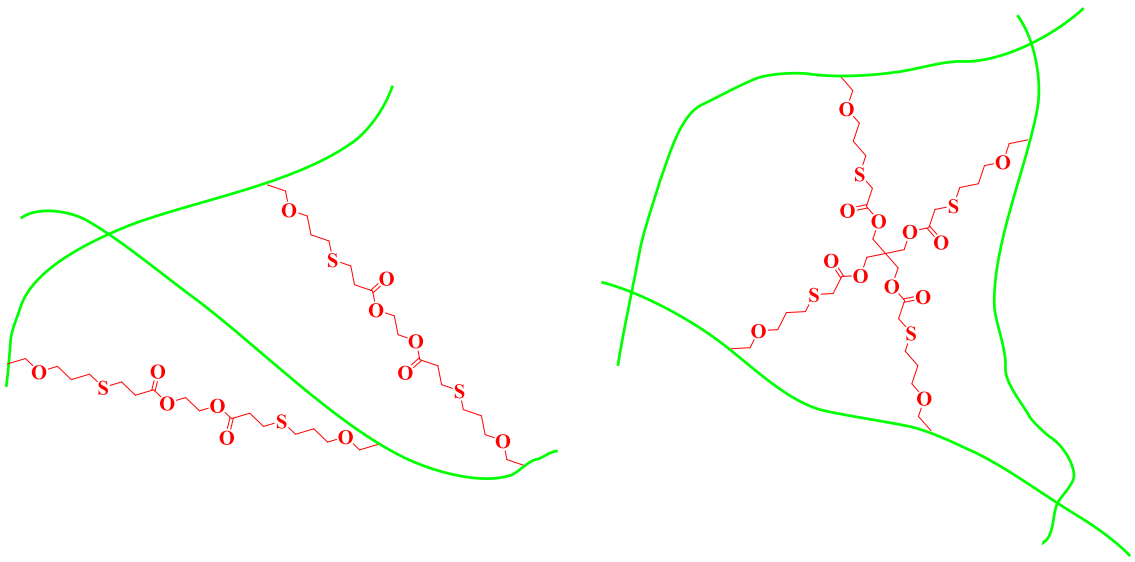

Figure IV-9. Carton drawings of **a** and **b** based cross-linked polycarbonates.

Surface Functionalization of Cross-linked Polymer Films. Surface functionalization of the cross-linked polymer films by thoil-ene reactions was investigated. *N*-acetyl-*L*-cysteine (NAC) was chosen since its amide group can be easily detected in infrared spectroscopy. Additionally, its carboxyl group has the potential for bioconjugation which provides a platform for the development of biomaterials. The cross-linked polycarbonate films with 25% double bond conversion were selected and submerged into a solution of NAC in THF followed by exposure to UV irradiation. The successful attachment of NAC onto the film was confirmed by ATR-FTIR spectroscopy (Figure IV-10). The C=O and C-N stretching peaks of the NAC amide group were observed at 1635 and 1527 cm^{-1}, respectively. XPS analysis was also performed on the functionalized films (Figure IV-11). The availability of NAC on the surface was

confirmed by the presence of N_{1s} emission at 398 eV which was attributed to the NH group.

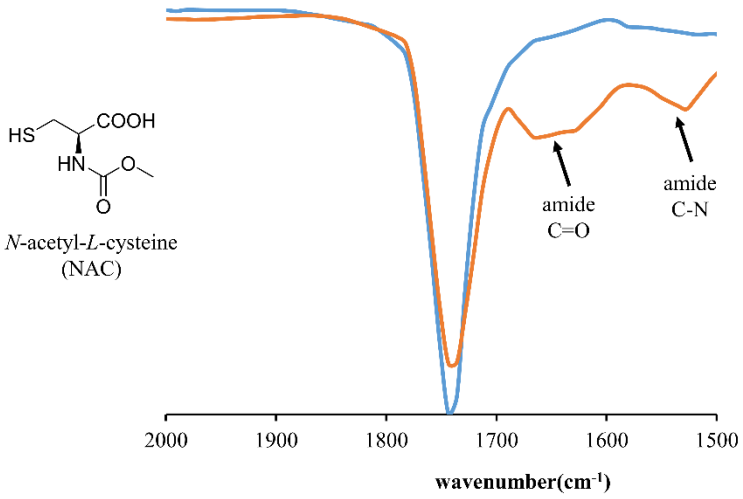

Figure IV-10. ATR-IR spectra of cross-linked PC films without functionalization (blue) and the NAC functionalized cross-linked film (orange).

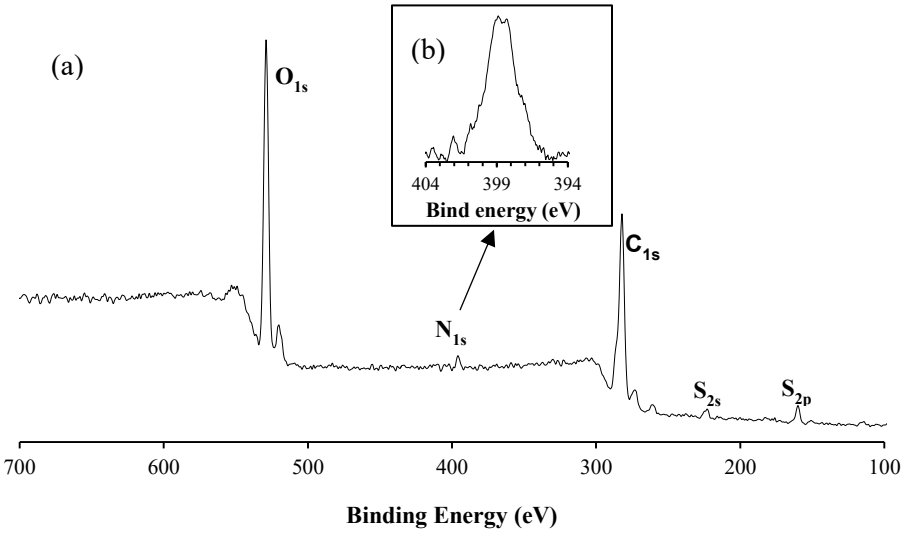

Figure IV-11. (a) XPS low-resolution survey spectra of NAC functionalized film. (b) XPS narrow scan of the N_{1s} region of the NAC functionalized film.

In order to introduce the amine functional group, 2-(Boc-amino)ethanethiol was used as the mono-thiol. Following a similar procedure as employed for NAC, 2-(Boc-amino)ethanethiol was attached to the films as confirmed by ATR-IR. As Figure IV-12 shows, there was a shoulder at the C=O peak region which arose from the Boc C=O group. The peak at 1512 cm^{-1} was associated with the C-N stretching. Deprotection of Boc protected amine groups was performed by submerging the film in trifluoroacetic acid.[20] Unfortunately, the film surface was shattered subsequent to being removed from the acid. Most likely, the film underwent degradation in the presence of a strong acid. Since it was inevitable for 2-(Boc-amino)ethanethiol to diffuse into the film to react with the alkene moieties, another possible reason was that the escaping of CO_2 coming from the deprotection of Boc groups destroyed the integrity of the film.

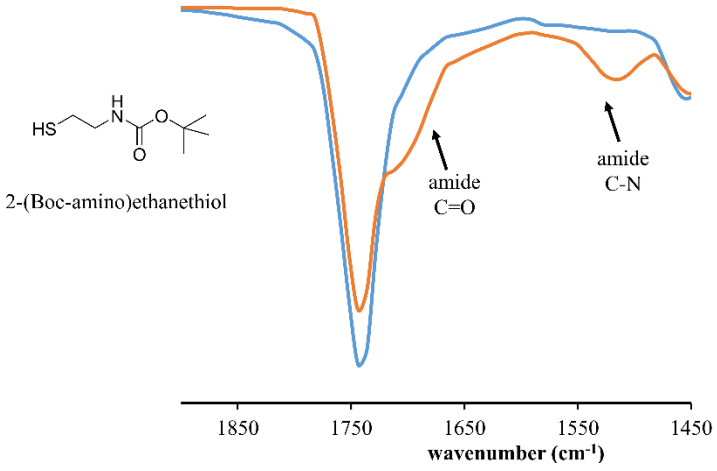

Figure IV-12. ATR-IR spectra of cross-linked PC films without functionalization (blue) and 2-(Boc-amino)ethanethiol functionalized cross-linked film (orange).

Conclusions

The kinetic study of terpolymerization of propylene oxide, vinyl oxiranes and CO_2 provided information about how the pendant vinyl group distributes themselves along the polymer chain. Terpolymers of allyl glycidyl ether/propylene oxide/CO_2 produced a more even or random distribution of vinyl groups in the terpolymer chain as compared with the terpolymer derived from 2-vinyloxirane/propylene oxide/CO_2. The terpolymer of allyl glycidyl ether/propylene oxide/CO_2 was chosen for the preparation of cross-linked polymer films, where a dithiol and a tetrathiol were used as cross-linkers. FT-Raman spectra indicated that the SH groups reacted quantitatively with the vinyl groups of the polymer. The mechanical and thermal properties of the cross-linked films with different cross-linking densities were tested using dynamic mechanical analysis (DMA). For dithiol based films, the changes of T_g (as defined by the peak of tanδ curves) were negligible. This is thought to be due to the flexibility of the cross-linker. When a more rigid tetrathiol was used as cross-linker, the T_g of the obtained films increased with increasing cross-linking density. With regard to storage modulus, when the conversion of double bond was only 20%, the films obtained showed a decreasing rubbery moduli as temperature increased. With higher cross-linking densities, the rubbery moduli of the films reached a plateau after the transition. Additionally, surface-functionalization of cross-linked films were achieved by thiol-ene grafting of *N*-acetyl-*L*-cysteine onto the surface as confirmed by IR and XPS spectroscopy. The functionalized films provide an example of biodegradable material for potential biomedical applications.

Experimental

Materials and Methods. Allyl glycidyl ether (97%, Alfa) and 2-vinyloxirane (98%, Alfa) were distilled over CaH_2 under reduced pressure prior to use. Ethylene glycol *bis*(3-mercaptoproionate) and pentaerythritol *tetrakis*(mercaptoacetate) were purchased from Wako. 2,2-Dimethoxy-2-phenylacetophenone (DMPA) was obtained from TCl (98%). *N*-acetyl-*L*-cysteine and 2-(Boc-amino)ethanethiol were acquired from Amresco and Sigma-Aldrich, respectively. Tetrahydrofuran (THF), dichloromethane, and toluene were purified using an MBraun manual solvent purification system packed with Alcoa F200 activated alumina desiccant. Bone-dry carbon dioxide supplied in a high-pressure cylinder and equipped with a liquid dip tube was purchased from Scott Specialty Gases. The CO_2 was further purified by passing through two steel columns packed with 4 Å molecular sieves that had been dried under vacuum at $\geq$200 ^{o}C.

Characterization Techniques. ^{1}H NMR spectra were recorded on a Mercury 300 MHz spectrometer in $CDCl_3$. Gel Permeation Chromatography (GPC) measurements were performed with a Malvern modular GPC apparatus equipped with ViscoGEL I-series columns (H & L) using THF as eluent, and the molecular weights were calculated based on polystyrene standards. Attenuated Total Reflection Fourier Transform Infrared (ATR-FTIR) and Fourier Transform Raman Spectroscopy (FT-Raman) spectra were measured in the solid state using a SHIMADZU IR Affinity-1 spectrophotometer and Horiba Jobin-Yvon LabRam IR system using a 785 nm laser line, respectively. Differential Scanning Calorimetry (DSC) measurements were performed with a polymer DSC instrument by Mettler Toledo at a heating rate of 5 ^{o}C/min. The polymer samples were cured using a

CL-1000 ultraviolet cross-linker (UVP, Inc.) with the UV light intensity at 365 nm being 1000 mJ/cm^2. Dynamic Mechanical Analysis (DMA) of polymer films was conducted using a DMA analyzer in compression mode (Mettler Toledo TT-DMA system). The specimens with approximate dimensions of 3.50 mm × 2.60 mm × 0.65 mm were analyzed at a frequency of 1 Hz with a heating rate of 3 ºC/min in air. X-ray photoelectron spectroscopy (XPS) spectra were acquired from an Omicron XPS system with Argus detector. The system uses Omicron's DAR 400 dual Mg/Al X-ray source for XPS measurements.

General Terpolymerization Reactions. The catalyst and epoxides were added to a 15 mL stainless steel reactor which had been previously dried at 170 ºC for 6 hours, and pressurized with CO_2 at 2.5 MPa. Following the allotted reaction time at ambient temperature, the reactor was cooled in an ice bath for 10 minutes prior to depressurization. An aliquot of the solution was analyzed by ^{1}H NMR to calculate the relative conversions of the two epoxides. The bulk polymer was isolated by dissolution in minimal amounts of dichloromethane, followed by precipitation in 1M HCl in methanol. This procedure was repeated 2 – 3 times to completely remove the catalyst. The polymer was subsequently dried in a vacuum oven.

Terpolymerization Reactions of Propylene Oxide (PO)/ 2-Vinyloxirane (VIO) and CO_2 (Table IV-1). The general terpolymerization procedure was followed. The bifunctional (salen)Co^{III}DNP complex (0.0035 g, 0.003 mmol) was used as the catalyst. Various ratios of PO and VIO were used, and the total volumes were maintained at 0.60 mL.

Terpolymerization Reactions of Propylene Oxide (PO)/Allyl Glycidyl Ether (AGE) and CO_2 (Table IV-2). The general terpolymerization procedure was followed. The binary catalyst system (salen)Co^{III}DNP/PPNDNP (0.0040 g, 0.005 mmol) was employed as the catalyst. Various ratios of PO and AGE were used and the total volumes were maintained at 1.18 mL. The precipitation step was repeated 2-3 times to completely remove all residual catalyst. For the first precipitation cycle, ca. 0.5 g of *p*-methoxyphenol was added to the dichloromethane solution to forestall self-cross-linking.

Preparation of Cross-linked Polycarbonate Films. The PO/AGE/CO_2 terpolymer was prepared following the general terpolymerization procedure. The binary catalyst system (salen)Co^{III}DNP/PPNDNP (0.0874 mmol), PO (4.6 mL, 65.7 mmol), AGE (2.59 mL, 21.8 mmol) and 6 mL dichloromethane/toluene (1:1 by volume) mixture were added into a 50 mL autoclave, and pressurized to 2.5 MPa. After 24 h at room temperature, the CO_2 pressure was slowly released. The crude polymer was dissolved in CH_2Cl_2 and precipitated from methanol. The process was repeated 2-3 times to completely remove all residual catalyst. For the first precipitation cycle, ca. 0.5 g of *p*-methoxyphenol was added to the dichloromethane solution to forestall self-cross-linking. The isolated polymer has 28% allyl glycidyl ether carbonate unit (from ^{1}H NMR analysis). GPC: M_n = 23900 g/mol, PDI = 1.146. DSC: T_g = 18.4 °C.

A glass mold was constructed by taping glass microscope slides together, the depth being 1 mm. 0.40 g of PO/AGE/CO_2 terpolymer was dissolved in 1 mL of dry tetrahydrofuran. Aliquots of 1.5 mM pentaerythritol *tetrakis*(mercaptoacetate) (1.5 mM in THF) and 2,2-dimethoxy-2-phenylacetophenone (0.4 mM in THF) were added to the

polymer solution to achieve various cross-linking ratios. The ratio of SH groups to initiator was kept at 60/1. The polymer solution was added into the glass mold, and it was covered with an additional glass slide. The polymer solution was cured with 365 nm UV light for 8 minutes on each side. A slightly yellow, transparent polymer film was obtained, and it was rinsed with tetrahydrofuran to remove the unreacted cross-linkers and initiator. The cross-linked polymer was dried in a vacuum oven at 60 °C thereafter. The same procedure was followed when using ethylene glycol *bis*(3-mercaptopropionate) as cross-linker.

General Procedure for Surface Functionalization of Polymer Films. Functional thiols (0.45 mmol) and DMPA (0.09 mmol) were mixed in 1 ml solvent and transferred onto the cross-linked film surface followed by UV curing. After 10 minutes, the film was taken out and washed with solvent to remove residue thiol and photoinitiator. The film was submerged in solvent overnight before drying in a vacuum oven for 48 h (60 °C).

For functionalization with 2-(Boc-amino)ethanethiol, THF was used as solvent. For functionalization with *N*-acetyl-*L*-cysteine, THF/methanol (3/2 volume) mixture was used.

Deprotection of Boc Group. The functionalized polymer film with 2-(Boc-amino)ethanethiol was submerged into trifluoroacetic acid for one hour followed by neutralizing with excess KOH solution and washing with deionized water.

CHAPTER V

SUMMARY AND CONCLUSIONS*

In the past three decades, the catalytic coupling of epoxides and carbon dioxide has become an important pathway to produce aliphatic polycarbonates. Indeed, this process has been commercialized by several companies including Empower Materials, Saudi Aramco, and Covestro for the production of poly(propylene carbonate) (PPC), poly(ethylene carbonate) (PEC), and poly(cyclohexene carbonate) (PCHC). Nevertheless, the lack of functional groups and relatively low glass transition temperatures of PPC, PEC and PCHC have limited their use in high value-added and functional materials. Hence, in order to expand the application scope of CO_2-based polycarbonates, novel synthetic strategies need to be developed to produce more diverse polycarbonates with improved performance.

Owing to their distinctive core-shell morphology and their tunable sizes and surface chemistries, polymeric micelles have attracted great attention in the biomedical field for applications in diagnostic imaging, drug and gene delivery and antimicrobial therapy. In Chapter II, we reported the facile preparation of functional micelles from a CO_2-derived triblock polycarbonate system. By judicious use of water as chain transfer reagent in the propylene oxide/CO_2 copolymerization, α,ω-dihydroxy telechelic

* Portions reprinted (adapted) from "Terpolymerization of Propylene Oxide and Vinyl Oxides with CO_2: Copolymer Cross-linking and Surface Modification *via* Thiol-ene Click Chemistry." Darensbourg, D. J.; Wang, Y. *Polym. Chem.*, **2015**, *6*, 1768-1776. Reproduced by permission of The Royal Society of Chemistry.

poly(propylene carbonate) was produced and served as macroinitiators in the subsequent allyl glycidyl ether/CO_2 coupling reaction. The resulting ABA block polycarbonate exhibited extremely narrow polydispersity index (PDI, ~ 1.01), confirming that the reaction system maintained its living character during the course of chain extension. The clickable alkene groups on the poly(allyl glycidyl ether carbonate) blocks were transformed with three different thiols by photoinitiated, radical-mediated thiol-ene chemistry, yielding amphiphilic CO_2-based polycarbonates with different charge types.

The self-assembly behavior of these amphiphilic polycarbonates was investigated. The polymer functionalized with 2-aminoethanethiol hydrochloride were shown to be soluble in water without micelle formation. This could be explained as being due to the low pH value of DI water (5.5), which would lead to a very high hydrophilic-hydrophobic ratio for the amino-containing cationic polymer. In contrast, amphiphilic polymers functionalized with mercaptoacetic acid and *L*-cysteine hydrochloride underwent self-assembly to afford uniform nanoparticles with similar intensity-averaged hydrodynamic diameters of 26±15 nm (by DLS). Transmission electron microscopy (TEM) measurements revealed the morphologies of these nanoparticles to be spherical. The surface charges of these micelles were found to coincide with the presence of their respective chemical functionalities. Currently, these degradable nanoparticles are being explored in various biomedical applications.

In our continued efforts towards the development of functional polycarbonate materials, in Chapter III we have designed and prepared poly(3,4-dihydroxybutyric acid carbonate) through copolymerization of *tert*-butyl 3,4-epoxybutanoate (^{t}Bu 3,4-EB) and

CO_2 followed by removal of the *tert*-butyl protecting group. Poly(3,4-dihydroxybutyric acid carbonate) is particularly attractive for biomaterial development, as it can degrade into nontoxic human metabolites in the human body. In addition, the pendant carboxylic groups provide a site for the attachment of biologically active materials, e.g. for drug delivery.

The catalytic coupling of ^{t}Bu 3,4-EB and CO_2 was carried out using bifunctional cobalt(III) salen catalysts in the presence of sterically unhindered nucleophiles as initiators. The resulting poly(*tert*-butyl 3,4-dihydroxybutanoate carbonate) (P^{t}BuDHBC) was shown to possess 100% head-to-tail regioselectivity. This implies that the bulky *tert*-butyl group promotes ring-opening of ^{t}Bu 3,4-EB to occur exclusively at the C$_\beta$-O bond during the copolymerization reactions. The *tert*-butyl group in P^{t}BuDHBC was cleaved by trifluoroacetic acid to afford poly(3,4-dihydroxybutyric acid carbonate). Poly(3,4-dihydroxybutyric acid carbonate) is not soluble in common organic solvent but dissolves in methanol and DMSO, indicating its enhanced hydrophilicity due to the presence of the carboxylic acid groups. ^{1}H NMR spectroscopy was employed to monitor the degradation of acetyl-capped poly(3,4-dihydroxybutyrate carbonate) in aqueous solution at pH 8 at 37 °C. Over a 5 day period, the polymer fully degraded into nontoxic biomasses, including β-hydroxy-γ-butylactone and 3,4-dihydroxybutyrate.

In an effort to construct polycarbonate-platinum conjugates, poly(3,4-dihydroxybutyric acid carbonate) was coupled with aspartate or glycine-aspartate followed by addition of $[(DACH)Pt(OH_2)_2][NO_3]_2$ (DACH = (*1R,2R*)-diaminocyclohexane). Platinum loadings of 21.3-29.5% were achieved. These polymer-

platinum conjugates could expand the repertoire of biocompatible and biodegradable polymers available for future anticancer pharmaceutics.

Post-polymerization modification has provided a powerful tool to access functional polycarbonates with enhanced hydrophilicity. In Chapter IV, we set out to employ the same approach to modify the thermal and mechanical properties of CO_2-PCs. We have prepared terpolymers of propylene oxide, vinyl epoxides and CO_2; whereby, the pendant alkene groups allows for postpolymerization cross-linking by thiol-ene click chemistry. To elucidate the microstructure of these terpolymers, Fineman-Ross analysis were carried out. For the terpolymerization reactions involving propylene oxide, 2-vinyl oxirane and CO_2, the reactivity parameters were r_{PO} = 3.74 and r_{VIO} = 0.224 at 25 °C. Hence, a 3:1 mixture of propylene oxide and 2-vinyl oxirane is anticipated to afford a tapered terpolymer structure. Less discrimination of epoxides was noted when carrying out the process using propylene oxide, allyl glycidyl ether, and CO_2, where the reactivity parameters were r_{PO} = 0.755 and r_{AGE} = 0.876 at 25 °C. The similar reactivity ratios between the two epoxides indicate a more even distribution of alkene groups along the polymer chain.

In order to enhance the polycarbonate's mechanical and thermal properties, the terpolymers from PO/AGE/CO_2, where the vinyl pendant groups are more randomly distributed in the polymeric material, were cross-linked *via* thiol-ene chemistry using two different thiols, ethylene glycol *bis*(3-mercaptoproionate) and pentaerythritol *tetrakis*(mercaptoacetate). FT-Raman spectroscopy provided evidence that successful cross-linking has occurred. Dynamic mechanical analysis measurements on these

terpolymers were performed as a function of the cross-link densities. Cross-linked films derived from the tetradentate cross-linker displayed a 50% increase in rubbery modulus between 50% and 100% C=C bond conversation; concomitantly, the T_g increased with increasing cross-link densities. In addition, the cross-linked films with 25% C=C bond conversion were reacted with *N*-acetyl-*L*-cysteine and 2-(Boc-amino)ethanethiol, and confirmed by FTIR and XPS, to provide surface functionalized films containing carboxyl or amine groups for various applications.

To conclude, the work presented in this dissertation highlighted the efforts we have made towards the development of more diverse functional CO_2 polycarbonate materials. Taking advantage of recent synthetic advances in the field, we have designed and prepared functional nanomaterials as well as polymer-drug conjugates from CO_2-derived polycarbonates, providing opportunities in biomedical applications. Over the past few decades, ring-opening polymerization of cyclic carbonate monomers has been the go-to-method to prepare polycarbonate materials investigated in biomedical applications. However, the demanding multistep synthesis of the cyclic monomers represents a major challenge for commercial application. Ring opening polymerization of CO_2 and epoxides can overcome this limitation, as many functional epoxides are commercially produced, or they can be readily prepared from olefins. Hence, the functional polycarbonate platforms presented in this dissertation have significant potential for use in commercial biomedical applications. In this dissertation, we have also developed synthetic strategies to modify the thermal mechanical properties of CO_2

copolymers. I hope that my small contributions to this field can help open up new application opportunities for CO_2-derived polycarbonates.

REFERENCES

1. Odian, G., *Principles of Polymerization*. 4th ed.; John Wiley &Sons, Inc.: Hoboken, New Jersey, 2004.

2. https://www.grandviewresearch.com/press-release/global-polycarbonate-market (accessed April 3, 2018)

3. Stevens, M. P., *Polymer Chemistry: An introduction*. 3rd ed.; Oxford University Press: New York, New York, 1999.

4. (a) Kim, S. Y.; Lee, K. E.; Han, S. S.; Jeong, B. *J. Phys. Chem. B* **2008,** *112*, 7420-7423; (b) Zhang, Y.; Zhuo, R.-X. *Biomaterials* **2005,** *26*, 2089-2094.

5. (a) Katz, A. R.; Mukherjee, D. P.; Kaganov, A. L.; Gordon, S. *Surg. Gynecol. Obstet.* **1985,** *161*, 213-222; (b) Moy, R. L.; Kaufman, A. J. *J. Dermatol. Surg. Oncol.* **1991,** *17*, 667-669.

6. (a) Sharifi, S.; Blanquer, S. B. G.; van Kooten, T. G.; Grijpma, D. W. *Acta Biomater.* **2012,** *8*, 4233-4243; (b) Zhang, C.; Sangaj, N.; Hwang, Y. S.; Phadke, A.; Chang, C.-W.; Varghese, S. *Acta Biomater.* **2011,** *7*, 3362-3369.

7. Fukuoka, S.; Tojo, M.; Hachiya, H.; Aminaka, M.; Hasegawa, K. *Polym. J.* **2007,** *39*, 91-114.

8. (a) Helou, M.; Miserque, O.; Brusson, J. M.; Carpentier, J. F.; Guillaume, S. M. *Chem. Eur. J.* **2010,** *16*, 13805-13813; (b) Ling, J.; Zhu, W. P.; Shen, Z. *Macromolecules* **2004,** *37*, 758-763.

9. Tamura, M.; Ito, K.; Honda, M.; Nakagawa, Y.; Sugimoto, H.; Tomishige, K. *Sci. Rep.* **2016,** *6*, 24038

10. (a) Inoue, S.; Koinuma, H.; Tsuruta, T. *J. Polym. Sci. B* **1969,** *7*, 287-292; (b) Inoue, S.; Koinuma, H.; Tsuruta, T. *Makromol. Chem.* **1969,** *130*, 210-220.

11. North, M.; Pasquale, R.; Young, C. *Green Chem.* **2010,** *12*, 1514-1539.

12. Darensbourg, D. J.; Yeung, A. D. *Polym. Chem.* **2014,** *5*, 3949-3962.

13. (a) Cyriac, A.; Lee, S. H.; Varghese, J. K.; Park, E. S.; Park, J. H.; Lee, B. Y. *Macromolecules* **2010,** *43*, 7398-7401; (b) Kember, M. R.; Copley, J.; Buchard, A.; Williams, C. K. *Polym. Chem.* **2012,** *3*, 1196-1201.

14. Inoue, S. *J. Polym. Sci. A* **2000,** *38*, 2861-2871.

15. (a) Ree, M.; Hwang, Y.; Kim, J. S.; Kim, H.; Kim, G.; Kim, H. *Catal. Today* **2006,** *115*, 134-145; (b) Klaus, S.; Lehenmeier, M. W.; Herdtweck, E.; Deglmann, P.; Ott, A. K.; Rieger, B. *J. Am. Chem. Soc.* **2011,** *133*, 13151-13161; (c) Varghese, J. K.; Park, D. S.; Jeon, J. Y.; Lee, B. Y. *J. Polym. Sci. A* **2013,** *51*, 4811-4818; (d) Zhang, X.-H.; Wei, R.-J.; Sun, X.-K.; Zhang, J.-F.; Du, B.-Y.; Fan, Z.-Q.; Qi, G.-R. *Polymer* **2011,** *52*, 5494-5502.

16. Aida, T.; Ishikawa, M.; Inoue, S. *Macromolecules* **1986,** *19*, 8-13.

17. (a) Darensbourg, D. J.; Holtcamp, M. W. *Macromolecules* **1995,** *28*, 7577-7579; (b) Darensbourg, D. J.; Holtcamp, M. W.; Struck, G. E.; Zimmer, M. S.; Niezgoda, S. A.; Rainey, P.; Robertson, J. B.; Draper, J. D.; Reibenspies, J. H. *J. Am. Chem. Soc.* **1999,** *121*, 107-116.

18. Cheng, M.; Lobkovsky, E. B.; Coates, G. W. *J. Am. Chem. Soc.* **1998,** *120*, 11018-11019.

19. (a) Chatterjee, C.; Chisholm, M. H. *Inorg. Chem.* **2011,** *50*, 4481-4492; (b) Sugimoto, H.; Ohshima, H.; Inoue, S. *J. Polym. Sci. A* **2003,** *41*, 3549-3555.

20. (a) Darensbourg, D. J.; Yarbrough, J. C. *J. Am. Chem. Soc.* **2002,** *124*, 6335-6342; (b) Qin, Z.; Thomas, C. M.; Lee, S.; Coates, G. W. *Angew. Chem. Int. Ed.* **2003,** *42*, 5484-5487; (c) Darensbourg, D. J.; Ulusoy, M.; Karroonnirum, O.; Poland, R. R.; Reibenspies, J. H.; Cetinkaya, B. *Macromolecules* **2009,** *42*, 6992-6998.

21. Kember, M. R.; Knight, P. D.; Reung, P. T. R.; Williams, C. K. *Angew. Chem. Int. Ed.* **2009,** *48*, 931-933.

22. Lu, X.-B.; Darensbourg, D. J. *Chem. Soc. Rev.* **2012,** *41*, 1462-1484.

23. (a) Ohkawara, T.; Suzuki, K.; Nakano, K.; Mori, S.; Nozaki, K. *J. Am. Chem. Soc.* **2014,** *136*, 10728-10735; (b) Liu, J.; Ren, W.-M.; Liu, Y.; Lu, X.-B. *Macromolecules* **2013,** *46*, 1343-1349; (c) Liu, Y.; Ren, W.-M.; Liu, C.; Fu, S.; Wang, M.; He, K.-K.; Li, R.-R.; Zhang, R.; Lu, X.-B. *Macromolecules* **2014,** *47*, 7775-7788.

24. (a) Nakano, K.; Kamada, T.; Nozaki, K. *Angew. Chem. Int. Ed.* **2006,** *45*, 7274-7277; (b) Sujith, S.; Min, J. K.; Seong, J. E.; Na, S. J.; Lee, B. Y. *Angew. Chem. Int. Ed.* **2008,** *47*, 7306-7309; (c) Noh, E. K.; Na, S. J.; Sujith, S.; Kim, S. W.; Lee, B. Y. *J. Am. Chem. Soc.* **2007,** *129*, 8082-8083; (d) Ren, W.-M.; Liu, Z.-W.; Wen, Y.-Q.; Zhang, R.; Lu, X.-B. *J. Am. Chem. Soc.* **2009,** *131*, 11509-11518; (e) Ren, W.-M.; Zhang, X.; Liu, Y.; Li, J.-F.; Wang, H.; Lu, X.-B. *Macromolecules* **2010,** *43*, 1396-1402.

25. http://www.saudiaramco.com/en/home/our-business/downstream/converge.html (accessed April 3, 2018)

26. http://empowermaterials.com/products (accessed April 3, 2018)

27. http://utech-polyurethane.com/information/econic-making-good-use-co2/ (accessed April 3, 2018).

28. https://www.co2-dreams.covestro.com/en (accessed April 3, 2018).

29. Poland, S. J.; Darensbourg, D. J. *Green Chem.* **2017,** *19*, 4990-5011.

30. (a) Wu, G.-P.; Wei, S.-H.; Ren, W.-M.; Lu, X.-B.; Li, B.; Zu, Y.-P.; Darensbourg, D. J. *Energy Environ. Sci.* **2011,** *4*, 5084-5092; (b) Darensbourg, D. J.; Fitch, S. B. *Inorg. Chem.* **2008,** *47*, 11868-11878; (c) Wu, G.-P.; Darensbourg, D. J.; Lu, X.-B. *J. Am. Chem. Soc.* **2012,** *134*, 17739-17745; (d) Wu, G.-P.; Zu, Y.-P.; Xu, P.-X.; Ren, W.-M.; Lu, X.-B. *Chem. Asian J.* **2013,** *8*, 1854-1862; (e) Wu, G.-P.; Wei, S.-H.; Lu, X.-B.; Ren, W.-M.; Darensbourg, D. J. *Macromolecules* **2010,** *43*, 9202-9204.

31. (a) Wu, G.-P.; Wei, S.-H.; Ren, W.-M.; Lu, X.-B.; Xu, T.-Q.; Darensbourg, D. J. *J. Am. Chem. Soc.* **2011,** *133*, 15191-15199; (b) Shen, Z.; Chen, X.; Zhang, Y. *Macromol. Chem. Phys.* **1994,** *195*, 2003-2011; (c) Sudakar, P.; Sivanesan, D.; Yoon, S. *Macromol. Rapid Commun.* **2016,** *37*, 788-793; (d) Wei, R.-J.; Zhang, X.-H.; Du, B.-Y.; Fan, Z.-Q.; Qi, G.-R. *Polymer* **2013,** *54*, 6357-6362.

32. Darensbourg, D. J.; Tsai, F.-T. *Macromolecules* **2014,** *47*, 3806-3813.

33. Zhang, Y.-Y.; Zhang, X.-H.; Wei, R.-J.; Du, B.-Y.; Fan, Z.-Q.; Qi, G.-R. *RSC Adv.* **2014,** *4*, 36183-36188.

34. Zhang, H.; Lin, X.; Chin, S.; Grinstaff, M. W. *J. Am. Chem. Soc.* **2015,** *137*, 12660-12666.

35. Tsai, F.-T.; Wang, Y.; Darensbourg, D. J. *J. Am. Chem. Soc.* **2016,** *138*, 4626-4633.

36. Scharfenberg, M.; Hilf, J.; Frey, H. *Adv. Funct. Mater.* **2018**, *28*, 1704302.

37. Hilf, J.; Frey, H. *Macromol. Rapid Commun.* **2013,** *34*, 1395-1400.

38. (a) Wang, Y.; Fan, J.; Darensbourg, D. J. *Angew. Chem. Int. Ed.* **2015,** *54*, 10206-10210; (b) Darensbourg, D. J.; Wang, Y. *Polym. Chem.* **2015,** *6*, 1768-1776; (c) Lukaszczyk, J.; Jaszcz, K.; Kuran, W.; Listos, T. *Macromol. Rapid Commun.* **2000,** *21*, 754-757; (d) Tan, C.-S.; Juan, C.-C.; Kuo, T.-W. *Polymer* **2004,** *45*, 1805-1814; (e) Tan, C.-S.; Kuo, T.-W. *J. Appl. Polym. Sci.* **2005,** *98*, 750-757; (f) Lukaszczyk, J.; Jaszcz, K.; Kuran, W.; Listos, T. *Macromol. Biosci.* **2001,** *1*, 282-289.

39. Hilf, J.; Scharfenberg, M.; Poon, J.; Moers, C.; Frey, H. *Macromol. Rapid Commun.* **2015,** *36*, 174-179.

40. Geschwind, J.; Frey, H. *Macromolecules* **2013,** *46*, 3280-3287.

41. Zhang, H.; Grinstaff, M. W. *J. Am. Chem. Soc.* **2013,** *135*, 6806-6809.

42. Kim, Y. J.; Matsunaga, Y. T. *J. Mater. Chem. B* **2017,** *5*, 4307-4321.

43. Zhou, Q.; Gu, L.; Gao, Y.; Qin, Y.; Wang, X.; Wang, F. *J. Polym. Sci. A* **2013,** *51*, 1893-1898.

44. Gu, L.; Qin, Y.; Gao, Y.; Wang, X.; Wang, F. *J. Polym. Sci. A* **2013,** *51*, 2834-2840.

45. Darensbourg, D. J.; Rodgers, J. L.; Fang, C. C. *Inorg. Chem.* **2003,** *42*, 4498-4500.

46. Kim, J. G.; Cowman, C. D.; LaPointe, A. M.; Wiesner, U.; Coates, G. W. *Macromolecules* **2011,** *44*, 1110-1113.

47. Duchateau, R.; van Meerendonk, W. J.; Yajjou, L.; Staal, B. B. P.; Koning, C. E.; Gruter, G. J. M. *Macromolecules* **2006,** *39*, 7900-7908.

48. (a) Darensbourg, D. J.; Chung, W.-C.; Arp, C. J.; Tsai, F.-T.; Kyran, S. J. *Macromolecules* **2014,** *47*, 7347-7353; (b) Honda, S.; Mori, T.; Goto, H.; Sugimoto, H. *Polymer* **2014,** *55*, 4832-4836; (c) Winkler, M.; Romain, C.; Meier, M. A. R.; Williams, C. K. *Green Chem.* **2015,** *17*, 300-306.

49. Darensbourg, D. J.; Chung, W. C.; Yeung, A. D.; Luna, M. *Macromolecules* **2015,** *48*, 1679-1687.

50. (a) Bonon, A. J.; Kozlov, Y. N.; Bahu, J. O.; Maciel, R.; Mandelli, D.; Shul'pin, G. B. *J. Catal.* **2014,** *319*, 71-86; (b) Charbonneau, L.; Kaliaguine, S. *Appl. Catal. A Gen.* **2017,** *533*, 1-8.

51. Byrne, C. M.; Allen, S. D.; Lobkovsky, E. B.; Coates, G. W. *J. Am. Chem. Soc.* **2004,** *126*, 11404-11405.

52. Reiter, M.; Vagin, S.; Kronast, A.; Jandl, C.; Rieger, B. *Chem. Sci.* **2017,** *8*, 1876-1882.

53. Carrodeguas, L. P.; Gonzalez-Fabra, J.; Castro-Gomez, F.; Bo, C.; Kleij, A. W. *Chem. Eur. J.* **2015,** *21*, 6115-6122.

54. Hauenstein, O.; Reiter, M.; Agarwal, S.; Rieger, B.; Greiner, A. *Green Chem.* **2016,** *18*, 760-770.

55. Hauenstein, O.; Rahman, M. M.; Elsayed, M.; Krause-Rehberg, R.; Agarwal, S.; Abetz, V.; Greiner, A. *Adv. Mater. Technol.* **2017,** *2*, 1700026.

56. Li, C.; Sablong, R. J.; Koning, C. E. *Angew. Chem. Int. Ed.* **2016,** *55*, 11572-11576.

57. Kindermann, N.; Cristofol, A.; Kleij, A. W. *ACS Catal.* **2017,** *7*, 3860-3863.

58. (a) Liu, Y.; Ren, W.-M.; He, K.-K.; Lu, X.-B. *Nat. Commun.* **2014,** *5*, 5687; (b) Liu, Y.; Wang, M.; Ren, W.-M.; He, K.-K.; Xu, Y.-C.; Liu, J.; Lu, X.-B. *Macromolecules* **2014,** *47*, 1269-1276; (c) Liu, Y.; Zhou, H.; Guo, J.-Z.; Ren, W.-M.; Lu, X.-B. *Angew. Chem. Int. Ed.* **2017,** *56*, 4862-4866.

59. Hoyle, C. E.; Bowman, C. N. *Angew. Chem. Int. Ed.* **2010,** *49*, 1540-1573.

60. Zhang, J.-F.; Ren, W.-M.; Sun, X.-K.; Meng, Y.; Du, B.-Y.; Zhang, X.-H. *Macromolecules* **2011,** *44*, 9882-9886.

61. Hauenstein, O.; Agarwal, S.; Greiner, A. *Nat. Commun.* **2016,** *7*, 11862.

62. Hu, Y.; Qiao, L.; Qin, Y.; Zhao, X.; Chen, X.; Wang, X.; Wang, F. *Macromolecules* **2009,** *42*, 9251-9254.

63. (a) Kember, M. R.; Williams, C. K. *J. Am. Chem. Soc.* **2012,** *134*, 15676-15679; (b) Darensbourg, D. J.; Wu, G.-P. *Angew. Chem. Int. Ed.* **2013,** *52*, 10602-10606.

64. Liu, S.; Zhao, X.; Guo, H.; Qin, Y.; Wang, X.; Wang, F. *Macromol. Rapid Commun.* **2017,** *38*, 1600754.

65. (a) Hilf, J.; Schulze, P.; Seiwert, J.; Frey, H. *Macromol. Rapid Commun.* **2014,** *35*, 198-203; (b) Scharfenberg, M.; Seiwert, J.; Scherger, M.; Preis, J.; Susewind, M.; Frey, H. *Macromolecules* **2017,** *50*, 6577-6585; (c) Liu, S.; Miao, Y.; Qiao, L.; Qin, Y.; Wang, X.; Chen, X.; Wang, F. *Polym. Chem.* **2015,** *6*, 7580-7585; (d) Liu, S.; Qin, Y.; Chen, X.; Wang, X.; Wang, F. *Polym. Chem.* **2014,** *5*, 6171-6179; (e) Sugimoto, H.; Goto, H.; Honda, S.; Yamada, R.; Manabe, Y.; Handa, S. *Polym. Chem.* **2016,** *7*, 3906-3912.

66. (a) Motokucho, S.; Sudo, A.; Sanda, F.; Endo, T. *J. Polym. Sci. A* **2004,** *42*, 2506-2511; (b) Scharfenberg, M.; Hofmann, S.; Preis, J.; Hilf, J.; Frey, H. *Macromolecules* **2017,** *50*, 6088-6097.

67. Inoue, K. *Prog. Polym. Sci.* **2000,** *25*, 453-571.

68. (a) Darensbourg, D. J.; Wilson, S. J. *J. Am. Chem. Soc.* **2011,** *133*, 18610-18613; (b) Darensbourg, D. J.; Wilson, S. J. *Macromolecules* **2013,** *46*, 5929-5934.

69. Darensbourg, D. J.; Kyran, S. J. *ACS Catal.* **2015,** *5*, 5421-5430.

70. Liu, Y.; Wang, M.; Ren, W.-M.; Xu, Y.-C.; Lu, X.-B. *Angew. Chem. Int. Ed.* **2015,** *54*, 7042-7046.

71. (a) Childers, M. I.; Longo, J. M.; Van Zee, N. J.; LaPointe, A. M.; Coates, G. W. *Chem. Rev.* **2014,** *114*, 8129-8152; (b) Darensbourg, D. J.; Wilson, S. J. *Green Chem.* **2012,** *14*, 2665-2671; (c) Kielland, N.; Whiteoak, C. J.; Kleij, A. W. *Adv. Synth. Catal.* **2013,** *355*, 2115-2138; (d) Lu, X.-B.; Ren, W.-M.; Wu, G.-P. *Acc. Chem. Res.* **2012,** *45*, 1721-1735; (e) Paul, S.; Zhu, Y.; Romain, C.; Brooks, R.; Saini, P. K.; Williams, C. K. *Chem. Commun.* **2015,** *51*, 6459-6479.

72. (a) Ellis, W. C.; Jung, Y.; Mulzer, M.; Di Girolamo, R.; Lobkovsky, E. B.; Coates, G. W. *Chem. Sci.* **2014,** *5*, 4004-4011; (b) Abbina, S.; Du, G. D. *Organometallics* **2012,** *31*, 7394-7403; (c) Cheng, M.; Darling, N. A.; Lobkovsky, E. B.; Coates, G. W. *Chem. Commun.* **2000,** *20*, 2007-2008; (d) Nozaki, K.; Nakano, K.; Hiyama, T. *J. Am. Chem. Soc.* **1999,** *121*, 11008-11009; (e) Xiao, Y.; Wang, Z.; Ding, K. *Chem. Eur. J.* **2005,** *11*, 3668-3678.

73. (a) Wu, G.-P.; Ren, W.-M.; Luo, Y.; Li, B.; Zhang, W.-Z.; Lu, X.-B. *J. Am. Chem. Soc.* **2012,** *134*, 5682-5688; (b) Liu, Y.; Ren, W.-M.; Liu, J.; Lu, X.-B. *Angew. Chem. Int. Ed.* **2013,** *52*, 11594-11598; (c) Shi, L.; Lu, X.-B.; Zhang, R.; Peng, X.-J.; Zhang, C.-Q.; Li, J.-F.; Peng, X.-M. *Macromolecules* **2006,** *39*, 5679-5685.

74. Nishioka, K.; Goto, H.; Sugimoto, H. *Macromolecules* **2012,** *45*, 8172-8192.

75. (a) Liu, Y.; Ren, W.-M.; Wang, M.; Liu, C.; Lu, X.-B. *Angew. Chem. Int. Ed.* **2015,** *54*, 2241-2244; (b) Liu, Y.; Ren, W.-M.; Zhang, W.-P.; Zhao, R.-R.; Lu, X.-B. *Nat. Commun.* **2015,** *6*, 8594.

76. Auriemma, F.; De Rosa, C.; Di Caprio, M. R.; Di Girolamo, R.; Ellis, W. C.; Coates, G. W. *Angew. Chem. Int. Ed.* **2015,** *54*, 1215-1218.

77. Auriemma, F.; De Rosa, C.; Di Caprio, M. R.; Di Girolamo, R.; Coates, G. W. *Macromolecules* **2015,** *48*, 2534-2550.

78. (a) Cohen, C. T.; Chu, T.; Coates, G. W. *Abstr. Pap. Am. Chem. S.* **2005,** *230*, U2268-U2268; (b) Li, B.; Wu, G.-P.; Ren, W.-M.; Wang, Y.-M.; Rao, D.-Y.; Lu, X.-B. *J. Polym. Sci. A* **2008,** *46*, 6102-6113; (c) Li, B.; Zhang, R.; Lu, X.-B. *Macromolecules* **2007,** *40*, 2303-2307; (d) Lu, X.-B.; Liang, B.; Zhang, Y.-J.; Tian, Y.-Z.; Wang, Y.-M.;

Bai, C.-X.; Wang, H.; Zhang, R. *J. Am. Chem. Soc.* **2004,** *126*, 3732-3733; (e) Nakano, K.; Hashimoto, S.; Nakamura, M.; Kamada, T.; Nozaki, K. *Angew. Chem. Int. Ed.* **2011,** *50*, 4868-4871; (f) Ren, W.; Zhang, W.; Lu, X. *Sci. China Chem.* **2010,** *53*, 1646-1652; (g) Salmeia, K. A.; Vagin, S.; Anderson, C. E.; Rieger, B. *Macromolecules* **2012,** *45*, 8604-8613; (h) Ren, W.-M.; Liu, Y.; Wu, G.-P.; Liu, J.; Lu, X.-B. *J. Polym. Sci. A* **2011,** *49*, 4894-4901.

79. (a) Ren, W.-M.; Yue, T.-J.; Zhang, X.; Gu, G.-G.; Liu, Y.; Lu, X.-B. *Macromolecules* **2017,** *50*, 7062-7069; (b) Wu, G.-P.; Xu, P.-X.; Lu, X.-B.; Zu, Y.-P.; Wei, S.-H.; Ren, W.-M.; Darensbourg, D. J. *Macromolecules* **2013,** *46*, 2128-2133; (c) Wei, R.-J.; Zhang, X.-H.; Du, B.-Y.; Sun, X.-K.; Fan, Z.-Q.; Qi, G.-R. *Macromolecules* **2013,** *46*, 3693-3697.

80. Seong, J. E.; Na, S. J.; Cyriac, A.; Kim, B. W.; Lee, B. Y. *Macromolecules* **2010,** *43*, 903-908.

81. Zhang, H.; Liu, B.; Ding, H.; Chen, J.; Duan, Z. *Polymer* **2017,** *129*, 5-11.

82. Cherian, A. E.; Sun, F. C.; Sheiko, S. S.; Coates, G. W. *J. Am. Chem. Soc.* **2007,** *129*, 11350-11351.

83. Taherimehr, M.; Serta, J. P. C. C.; Kleij, A. W.; Whiteoak, C. J.; Pescarmona, P. P. *ChemSusChem* **2015,** *8*, 1034-1042.

84. Martin, C.; Kleij, A. W. *Macromolecules* **2016,** *49*, 6285-6295.

85. Li, C.; Johansson, M.; Sablong, R. J.; Koning, C. E. *Eur. Polym. J.* **2017,** *96*, 337-349.

86. Tao, Y.; Wang, X.; Zhao, X.; Li, J.; Wang, F. *J. Polym. Sci. A* **2006,** *44*, 5329-5336.

87. (a) Li, C.; van Berkel, S.; Sablong, R. J.; Koning, C. E. *Eur. Polym. J.* **2016,** *85*, 466-477; (b) Li, C.; Sablong, R. J.; Koning, C. E. *Eur. Polym. J.* **2015,** *67*, 449-458; (c) Chen, J.-X.; Zhang, C.-F.; Gao, W.-X.; Jin, H.-L.; Ding, J.-C.; Wu, H.-Y. *J. Braz. Chem. Soc.* **2010,** *21*, 1552-1556.

88. (a) Chisholm, M. H.; Zhou, Z. *J. Mater. Chem.* **2004,** *14*, 3081-3092; (b) Coates, G. W.; Moore, D. R. *Angew. Chem. Int. Ed.* **2004,** *43*, 6618-6639; (c) Darensbourg, D. J. *Chem. Rev.* **2007,** *107*, 2388-2410; (d) Darensbourg, D. J.; Holtcamp, M. W. *Coord. Chem. Rev.* **1996,** *153*, 155-174; (e) Darensbourg, D. J.; Mackiewicz, R. M.; Phelps, A. L.; Billodeaux, D. R. *Acc. Chem. Res.* **2004,** *37*, 836-844; (f) Kember, M. R.; Buchard, A.; Williams, C. K. *Chem. Commun.* **2011,** *47*, 141-163; (g) Klaus, S.; Lehenmeier, M. W.; Anderson, C. E.; Rieger, B. *Coord. Chem. Rev.* **2011,** *255*, 1460-1479; (h) Luinstra, G. A. *Polym. Rev.* **2008,** *48*, 192-219; (i) Qin, Y.; Wang, X. *Biotechnol. J.* **2010,** *5*, 1164-1180; (j) Sugimoto, H.; Inoue, S. *J. Polym. Sci. A* **2004,** *42*, 5561-5573.

89. (a) Zhang, H.; Grinstaff, M. W. *J. Appl. Polym. Sci.* **2014,** *131*, 39893; (b) Hilf, J.; Phillips, A.; Frey, H. *Polym. Chem.* **2014,** *5*, 814-818; (c) Wu, X.; Zhao, H.; Nornberg, B.; Theato, P.; Luinstra, G. A. *Macromolecules* **2014,** *47*, 492-497.

90. Hilf, J.; Scharfenberg, M.; Poon, J.; Moers, C.; Frey, H. *Macromol. Rapid Commun.* **2015,** *36*, 174-179.

91. (a) Wang, H.; Dong, J. H.; Qiu, K. Y. *J. Polym. Sci. A* **1998,** *36*, 695-702; (b) Melchiors, M.; Keul, H.; Hocker, H. *Polymer* **1996,** *37*, 1519-1527; (c) Ling, J.; Chen,

W.; Shen, Z. *J. Polym. Sci. A* **2005,** *43*, 1787-1796; (d) Chan, J. M. W.; Ke, X.; Sardon, H.; Engler, A. C.; Yang, Y. Y.; Hedrick, J. L. *Chem. Sci.* **2014,** *5*, 3294-3300; (e) Liu, S. Q.; Yang, C.; Huang, Y.; Ding, X.; Li, Y.; Fan, W. M.; Hedrick, J. L.; Yang, Y.-Y. *Adv. Mater.* **2012,** *24*, 6484-6489; (f) Nederberg, F.; Zhang, Y.; Tan, J. P. K.; Xu, K.; Wang, H.; Yang, C.; Gao, S.; Guo, X. D.; Fukushima, K.; Li, L.; Hedrick, J. L.; Yang, Y.-Y. *Nat. Chem.* **2011,** *3*, 409-414.

92. Movassaghian, S.; Merkel, O. M.; Torchilin, V. P. *WIREs Nanomed. Nanobiotechnol.* **2015,** *7*, 691-707.

93. (a) Obermeier, B.; Frey, H. *Bioconjug. Chem.* **2011,** *22*, 436-444; (b) Fleischmann, C.; Gopez, J.; Lundberg, P.; Ritter, H.; Killops, K. L.; Hawker, C. J.; Klinger, D. *Polym. Chem.* **2015,** *6*, 2029-2037; (c) Lee, B. F.; Kade, M. J.; Chute, J. A.; Gupta, N.; Campos, L. M.; Fredrickson, G. H.; Kramer, E. J.; Lynd, N. A.; Hawker, C. J. *J. Polym. Sci. A* **2011,** *49*, 4498-4504.

94. (a) Kember, M. R.; White, A. J. P.; Williams, C. K. *Macromolecules* **2010,** *43*, 2291-2298; (b) Sugimoto, H.; Ohtsuka, H.; Inoue, S. *J. Polym. Sci. A* **2005,** *43*, 4172-4186.

95. (a) Cowman, C. D.; Padgett, E.; Tan, K. W.; Hovden, R.; Gu, Y.; Andrejevic, N.; Muller, D.; Coates, G. W.; Wiesner, U. *J. Am. Chem. Soc.* **2015,** *137*, 6026-6033; (b) Hilf, J.; Schulze, P.; Frey, H. *Macromol. Chem. Phys.* **2013,** *214*, 2848-2855.

96. Rodriguez, J.; Nieto, R. M.; Blanco, M.; Valeriote, F. A.; Jimenez, C.; Crews, P. *Org. Lett.* **2014,** *16*, 464-467.

97. Ferris, C.; de Paz, M. V.; Galbis, J. A. *Macromol. Chem. Phys.* **2012,** *213*, 480-488.

98. Coates, G. W.; Hillmyer, M. A. *Macromolecules* **2009,** *42*, 7987-7989.

99. (a) You, L.; Schlaad, H. *J. Am. Chem. Soc.* **2006,** *128*, 13336-3337; (b) Nair, L. S.; Laurencin, C. T. *Prog. Polym. Sci.* **2007,** *32*, 762-798; (c) Wang, R.; Chen, W.; Meng, F.; Cheng, R.; Deng, C.; Feijen, J.; Zhong, Z. *Macromolecules* **2011,** *44*, 6009-6016.

100. (a) Bouatra, S.; Aziat, F.; Mandal, R.; Guo, A. C.; Wilson, M. R.; Knox, C.; Bjorndahl, T. C.; Krishnamurthy, R.; Saleem, F.; Liu, P.; Dame, Z. T.; Poelzer, J.; Huynh, J.; Yallou, F. S.; Psychogios, N.; Dong, E.; Bogumil, R.; Roehring, C.; Wishart, D. S. *PLoS ONE* **2013,** *8*, E73076-E73103; (b) Fell, V.; Lee, C. R.; Pollitt, R. J. *Biochemical Med.* **1975,** *13*, 40-45; (c) Hoffmann, G. F.; Seppel, C. K.; Holmes, B.; Mitchell, L.; Christen, H. J.; Hanefeld, F.; Rating, D.; Nyhan, W. L. *J. Chrom. B Biomed. Sci. Appl.* **1993,** *617*, 1-10.

101. (a) Kelland, L. *Nat. Rev. Cancer* **2007,** *7*, 573-584; (b) Zhang, F.; Elsabahy, M.; Zhang, S.; Lin, L. Y.; Zou, J.; Wooley, K. L. *Nanoscale* **2013,** *5*, 3220-3225; (c) Huynh, V. T.; Chen, G.; de Souza, P.; Stenzel, M. H. *Biomacromolecules* **2011,** *12*, 1738-1751; (d) Lee, S. M.; O'Halloran, T. V.; Nguyen, S. T. *J. Am. Chem. Soc.* **2010,** *132*, 17130-17138; (e) Sood, P.; Thurmond, K. B.; Jacob, J. E.; Waller, L. K.; Silva, G. O.; Stewart, D. R.; Nowotnik, D. P. *Bioconjug. Chem.* **2006,** *17*, 1270-1279.

102. (a) Darensbourg, D. J.; Wei, S.-H. *Macromolecules* **2012,** *45*, 5916-5922; (b) Darensbourg, D. J.; Wei, S.-H.; Yeung, A. D.; Ellis, W. C. *Macromolecules* **2013,** *46*, 5850-5855.

103. Luinstra, G. A.; Borchardt, E. *Adv. Polym. Sci.* **2012,** *245*, 29-48.

104. Aslan, K.; Holley, P.; Geddes, C. D. *J. Mater. Chem.* **2006,** *16*, 2846-2852.

105. Fineman, M.; Ross, S. D. *J. Polym. Sci.* **1950,** *5*, 259-262.

APPENDIX A

^{1}H NMR SPECTRA IN CHAPTER III

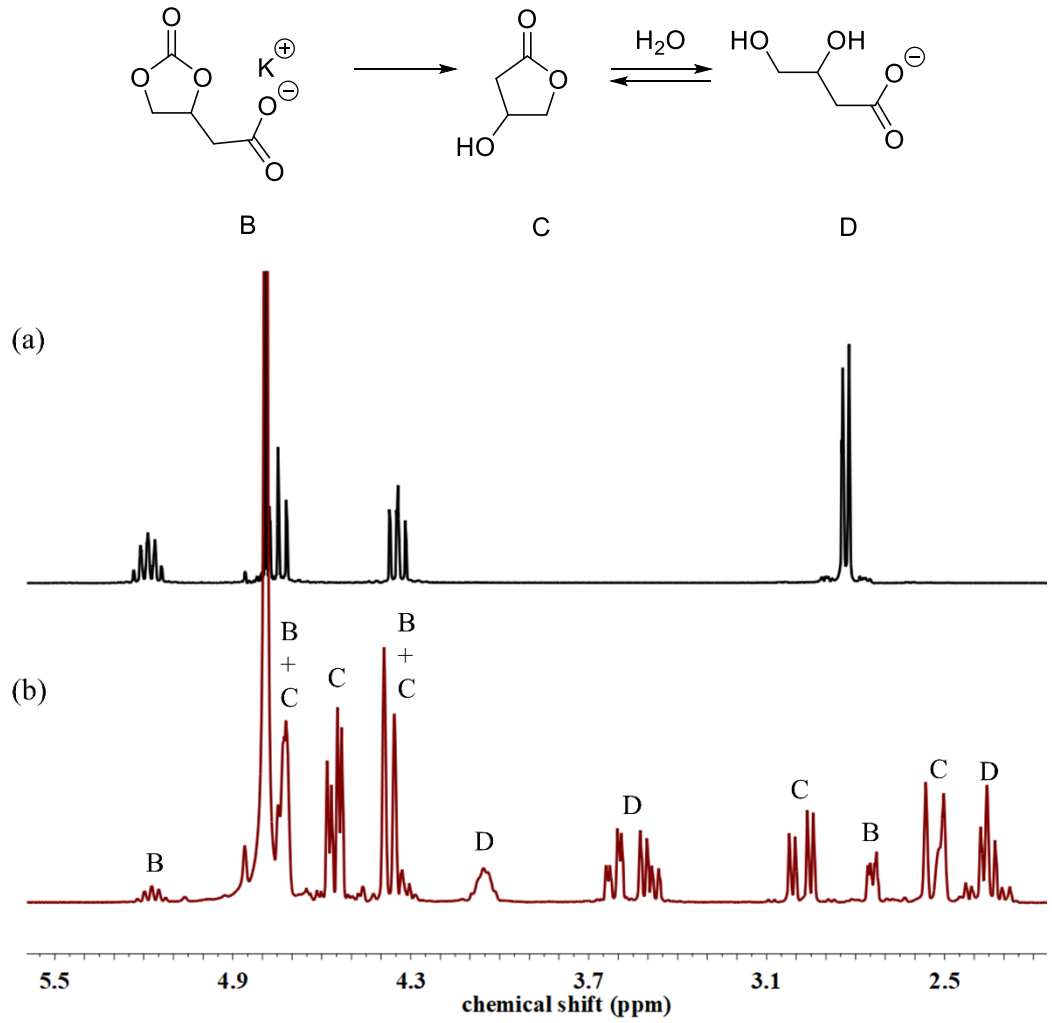

Figure A-1. Degradation of 3,4-dihydroxybutyrate cyclic carbonate in D_2O (pH =8) at 37 °C. (a) 0 h, (b) after 45 h. B: cyclic carbonate; C: *β*-hydroxy-*γ*-butyrolactone; D: 3,4-dihydroxybutyrate.

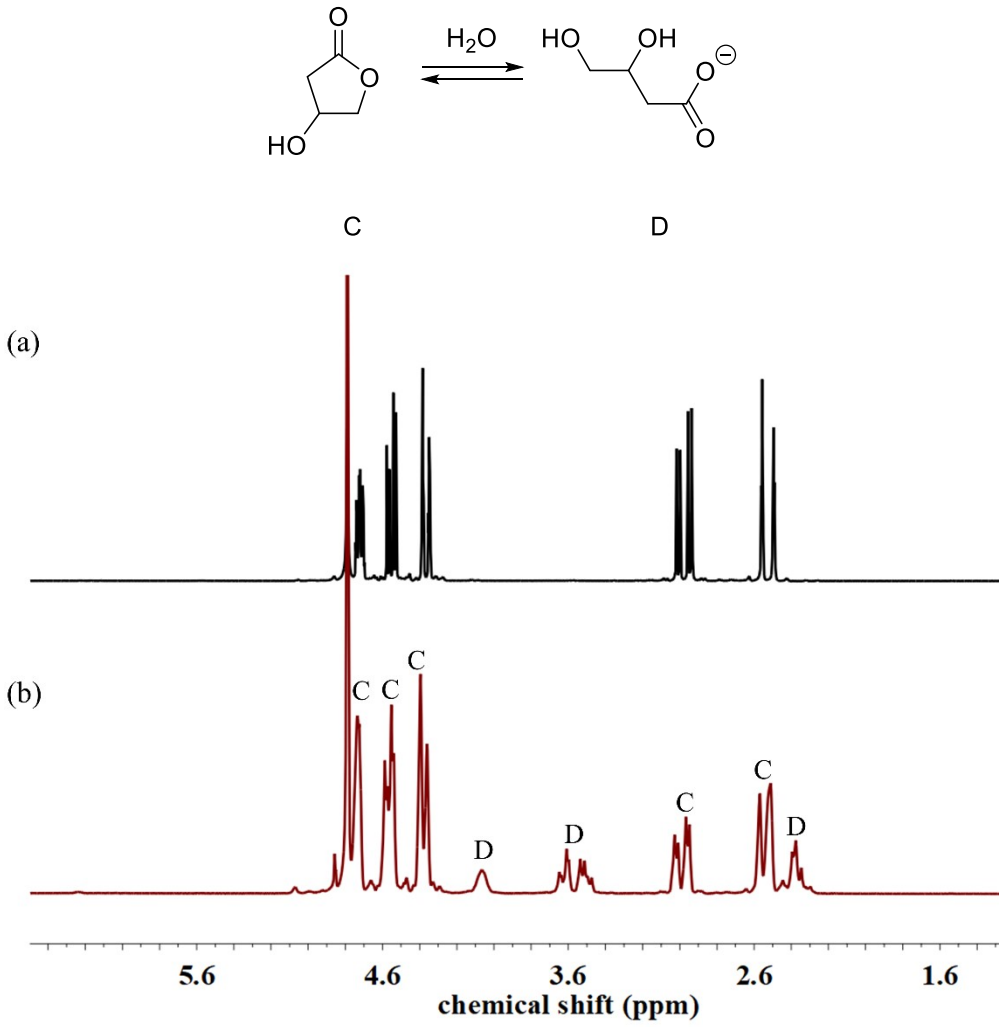

Figure A-2. Hydrolysis of *β*-hydroxy-*γ*-butyrolactone in D_2O (pH = 8) at 37 °C. (a) 0h, (b) after 140 h. C: *β*-hydroxy-*γ*-butyrolactone; D: 3,4-dihydroxybutyrate.

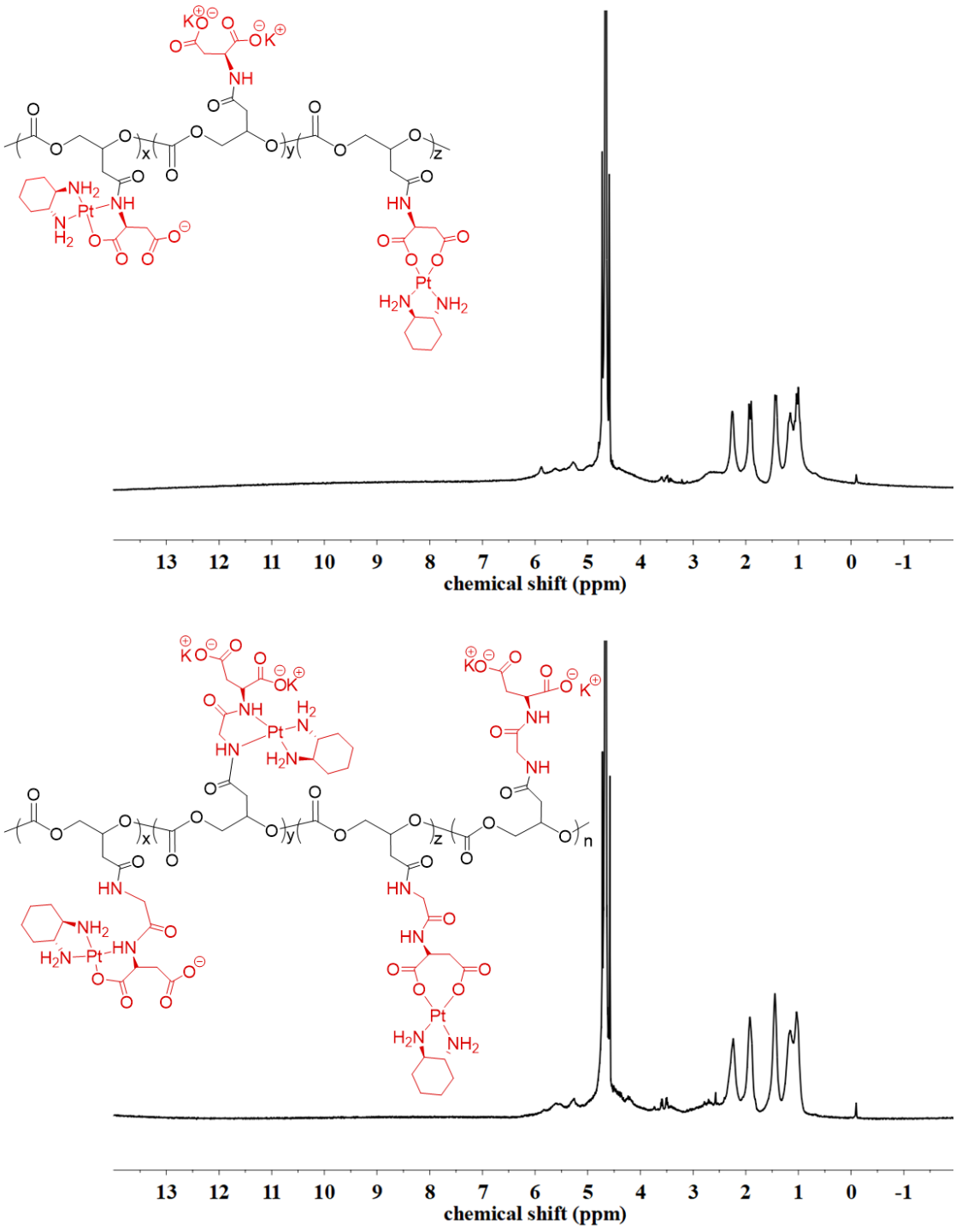

Figure A-3. ^{1}H NMR spectra of (top) PDHBAC-Asp-Pt, and (bottom) PDHBAC-Gly-Asp-Pt in D_2O.